The role of endocannabinoid system in brain aging

Thesis

Submitted for a Doctoral Degree in Natural Sciences

(Dr. rer. nat.)

Faculty of Mathematics and Natural Sciences

Rheinische Friedrich Wilhelms University, Bonn

submitted by

Anastasia Piyanova

from Moscow

Bonn, 29.03.12

Prepared with the consent of the Faculty of Mathematics and Natural Sciences,

Rheinische Friedrich Wilhelms University, Bonn

1. Reviewer: Priv.-Doz. Dr. Andras Bilkei-Gorzo

2. Reviewer: Prof. Dr. Gerhard von der Emde

Examination date: 28.06.12

Year of publication: 2012

Disclosure statement

I hereby declare that I prepared this thesis entitled: "The role of endocannabinoid system in brain aging" by myself except where otherwise stated. All text passages that are literally or correspondingly taken from published or unpublished papers are indicated as such. All materials or services provided by other people are equally indicated. Part of this thesis was published as listed:

> Albayram O, Alferink J, Pitsch J, Piyanova A, Neitzert K, Poppensieker K, Mauer D, Michel K, Legler A, Becker A, Monory K, Lutz B, Zimmer A, Bilkei-Gorzo A. Role of CB1 cannabinoid receptors on GABAergic neurons in brain aging. *Proc Natl Acad Sci U S A* 2011 Jul 5; 108(27):11256-61. Epub 2011 Jun 20

Bonn, den 29.03.12 Anastasia Piyanova

All diseases run into one, old age. (Ralph Waldo Emerson)

Abbreviations

2-AG = 2-arachidonoylglycerol

2D-PAGE = two-dimensional polyacrylamide gel electrophoresis

AA = arachidonic acid

ACN = acetonitrile

AEA = anandamide

Akt (protein kinase B, PKB) = alpha serine/threonine-protein kinase

APP/PS1 = amyloid precursor protein/presenilin 1

BCA = bicinchoninic acid

BDNF = brain-derived neurotrophic factor

BSA = bovine serum albumine

BrdU = 5-bromo-2'-deoxyuridine

CA1/2/3 = cornu ammonis areas 1,2,3

CCD = charge-coupled device

CB1, CB1R, Cnr1 = cannabinoid receptor type 1

CB2, Cnr2 = cannabinoid receptor type 2

cDNA = complementary DNA

CO_2 = carbon dioxide

$Cnr1^{+/+}$ = wildtype (for cannabinoid receptor 1)

$Cnr1^{-/-}$ = knockout (for cannabinoid receptor 1)

Ct = cycle threshold

$CuSO_4$ = copper (II) sulfate

DAPI = 4',6-diamidino-2-phenylindole

DAGLα = diacylglycerol lipase alpha

DAGLβ = diacylglycerol lipase beta

DEPC = diethylpyrocarbonate

DG = dentate gyrus

DNA = deoxyribonucleic acid

DNPH = 2,4-dinitrophenylhydrazine

DTT = dithiothreitol

EC = endocannabinoid

ECL = enhanced chemiluminescence

EDTA = ethylenediaminetetraacetic acid

e.g. = for example

FA = formic acid

FAAH = fatty acid amide hydrolase

FADD = Fas-associated protein with death domain

GABA = gamma-aminobutyric acid

GAPDH = glyceraldehyde 3–phosphate dehydrogenase

h = hours (s)

H_2O = water

H_2O_2 = hydrogen peroxide

H_3PO_4 = phosphoric acid

HCl = hydrochloric acid

HRP = horseradish peroxidase

HTPLC = high-performance thin-layer chromatography

Iba1 = ionized calcium binding adaptor molecule 1

IEF = isoelectric focusing

IL6 = interleukin 6

IPG = immobilized pH gradient

Kir = inwardly rectifying potassium channels

LAMP2 = lysosomal-associated membrane protein 2

LC-ESI/QTOF-MS = high performance liquid chromatography coupled with electrospray ionization-quadripole/time of flight hybrid mass spectrometry

LC3 = microtubule-associated protein light chain 3

LC-MS/MS = liquid chromatography/tandem mass spectrometry

LDS (buffer) = lithium dodecyl sulfate

MAGL = monoacylglycerol lipase

MES (buffer) = 2-(N-morpholino)ethanesulfonic acid

milliQ (™ Millipore) = ultrapure water

MOPS (buffer) = 3-(N-morpholino)propanesulfonic acid

MRM = multiple-reaction monitoring

mRNA = messenger RNA

mtDNA = mitochondrial DNA

mTOR = mammalian target of rapamycin

NeuN = neuronal nuclear antigen

n.s. = not significant

OEA = oleoylethanolamide

p62 (SQSTM1) = sequestome 1

PARP = Poly (ADP-ribose) polymerase

PBS = phosphate buffered saline

PC = personal computer

PFA = paraformaldehyde

PEA = palmithoylethanolamide

qPCR (RT-PCR) = quantitative (reverse-transcriptase) polymerase chain reaction

RIPA (buffer) = radioimmunoprecipitation assay

RNA = ribonucleic acid

ROS = reactive oxygen species

RT = reverse transcriptase

SDS = sodium dodecyl sulphate

TBARS = thiobarbituric acid reactive substances

TBS = Tris-buffered saline

TBST = Tris-buffered saline with Tween 20

TCA = trichloroacetic acid

TLC = thin-layer chromatography

SDS-PAGE = sodium dodecyl sulphate polyacrylamide gel electrophoresis

SEM = standard error of mean

WT = wildtype

1. Abstract (summary)

Endocannabinoid system has recently been shown to play a role in brain aging. Mice lacking cannabinoid CB1 receptors (CB1 receptor knockout, Cnr1$^{-/-}$ mice) show signs of accelerated aging specific to the brain and cognitive functions. The mechanisms by which the absence of CB1 receptor deficiency induces accelerated brain aging have not been identified yet. The present work shows that CB1 receptor absence can enhance age-related accumulation of aging marker lipofuscin. Knockout of CB1 receptors also leads to a decrease in cathpesin D expression, as well as changes in autophagic pathway. However, the absence of CB1 receptor does not affect age-related oxidative stress or reduction in the rate of neurogenesis. We next asked if the endocannabinoid system itself undergoes age-related changes and assessed the levels of 2-arachidonoylglycerol (2-AG), the major ligand of the CB1 receptor, and the enzymes responsible for its metabolism in the hippocampus. The expression of the enzymes involved in the synthesis and degradation of 2-AG decreases with age, leaving the basal 2-AG levels unaltered. However, this general decrease in the production of metabolic enzymes for 2-AG might be detrimental in some cases, when an increased synthesis of this endocannabinoid is needed (e.g., excitotoxicity). No change in the levels of anandamide (AEA) or oleylethanolamide (OEA) is observed in aging. In addition, an increase in palmitoylethanolamide (PEA) levels is present in aged animals.

2. Introduction

Endocannabinoid system is a neurotransmitter system, which includes several neuromodulatory lipids (endocannabinoids), their receptors (cannabinoid receptor type 1, CB1, and 2, CB2) and a set of enzymes that synthesize and degrade endocannabinoids. The endocannabinoid system has been recently identified as a new target for interfering with age-related cognitive decline by decreasing age-related neuroinflammation and increasing neurogenesis (Marchalant et al. 2009a; Marchalant et al. 2009b). In the previous studies from our group, it has been shown that mice lacking the CB1 receptor, the principal endocannabinoid receptor in the central nervous system, suffer from early age-related memory dysfunctions and impaired learning, accompanied by neuronal loss and increased neuroinflammation (Albayram et al. 2011; Bilkei-Gorzo et al. 2012; Bilkei-Gorzo et al. 2005). However, the mechanisms contributing to this phenotype are not fully understood yet. Endocannabinoid system has many anti-aging properties: its activity can protect against oxidative stress, excitotoxicity, inflammation and increase neurogenesis (Aguado et al. 2005; Aguado et al. 2007; Jin et al. 2004; Kim et al. 2005; Marchalant et al. 2009a; Marchalant et al. 2009b; Marsicano et al. 2002; McCarron et al. 2003; Mulder et al. 2008). CB1 receptors are an important component of a negative feedback loop that controls neuronal excitability protecting the neurons from excessive overactivation by acting retrogradely to reduce neurotransmitter release (Di Marzo 2011). There is also some recent evidence that CB1 receptors are widely present intracellularly, namely, on lysosomes and mitochondria (Benard et al. 2012; Rozenfeld and Devi 2008). Therefore, there is a variety of possible mechanisms and pathways through which the endocannabinoid system can protect against accelerated aging, both through and independent from CB1 receptor signaling. In the next section (2.1) the mechanisms known to contribute to aging are presented, whereas section 2.2 provides general information about the endocannabinoid system. Section 2.3 focuses specifically on the evidence that endocannabinoid system plays a protective role in brain aging, which then leads to the main aims of the present work (section 2.4).

2.1 **Aging of the brain: theories and mechanisms**

The old believe everything, the middle-aged suspect everything, the young know everything.

(Oscar Wilde)

The fear of age-related disabilities is becoming one of the major concerns in the modern society, as the life expectancy progressively increases (Oeppen and Vaupel 2002). Aging of the brain is the major risk factor for neurodegenerative diseases: the probability of developing Alzheimer's disease increases up to 50% after the age of 85 (Bishop *et al.* 2010). Neurodegenerative diseases share many common mechanisms with normal brain aging, such as an increase in reactive oxygen species' (ROS) production by the mitochondria which results in increased oxidative stress, as well as synaptic loss and decreased neurogenesis. These processes are exacerbated in Parkinson's, Huntington's and Alzheimer's disease (AD) along with some other changes that are usually not typical for normal brain aging, such as massive neuronal loss (see Fig.2.1.1).

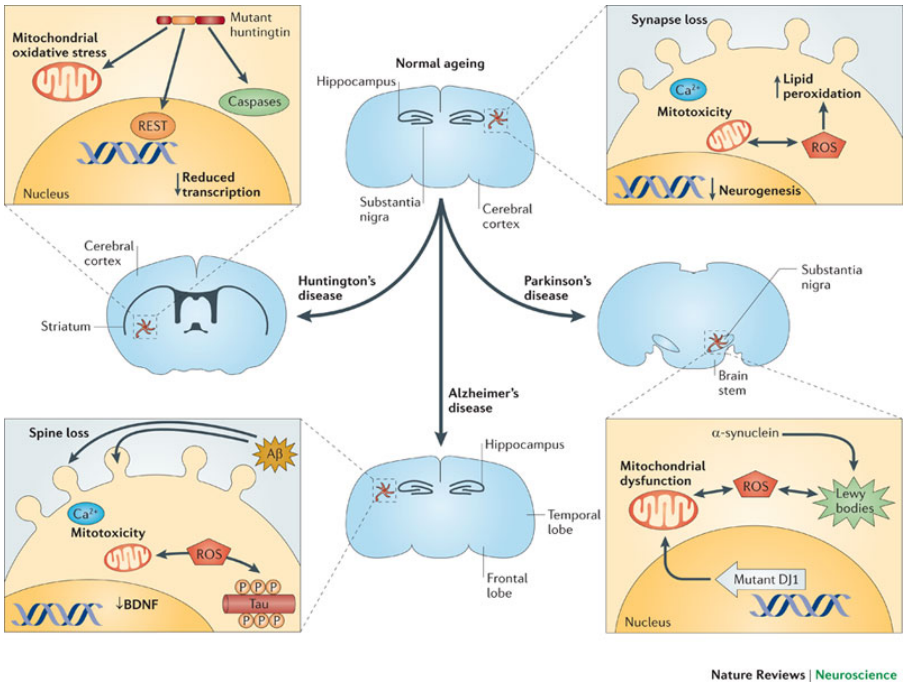

Fig.2.1.1. Normal and pathological processes that occur in the brain during aging (from: Stranahan & Mattson, *Nat Rev Neurosci* 2012).

Multiple lines of evidence suggest that the ability to resist oxidative stress is crucial in aging. „The free radical theory of aging“ (Harman 1956) or its modified version, „the mitochondrial theory of aging“ (Miquel *et al.* 1980; Sastre *et al.* 2003), have received wide acceptance in the scientific world over the past decades. This evidence supporting this theory comes not only from studies showing an increase in oxidative damage to cellular macromolecules in aged animals (Dubey et al. 1996; Navarro et al. 2002), but also from the fact that aging has been associated with reduced mitochondrial function which can lead to ROS production (Golden et al. 2002; Sastre et al. 2003). For instance, mtDNA mutations shorten lifespan, and overexpression of one of the most potent enzymes involved in protection against oxidative stress - catalase – can lead to an increased lifespan, which supports the free radical theory of aging (Muller et al. 2007). However, a reduction in mitochondrial respiration and activity during aging might also be compensatory and beneficial for the organism, and modestly increased concentrations of ROS can promote longevity through a process called hormesis, by which exposure to low levels of stressor can activate repair mechanisms beneficial for the cell or organism (Calabrese et al. 2007; Stranahan and Mattson 2012). Oxidative stress can also contribute to epigenetic changes during aging; for example, oxidation of promoter regions can induce gene silencing (Lu et al. 2004). Nevertheless, the oxidative stress theory of aging has been extensively critisized in the last years (Blagosklonny 2007; 2008; 2010; Lapointe and Hekimi 2010), implying that aging is rather programmed than stochastic as suggested by the oxidative stress theory. These studies propose the mammalian target of rapamycin (mTOR) as a major determinant of aging. It is known that mTOR activation can inhibit autophagy, which in turn would compromise the ability of the cell to degrade damaged macromolecules and organells. Indeed, treating mice with rapamycin, which is known to inhibit mTOR-mediated signaling, has been shown to extend lifespan (Miller et al. 2009). It also reduces formation of protein aggregates in animal models of neurodegenerative diseases. However, mTOR signaling also has some beneficial functions: activating mTOR can promote neuronal survival (together with BDNF) and induce dendritic spine formation (Bano et al. 2011).

Furthermore, aging is often accompanied by an increased generation of abnormal macromolecules, like aggregated and misfolded proteins (Nakanishi *et al.* 1997). Accordingly, molecular repair and degradation systems that usually respond to such damage tend to fail to react properly with increasing age. In general, cells become less able to respond to stress (Stranahan and Mattson 2012). Accumulation of molecular damage is particularly detrimental to postmitotic cells, like neurons, that cannot get rid of toxic waste products by cell division. Instead they have to activate internal degradative systems, like the proteasome (Low 2011) or autophagy (Cuervo 2008). Macroautophagy (often referred to as simply autophagy), a largely unspecific process of cytoplasmic sequestration leading to degradation of defective organelles and macromolecules (Klionsky *et al.* 2007), has been shown to play a major role in aging and neurodegenerative disorders (Rubinsztein et al. 2011). Autophagy deficiency results in accumulation of ubiquitinylated proteins, similar to the case of neurodegenerative disorders (Komatsu et al. 2007). Sometimes there is an increase in the number of autophagosomes, but the efficiency of autophagic degradation is poor (Martinez-Vicente et al. 2010; Wong and Cuervo 2010). Different reasons can account for that: deficient transport of autophagosomes to the degradation site or impaired cargo transport, deficiency in cargo recognition, impairment of fusion between autophagosomes and lysosomes or insufficient proteolytic degradation after the fusion. Changes that are initiated in the lysosomes can be primary reasons for autophagy deficits (Settembre et al. 2008a; Settembre et al. 2008b); see Fig. 2.1.3. Such changes include reduced acidification, accumulation of degradation products, decreased levels of lysosomal enzymes or their activity (Wong and Cuervo 2010). Lysosomal enzyme deficiencies often lead to conditions known as lysosomal storage disorders, many of which are also associated with autophagy malfunction and neurological symptoms (Wong and Cuervo 2010).

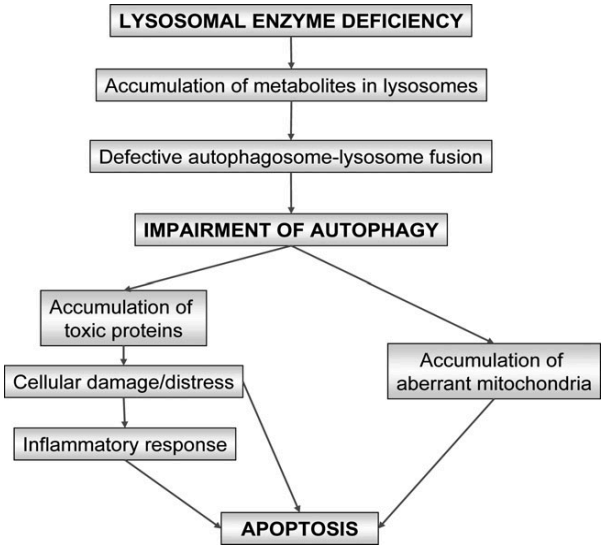

Fig.2.1.2. A model of lysosomal storage disorders proposed in Settembre et al, 2008 (Settembre et al. 2008a).

One of the prominent lysosomal enzymes that have been implicated in such conditions in animal models is cathepsin D (Koike et al. 2000; Nakanishi 2003; Nakanishi and Wu 2009; Nakanishi et al. 2001; Walls et al. 2007; Yamasaki et al. 2007). Knockdown of cathepsin D has also been demonstrated to cause multiple deficits and premature death in zebrafish (Follo et al. 2011). The brains of cathepsin D-deficient mice exhibit signs of impaired autophagy, increased neuroinflammation and neuronal loss, as well as massive lipofuscin accumulation (Yamasaki et al. 2007). Lipofuscin is a widely used aging marker (Terman and Brunk 2004). However, its accumulation is associated not only with increasing age, but also with lysosomal dysfunctions, like in the case of lysosomal storage disorders. It mostly consists of lysosomal degradation products: oxidized and misfolded proteins, damaged and partially degraded non-functional organelles, such as mitochondria (Dunlop et al. 2009; Terman and Brunk 2004). The accumulation of lipofuscin is characteristic of failing lysosomal and autophagic degradation process (Brunk and Terman 2002) and can be attributed to a loss-of-function of degradation enzymes, such as cathepsin D (Koike *et al.* 2000). Lipofuscin is known to have a very broad spectrum autofluorescence which disturbs fluorescent stainings, but is very useful for the

lipofuscin quantification (Gray and Woulfe 2005). There has been a debate since years, if lipofuscin accumulation in aging is just a marker or can actively contribute to age-related impairments. Since it is located in the lysosomes in the presence of enzymes that usually degrade any cellular material, one can conclude that lipofuscin is non-degradable (Brunk et al. 1992). Its presence can be detrimental to the normal lysosomal function, since the enzymes normally used for degradation of damaged macromolecules are recruited to attack lipofuscin – without any success. The only way for the cells to get rid of lipofuscin is to divide, which is why its accumulation is very characteristic of post-mitotic tissues.

In conclusion, aging is accompanied by various changes on the cellular and molecular level that lead to a shift in homeostasis, ultimately increasing the chance of neuronal dysfunction.

2.2 The endocannabinoid system

Endocannabinoid system is a neurotransmitter system that comprizes cannabinoid receptors (cannabinoid type 1, CB1, and type 2, CB2, and potentially other putative cannabinoid receptors), their endogenous ligands, the endocannabinoids, as well as their synthesis and degradaton enzymes. CB1 receptors are mainly expressed in the central nervous system, whereas CB2 receptors are mostly found in the periphery, e.g. on immune cells (Pertwee 1997). The CB1 receptor is the most abundant G-protein coupled-receptor in the brain (Di Marzo *et al.* 2004). The regions with the highest CB1 receptor expression are basal ganglia (striatum), cerebellum, hippocampus and cortex (Herkenham et al. 1991a; Herkenham et al. 1991b; Herkenham et al. 1990; Mailleux and Vanderhaeghen 1992; Matsuda et al. 1993). Binding of the ligands to CB1 receptors leads to changes in the activation state of multiple intracellular pathways, some of which are presented in Fig.2.2.1, like the activation of MAP kinases, inhibition of adenylate cyclase (AC), as well as inhibition of calcium (Ca^{2+}) channels and activation of inwardly rectifying potassium (K^{+}) channels (Kir) (Di Marzo et al. 2004).

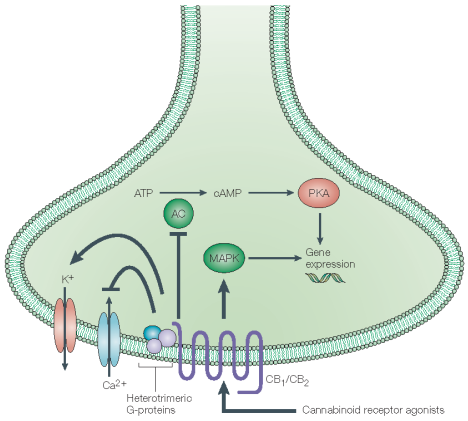

Fig.2.2.1. Signal transduction pathways related to cannabinoid receptor activation (from: Di Marzo, 2004).

2-AG and anandamide (AEA) are the two best-characterized endocannabinoids and the major endogenous ligands of the CB1 receptor. Pathways involved in the synthesis and degradation of these two endocannabinoids and their localization are presented in Fig.2.2.2 (Di Marzo et al. 2004).

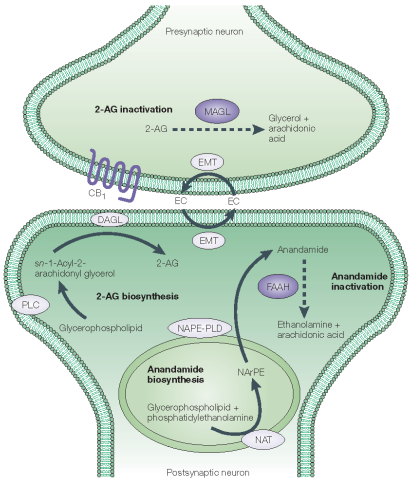

Fig 2.2.2. Schematic representation of the metabolic pathways of the endocannabinoids and their subcellular localization (from: Di Marzo, 2004).

There are four alternative pathways for AEA biosynthesis, and its major degrading enzyme is the fatty acid amide hydrolase (FAAH) (Di Marzo 2011). 2-AG is synthesized by diacylglycerol lipase (DAGL) α and β isoforms (Di Marzo 2011). DAGLα activity is the most prevalent in the brain,

whereas DAGLβ is the prominent enzyme for 2-AG synthesis in the liver (Bisogno *et al.* 2003). Genetic deletion of DAGLα produces 80% decrease in 2-AG levels in the brain, whereas knockout of DAGLβ elicits a 50% decrease in 2-AG levels in the brain and 90% in the liver (Gao *et al.* 2010). 2-AG is mainly degraded by monoacylglycerol lipase (MAGL), yielding arachidonic acid and glycerol (Lichtman *et al.* 2010).

Although endocannabinoids are produced on demand and rapidly degraded, their concentrations in the brain have been shown to follow certain patterns, such as circadian rhythms (Vaughn *et al.* 2010). There are diurnal variations in the levels of AEA and 2-AG in different brain areas (nucleus accumbens, hippocampus, prefrontal cortex, striatum), as well as in FAAH, MAGL and DAGL activities (Valenti *et al.* 2004). However, the changes in MAGL and DAGL activity were only present in the striatum and not in the hippocampus, which indicates a different mechanism of the regulation of endocannabinoid levels depending on the brain region.

Several other endocannabinoids that do not bind to CB1 or CB2 receptors have been recently identified in the brain (so called non-classical or orphan endocannabinoids), like oleoylethanolamide (OEA) and palmithoylethanolamide (PEA) (O'Sullivan and Kendall 2010). OEA has been shown to bind to GPR 55, whereas PEA is a ligand of both GPR55 and GPR119 (Godlewski et al. 2009), which have been implicated as novel receptors of the endocannabinoid system(Brown 2007).

2.3 **The emerging role of the endocannabinoid system in brain aging**

Endocannabinoid system has been implicated in several age-related neurodegenerative diseases, such as Alzheimer's disease (Koppel and Davies 2008), Parkinson's and Huntington's disease (Bisogno and Di Marzo 2010). However, the direct evidence that the activity of the endocannabinoid system protects from the deleterious effects of normal brain aging has been provided using the mice lacking CB1 receptors (Bilkei-Gorzo et al. 2010; Bilkei-Gorzo et al.

2005). These mice showed age-dependent deficits in multiple behavioural paradigms (operant learning, skill learning on the rota rod, memory deficits in the partner recognition test – shown in Fig.2.3.1), as well as an age-related loss of pyramidal neurons in the hippocampus that accompanied the decline in cognitive performance (Bilkei-Gorzo *et al.* 2005); Fig.2.3.2. The reduction in neuronal density is first observed in the CA3 region of the hippocampus in young mice (6-8 weeks old). In mature mice, the number of neurons is also reduced in the CA1 region. These changes are further exacerbated in the old mice. The neuronal density is not changed in the CA2/CA3 region or the dentate gyrus (DG).

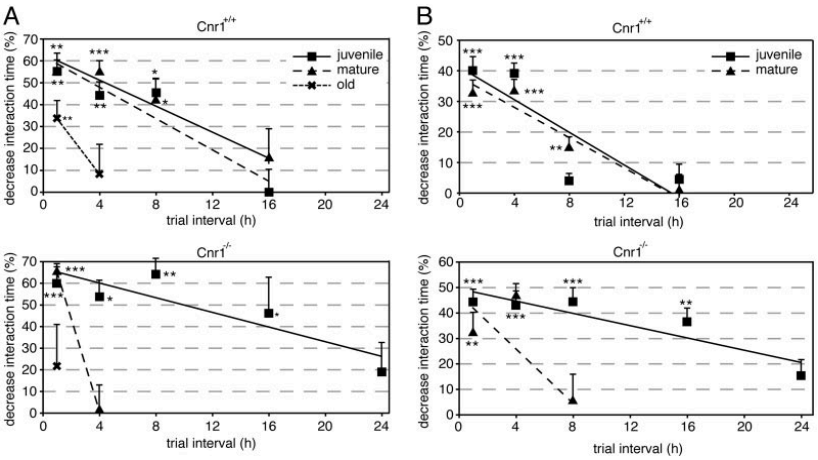

Fig.2.3.1. Performance of Cnr1$^{-/-}$ mice (vs. Cnr1$^{+/+}$) in the partner recognition test (from: Bilkei-Gorzo, 2005); A – mice on the C57BL6/J background; B – mice on the CD1 background. Trial interval (h) represents the time between the two presentations of the partner mouse.

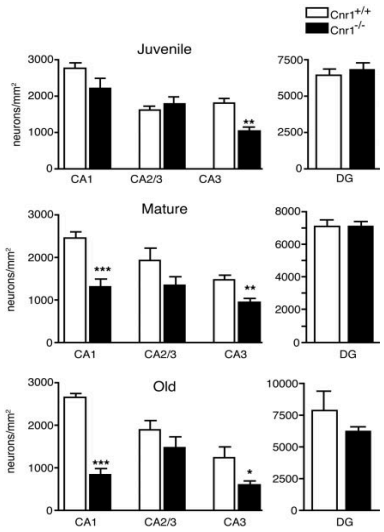

Fig.2.3.2. Neuronal density in different hippocampal regions in $Cnr1^{+/+}$ and $Cnr1^{-/-}$ mice of different ages (from: Bilkei-Gorzo, 2005).

Interestingly, this age-related phenotype seems to be specific for the brain and cognitive functions (Bilkei-Gorzo et al. 2012). We have demonstrated that CB1 knockout animals exhibit deficits in social memory (partner recognition) very early in their life (at the age of 3 months vs. 6 months in the case of WT). However, their sensory and motor functions were similar to the WT mice. Also, no signs of accelerated aging were found in the peripheral organs (except for the skin, which also showed an age-related phenotype in the CB1 knockout mice at 12 months of age).

Later, our group has shown that the degeneration of pyramidal neurons in the CB1 receptor knockout mice was accompanied by increased neuroinflammation as suggested by microglia activation and increased expression of a pro-inflammatory and aging-related cytokine IL-6 (Albayram et al. 2011). Interestingly, neuronal loss and changes in the inflammatory profile were restricted to the hippocampus – those changes were absent in the striatum, which is also known for high CB1 receptor density and in different cortical regions. The onset of microglial activation started at 12 months of age, whereas learning impairments and pyramidal cell loss preceded it (Albayram et al. 2011; Bilkei-Gorzo et al. 2010; Bilkei-Gorzo et al. 2005). Therefore, other reasons for the observed neuronal loss should exist.

There are several lines of evidence that the endocannabinoid system may play a role in the formation and clearance of oxidized macromolecules. Endocannabinoids are known to possess antioxidant-like properties (Mechoulam *et al.* 1998), for example, 2-AG is known to directly inhibit ROS formation *in vitro* (Gallily *et al.* 2000), which could explain the neuroprotective effect of endocannabinoid system activity (Kim *et al.* 2005). Some studies also show that cannabinoids regulate autophagy in human cancer cells – it has been demonstrated for glioma (Salazar et al. 2009), pancreatic adenocarcinoma (Donadelli *et al.* 2011), hepatocellular carcinoma (Vara et al. 2011). Therefore, it still remains to be shown if CB1 receptor activity can regulate autophagic processes in normal, non-transformed cells. If such a regulation takes plays, it could certainly also contribute to the neuroprotective role of CB1 receptors.

There is a growing body of evidence showing that the endocannabinoid system itself undergoes age-related changes. Earlier studies suggest an age-related decrease in CB1 receptor expression (Berrendero et al. 1998; Romero et al. 1998) and coupling in the forebrain. Some studies have also reported diminished anandamide levels during aging using CB1 knockout mice (Maccarrone et al. 2001; Maccarrone et al. 2002; Wang et al. 2003), while others found no significant differences in the endocannabinoid (EC) levels in aging in different brain regions (Wang et al. 2003). However, no data exists so far on the age-related changes in the endocannabinoid levels in the hippocampus. Also, the data available on the changes in activity and expression of the enzymes involved in the metabolism of EC are rather scarce: only changes in FAAH activity have been demonstrated so far (Maccarrone et al. 2001). One of the reasons for that is probably the complexity for the synthesis of AEA (Di Marzo 2011). However, it is easier to dissect the age-related changes in 2-AG metabolism, since there are only three main enzymes that are primarily responsible for the major part of it – DAGLα, DAGLβ and MAGL (mentioned in the previous section). Although there are some other enzymes involved in the metabolism of 2-AG (Di Marzo 2011), these three are responsible for approximately 80% of synthesis and degradation of 2-AG.

In conclusion, endocannabinoid system has emerged as a new pharmacological target in respect to age-related diseases and aging itself (Paradisi et al. 2006), however, mechanisms contributing to its protective effects, as well as the extent to which its activity changes with age have not been fully identified yet.

2.4 Aims of this work

The first aim of this work was to investigate the mechanisms contributing to the aging phenotype of the CB1 knockout mice. First, changes in neurogenesis and apoptotic markers in the $Cnr1^{-/-}$ mice of different ages were assessed to find out, if a decrease in neurogenesis and/or increase in apoptosis or cellular stress can account for the observed neuronal loss in the knockout strain with increasing age. Another possibility would be that the presence of CB1 receptors is essential for protection against age-related oxidative stress in the brain, therefore the levels of oxidative stress markers (lipid peroxidation, protein carbonylation, DNA oxidation) were investigated in the brains of CB1 receptor knockout mice in comparison to WT at different ages. There is evidence that CB1 receptor presence can affect lysosomal integrity, as well as autophagy (Gowran and Campbell 2008; Salazar et al. 2009; Vara et al. 2011). Thus, the lack of CB1 receptors may lead to an impairment of degradation of damaged macromolecules via autophagolysosomal pathway that would result in higher accumulation of cellular trash. Therefore, the lysosomal function and autophagy levels in the knockout mice were assessed.

The second aim of this work was to investigate the age-related changes in the endocannabinoid system itself, particularly the changes in the endocannabinoid levels, mainly 2-arachidonoylglycerol (2-AG) and the enzymes responsible for 2-AG metabolism. If the activity of the endocannabinoid system goes down with age, it can contribute to the onset and development of age-related diseases and represent an attractive therapeutic target for

pharmacological manipulation, as has been already suggested previously for some age-related conditions (Paradisi et al. 2006).

3. Materials and Methods

If not indicated differently, all applied chemicals are products from Invitrogen, Fluka, Sigma-Aldrich, Merck, Millipore, Roche and Carl Roth. All the ready-to-use buffers and transfer stacks for Western blots were bought from Invitrogen (as indicated in the text). TaqMan® gene expression assays were purchased from Applied Biosystems. For the endocannabinoid measurements, anandamide (AEA), 2-arachidonoylglycerol (2-AG), oleylethanolamide (OEA), palmitoylethanolamide (PEA), arachidonic acid (AA), and their deuterated analogues AEA-d_4, 2-AG-d_5, OEA-d_2, PEA-d_4, and AA-d_8 were obtained from Cayman Chemicals (Ann Arbor, Michigan, USA). Water (H_2O), acetonitrile (ACN), formic acid (FA), ethylacetate, and hexane (all of Fluka LC-MS grade) were obtained from Sigma-Aldrich (Munich, Germany).

3.1 **Equipment**

Autosampler	Linomat® 4, CAMAG, Berlin, Germany
	CTC HTC PAL autosampler, CTC Analytics AG, Zwingen, Switzerland
Analytical balance	BP 121 S, Sartorius
Bioanalyzer	Agilent 2100 bioanalyzer, Agilent Technologies
Blotting devices	iBlot® Dry Blotting Device, Invitrogen (Life Technologies)
	Mini-Cell XCell™ Blot Module, Invitrogen (Life Technologies)
CCD cameras	AxioCam MRm, Zeiss
	KY-F75U, JVC
Centrifuges	Biofuge fresco, Heraeus Instruments

	Biofuge pico, Heraeus Instruments
Cryostate	CM 3050 S, Leica
Film developing machine	CP 1000 AGFA Healthcare N.V.
Homogenisers	Precellys® 24, Bertin Technologies
	Ultra-Turrex®, IKA Werke, Staufen, Germany
	Ultrasound homogenizer, Bandelin Sonoplus, Berlin, Germany
	1 ml glass homogeniser, Wheaton, USA
HTPLC running chamber	CAMAG, Berlin, Germany
LC system	Agilent 1200 series, Agilent, Waldbronn, Germany
Mass spectrometer	5500 QTrap triple-quadrupole linear ion trap MS,
	AB SCIEX, Darmstadt
Magnetic stirrer	MR 3001 K, Heidolph, Fisher
Microscope	Axioplan 2, Zeiss
	Axioscope 40, Zeiss
PCR iCycler	iCycler, Bio-Rad Laboratories
pH meter	inoLab, WTW
Real-Time Cycler	7500 Real-Time PCR Detection System,
	Applied Biosystems
Scanner	Epson Perfection 4990, Epson

Spectrophotometers	MRX TCII, Dynex
	NanoDrop ND-1000, Thermo Scientific
	Ultrospec 2100 *pro*, GE Healthcare
Power Supply	PowerEase® 500, Invitrogen (Life Technologies)
TLC scanner 3	CAMAG, Berlin, Germany
Vortexer	Vortex-Genie 2, Scientific Industries
ZOOM® IPGRunner™ System	Invitrogen (Life Technologies)

3.2 **Software and databases**

Analyst	Version 1.5.1; AB SCIEX
AxioVision LE	Carl Zeiss, Germany
ImageJ	Wayne Rasband, NIH, USA Version 1.41o
Microsoft Office 2008	Microsoft Germany
Prism	GraphPad Software, Inc. Version 4 (2003)
Sequence Detection Software	Applied Biosystems, Version 2.2.2
Statistika	StatSoft, Inc. Version 6 (2001)
EndNote X1	The Thomson Corporation (2007)
PubMed MEDLINE	http://www.ncbi.nlm.nih.gov/pubmed

3.3 **Antibodies**

3.3.1 Primary Antibodies

Monoclonal anti-β-actin - Sigma, A 5441

Rat monoclonal (BU1/75 (ICR1)) anti-BrdU – Abcam, ab6326

Mouse monoclonal anti-Neuronal Nuclei (NeuN) (Alexa Fluor® 488 conjugated antibody) - Millipore, MAB377X

Rabbit monoclonal anti-human/mouse cleaved caspase 3 (Asp175) – R&D Systems, MAB835

Rabbit polyclonal anti-caspase 8 – Abcam, ab4052

Rabbit monoclonal (E23) anti-caspase 9 – Abcam, ab32539

Guinea pig polyclonal anti-p62/ SQSTM1 - Progen, Queensland, Australia

Goat polyclonal anti-cathepsin D antibody (C-20) – Santa Cruz Biotechnology, Inc., sc-6486

Mouse monoclonal anti-8-hydroxyguanosine – Abnova, MAB 1998

Rabbit polyclonal anti-LC3B – Sigma, L7543-200UL

Rabbit polyclonal anti-phospho-Akt (Ser473) – Cell Signaling, 9271 S

Rabbit polyclonal anti-Akt, non-phosphorylated – Cell Signaling, 9272 S

Rabbit polyclonal anti-phospho-mTOR - (Ser2448) – Cell Signaling, 2971 S

Rabbit polyclonal anti-mTOR – Abcam, ab2732

Monoclonal anti-α-tubulin – Sigma, T8203-200UL

3.3.2 Secondary Antibodies

Alexa Fluor® 594 goat anti-rabbit IgG - Life Technologies, A21207

Alexa Fluor® 647 donkey anti-rabbit IgG - Life Technologies, A3157

Peroxidase-conjugated donkey anti-goat IgG - Jackson IR, 705-035-003

Peroxidase-conjugated goat anti-guinea pig IgG – Abcam, ab102365

Peroxidase-conjugated goat anti-rabbit IgG - Jackson IR, 111-035-003

Peroxidase-conjugated goat anti-rabbit IgG – Thermo Scientific (Pierce), 32260

Peroxidase-conjugated rabbit anti-mouse – Sigma, A9044-2ML

3.4 **Kits**

Mouse On Mouse Blocking Kit – Vector Laboratories, BMK-2202

OxyBlot™ Protein Oxidation Detection Kit – Millipore, S7150

ProteoExtract Protein Precipitation Kit – Calbiochem, 539180

Pierce® BCA Protein Assay Kit – Thermo Scientific, 23225

RNA 6000 Nano LabChip® Kit – Agilent Technologies, 5067-1548

SuperScript First-Strand Synthesis System – Invitrogen (Life Technologies), 18080-051

3.5 **Animals**

Male and female WT ($Cnr1^{+/+}$) and cannabinoid receptor 1 (CB1) knockout ($Cnr1^{-/-}$) mice of different ages (2 months, 5 months, 12 months) were derived from a heterozygous $Cnr1^{+/-}$ breeding colony on a congenic C57BL/6J background maintained at the House of Experimental Therapy, University of Bonn. Mice received food and water *ad libitum*, were group-housed as single sex littermates and were kept on a reversed light-dark cycle (dark period between 9 am and 7 pm). Animal care and conduction of all experiments followed the guidelines of the 1998

German Animal Protection Law. Young (2-month-old) and old (15-month-old) C57BL6/J mice for the gene expression studies and endocannabinoid measurements, described in section 4.2 ("Age-related changes of the endocannabinoid system"; indicated accordingly in the text), were purchased from Charles River, France, and habituated to the above mentioned animal facility for 2 weeks before sacrifice (this period should be enough to lower the stress level caused by transportation and new environment).

3.6 Tissue preparation methods

3.6.1 Brain isolation and punch technique (isolation of brain areas)

For brain isolation in most experiments, the mice were anaesthesized with CO_2 and killed by decapitation. For endocannabinoid measurements, mice were sacrificed by cervical dislocation. Brains were then rapidly isolated and frozen in dry ice cooled isopentane and stored at - 80°C until assayed. In some cases, brain parts were punched out from freshly isolated brains (Palkovits 1983), but for most experiments brain areas were isolated at -20 °C from frozen specimen using the punch technique (Palkovits 1983). Punch technique allows precise isolation of small brain areas using visible landmarks on the brain slice. The areas were identified using the mouse brain atlas (Paxinos, 2001).

Prior to punching, brains were pre-equilibrated to the temperature within the cryostate for 1 hour. The sections were then sectioned into approximately 1 mm thick pieces using the brain matrix or per hand with a sharp cooled razor blade. Blunted stainless steel needles (10G, 12G and 17G, Harvard Apparatus) were then used to punch out the areas of interest resting on the metallic surface within the cryostate.

3.6.2 Transcardial perfusion

Mice were deeply anaesthesized with a mixture of ketamine and xylazine. The chest was opened and a catheter with a 25G needle was inserted into the left ventricle; the right atrium was cut open. The animals were then perfused with 20 ml cold phosphate-buffered saline (PBS) using a

pump and 50 ml syringes to wash the blood out, followed by 20 ml 4% parafolmadehyde (PFA) in PBS to allow fixation of brain tissue. After the perfusion, brains were isolated and kept in a 4% PFA solution for 24h at 4 °C. Subsequently, the brains were kept another 48-72h in a 10% sucrose solution and then frozen in dry ice cooled isopentane.

3.6.3 Preparation of frozen brain slices for histology

Brains were generally stored at -80°C until further processing. Brains were then embedded in Tissue-Tek O.C.T. Compound (Sakura Finetek, Zoeterwoude, Netherland) and cut into 16 μm sections using a cryostat (Leica CM 3050, Leica Microsystems) according to the mouse brain atlas (Paxinos, 2001). Alternatively, 40 μm free-floating sections were prepared to the analysis of neurogenesis (as described in the respective section).

3.7 Genotyping

The genotype of $Cnr1^{+/+}$ and $Cnr1^{-/-}$ mice was determined by PCR analysis of genomic DNA from the tails. Genotyping was performed with the help of A.Zimmer and K.Michel.

3.7.1 Sample preparation

Tail DNA (small tail pieces, maximum 0.2 cm long) was extracted using 75 μl of Alcalyc Lysis Reagent (25 mM NaOH, 0.2 mM dinatrium EDTA, pH 12) for 1 h in a PCR cycler at 95°C. The samples were then cooled down to 4°C, treated with 75 μl of Neutralization Reagent (40 mM TrisHCl, pH 5) were added to all samples and mixed by vortexing. 2 μl of the resulting product were used for the PCR.

3.7.2 Polimerase-chain reaction (PCR)

Custom primers were ordered at Life Technologies and had the following sequences (5' to 3'):

CB1 common – CTC CTG GCA CCT CTT TCT CAG TCA CG, CB1 knockout – TCT CTC GTG GGA TCA TTG, CB1 wildtype – TGT GTC TCC TGC TGG AAC.

For the PCR reaction, the extracted DNA (2 µl) was mixed with 10 µl of GoTaq Green Master Mix (Promega, Madison, WI, USA), primers (knockout, wildtype, common, diluted to 10mM; 1 µl of each), 0.3 µl of 50 mM $MgCl_2$ and filled with H_2O to 20 µl total. PCR reaction was performed in a PCR cycler (BioRad) using the following programm: 2 minutes at 95°C (1x time; denaturation step), 30s at 95°C followed by 30s at 65°C and 60s at 72°C (30x times; amplification), 5 minutes at 72°C (1x time; inactivation), 4°C (hold temperature).

3.7.3 Detection of PCR products: agarose gel electrophoresis and gel staining with ethidium bromide

After the PCR, samples were separated on a 1% agarose gel in TAE buffer (40 mM Tris-Acetate, EDTA, pH 8) for approximetely 1h at 120V and 400 mA using a 100 base pairs (bp) ladder in a gel-loading buffer (6x buffer containing 30% glycerol, 0.25% bromophenol blue and 0.25% Orange G dye) as a reference. The gels were then submerged in an ethidium bromide solution, and the bands were visualized using ChemiDoc system (BioRad Laboratories).

3.8 Oxidative stress determination: colorimetric assays and 2D-Western blots

3.8.1 Lipid peroxidation assay

Lipid peroxidation was assessed by measuring the presence of thiobarbituric acid reactive substances (TBARS) in different brain parts (hippocampus, amygdala, cortex, striatum, cerebellum) of Cnr1+/+ and Cnr1-/- mice as described previously (Bruce and Baudry 1995). The probes were homogenized in 50 mM phosphate buffer pH 7.4 (PBS) in the presence of deferoxamine. Equal volumes of homogenates were added to an aqueous solution containing acetic acid and thiobarbituric acid. An aliquot was also taken for protein content determination.

After heating this mixture to 95°C for 1 h a 1-butanol/pyridine solution was added, and TBARS were extracted into the organic layer by centrifugation at 4000 g for 10 min. The amounts of TBARS were determined by spectrophotometry at 532 nm on an Ultrospec 2100 *pro* UV/visible spectrophotometer (GE Healthcare, Freiburg, Germany) and calculated as nmol malondialdehyde equivalent per μg of protein according to a standard curve prepared from malonaldehyde bis-dimethyl acetal.

3.8.2 Protein carbonylation assay

Protein carbonyl content, as an index of protein oxidation, was measured as described in the literature (Dubey et al. 1996; Levine 2002; Levine et al. 1994; Reznick and Packer 1994). Briefly, tissue samples (hippocampus, amygdala, cortex, cerebellum) were homogenized in PBS in the presence of protease inhibitors and centrifuged at 11000 g for 15 min to sediment insoluble materials. The resulting supernatants were used for the reaction with 2,4-dinitrophenylhydrazine (DNPH) and protein content determination. For each sample, the supernatants were divided into two equal volumes – test probe (with DNPH) and blank (without DNPH). Samples were then incubated for 1 h at room temperature in the dark with continuous stirring and precipitated with equal volumes of 20% trichloroacetic acid (TCA) for 10 min on ice, centrifuged at 3000 g for 5 min, and supernatants were discarded. Protein pellets were washed in ethanol/ethyl acetate (1:1) mixture for three times to remove free DNPH and additional lipid contaminants. Final protein precipitates were dissolved in 6 M guanidine hydrochloride solution. The carbonyl content of both test and control samples was determined by spectrophotometry at 370 nm using molar extinction coefficient and expressed as nmol carbonyl per mg of soluble extracted protein.

3.8.3 Derivatization of protein carbonyls for 2D-Western blotting

Differential protein carbonylation (higher damage to specific proteins) by 2D-gel electrophoresis followed by immunoblotting against 2,4-DNPH was shown previously in AD (Aksenov et al. 2001); see Fig.3.8.3.

To determine if some proteins are more affected by oxidative stress than others, 2D-gel electrophoresis followed by Western blotting analysis of protein carbonyls using an antibody to 2,4-DNPH was performed. First, a similar procedure as in 3.8.2 was established: the protein carbonylation assay was carried out normally, but the final protein precipitates then were processed as described in 3.11.2. However, it often produces an altered spot pattern (Reinheckel *et al.* 2000) because the DNPH-procedure can alter the isoelectric point of proteins and affect their migration in the first dimension of the 2D-PAGE (Conrad *et al.* 2001; Hawkins *et al.* 2009). That is why the procedure was modified, and the incubation with DNPH was then performed after the first dimension: IPG-strips were incubated with 10 mM DNPH in 2.5 M HCl (or 2.5 HCl to serve as negative control for the specificity of the primary antibody) for 15 minutes as described (Hawkins et al. 2009; Reinheckel et al. 2000). Then the strips were processed as described in 3.11.2.

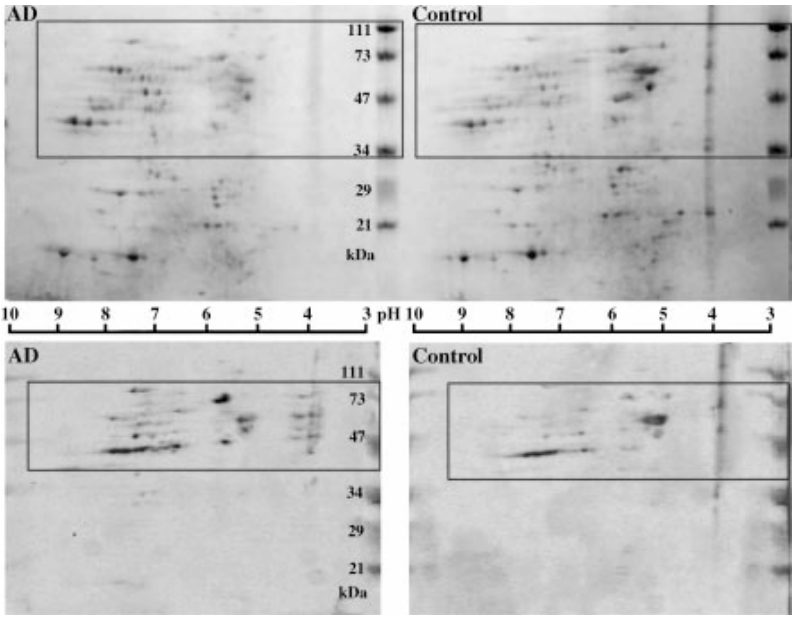

Fig.3.8.3. Two-dimensional gels (top) and Western blots (bottom) showing carbonylated proteins detected in AD patients and controls. Example from Aksenov et al, 2001.

3.9 Protein isolation

3.9.1 Protein isolation from frozen brain tissue

Frozen tissue specimen were briefly (for 30 s) sonicated in 1% SDS buffer (Sigma) or in RIPA buffer (150 mM NaCl; 10 mM Tris-HCl; pH 7.2; 0.1% Triton X-100; 1% sodium deoxycholate; 5 mM EDTA; Sigma) containing protease and phosphatase inhibitors (Complete Mini, Roche; PhosStop, Roche). Lysates were then clarified by centrifugation (13000 rpm for 10 minutes) to remove cell debris, and supernatants were transferred to fresh tubes. In some cases (e.g., prior to 2D-PAGE), protein precipitation and purufication was performed using ProteoExtract Protein Precipitation Kit (Calbiochem) as described by the manufacturer.

3.9.2 Protein isolation by TRIzol® protocol

After the separation of the aqueous phase (described in 3.14.1), the organic phase can be used for DNA and protein isolation. For this purpose, 240 μl of 100% ethanol was added to the tube; it was then reversed several times, allowed to sit at room temperature for 3 minutes and centrifuged for 5 minutes at 6000 rpm and 4 ^{o}C. The supernatant containing the proteins was then transferred to a fresh tube. 1ml of isopropyl alcohol was added to the supernatant, mixed and allowed to sit for 10 minutes at room temperature. The tube was then centrifuged at 11400 rpm and 4 ^{o}C for 10 minutes. The resulting supernatant was removed, and the protein pellet was washed for 3 times with 1 ml of 0.3 M guanidine hydrochloride in 95% ethanol and 1 time with 100% ethanol for 20 minutes followed by a centrifugation step (11400 rpm, 4^{o}C, 5 minutes). The pellet was then dried for approximately 30 minutes on the bench, until the alcohol evaporated

(it is important not to over-dry the pellet at this step). Then the pellet was dissolved in 1% SDS solution (containing protease inhibitors) first by using the tissue homogeniser (IKA® Werke, Germany), then for 1 hour at 50°C while shaking vigorously. The tubes were then centrifuged for 10 minutes at room temperature at 13000 rpm, and the resulting supernatant containing the isolated proteins was transferred to a new tube.

3.10 Protein content determination

Protein content was determined using a commercially available bicinchoninic acid (BCA) assay kit from Pierce (Thermo Scientific, Rockford, IL) using the microplate procedure described in the instructions to the kit. The absorbance was measured at 570 nm on a Revelation Microtiter Plate Reader (Dynex Technologies MRX-TC). Protein concentration was calculated from the optical density values according to the standard curve of bovine serum albumine.

3.11 Gel electrophoresis

All solutions, ready-to-use gels and transfer stacks for the iBlot® transfer system were purchased from Invitrogen, Life Technologies.

3.11.1 1D-gel electrophoresis (SDS-PAGE)

Sodium dodecyl sulfate polyacrylamide gel electrophoresis, or SDS-PAGE, is a widely used method to separate proteins according to their mobility in the electric field. Prior to SDS-PAGE, sample preparation was carried out as following (reduced samples; calculation example for the total loading volume of 10 µl):

- Sample - **x** µl (all samples have to contain the same amount of total protein!)
- LDS Sample Buffer 4x – 2.5 µl
- Sample Reducing Agent 10x – 1 µl
- Deionized water – up to 6.5 µl

The samples were then heated at 70°C for 10 minutes, cooled down on water ice and loaded onto pre-cast NuPAGE® Bis-Tris 4-12% gradient mini-gels (supplied by Life Technologies). Novex® Sharp Protein Stndard (Life Technologies, LC5800) was run on the same gel to visualize the protein molecular weight ranges. Gels were run using SureLock® Mini-Cell gel running system from Life Technologies in NuPAGE® MOPS or MES SDS running buffer for approximately 35-40 minutes (in MES buffer) or 50 minutes (in MOPS buffer) at 200V (constant), maximum current – 125 mA per gel.

3.11.2 2D-PAGE

5-10 µl of the protein homogenate (containing not more than 50 µg total protein; protein amount has to be the same for the samples to compare) was mixed with 155 µl rehydration buffer (Life Technologies), and the resulting mixture was loaded onto ZOOM® IPG Strips pH 3-10 (non-linear), and they were left to rehydrate over night . The next day, isoelectric focusing (IEF) was performed using ZOOM® IPG Runner Cassettes with the following protocol: 200 V for 20 min, 450 V for 15 min, 500 V for 4h. Following the IEF procedure IPG-strips are incubated with 10 mM DNPH in 2.5 M HCl, as described in 3.8.3 and then equilibrated in 1x NuPAGE LDS Buffer with 10x Sample Reducing Agent (both from Life Technologies), for 15 minutes followed by another 15 minutes of alkylation in 1x NuPAGE® LDS Buffer with 232 mg iodocetamide. The strips were then placed onto 4-12% NuPAGE® Bis-Tris gels (Life Technologies), covered with 500 µl 0.5% agarose solution in 1x MES running buffer (Life Technologies), and the gels were run in the second dimension (SDS-PAGE) as described in 3.11.1. Immediately after the run, some

gels were used for Western blotting (general procedure described in 3.12) and stained using the OxyBlot™ kit (Millipore) as described by the manufacturer, and others were stained with Coomassie blue for 1 hour to ensure that equal amount of protein was added onto the gels. The gels were then washed in milliQ water overnight to eliminate the background, and spots marked with Coomassie were visible on the next day.

3.12 Western Blotting

Western blotting was performed immediately after running the gels using 2 alternative protocols: semi-dry transfer using XCell II™ Blot Module and dry blotting using iBlot® system (both supplied by Life Technologies). After it has been established, that the second procedure is equally or more efficient that the prior one, all Western blotting experiments were performed using the iBlot® system. In the following two subsections, both procedures are described.

3.12.1 Semi-dry blotting

Semi-dry blotting was performed using the XCell II™ Blot Module as described by the manufacturer, using NuPAGE® Transfer Buffer 20x (Invitrogen; diluted 1:20) with 10% methanol (for 1 gel), at 30V constant for 1h (start current: 170 mA, end current: 110 mA).

3.12.2 Dry blotting

Dry blotting was performed immediately after running the gels using the iBlot® Dry Blotting system from Life Technologies following the manufacturer's instructions (Program 3, 20V, 7 minutes run time) using disposable anode and cathode stacks.

3.12.3 Protein detection by antibodies

Immediately after the transfer, the membrane was submerged in 5% milk in TBS-T (TBS + 0,1% Tween 20; = blocking buffer) and incubated for 1h at room temperature on a shaker. The membrane was then briefly washed with TBS-T (washing buffer) and incubated with a primary antibody in 5% BSA/TBS-T at 4°C overnight on an orbital shaker. Following primary antibodies were used for Western blots: anti-ß-actin (1:10000, Sigma), anti-Akt (1:5000, Cell Signalling), anti-caspase 9 (1:1000; Abcam), anti-cathepsin D (1:1000; Santa Cruz), anti-mTOR (1:1000; Abcam), anti-phospho-Akt (Ser473, 1:1000, Cell Signalling), anti-phospho-mTOR Ser2448 (1:1000; Cell Signaling), anti-LC3 (1:500; Sigma), anti-p62/SQSTM1 antibody (1:500; Progen). On the next day, the membrane was washed with TBS-T 3 times for 5 minutes and incubated with an appropriate horseradish peroxidase (HRP)-conjugated secondary antibody in 5% BSA/TBS-T (dilution: 1:2500-12000) for 1h at room temperature. It was subsequently washed for 3 times, and protein detection was carried out using the ECL kit (Pierce). The method was introduced by Thorpe and Kricka in 1986 and allows chemiluminescent detection of immobilized proteins. The principle of the method is oxidation of the substrate, such as luminol, by horseradish peroxidase (HRP) in the presence of hydrogen peroxide (H_2O_2). As a result of the reaction, luminol is converted to a reaction product in an excited state which then decays back to the ground state by emitting light (chemiluminescence), which is enhanced by enhancers contained in the kit components. The membrane is incubated in the ECL solution for 1 minute and then sealed between 2 overhead transparencies and transferred to an autoradiography film development cassette. A high performance autoradiography film (Amersham Hyperfilm® MP, GE Healthcare, Buckinghamshire, UK) is then placed on top of the membrane in the dark room, and left in the cassette for a certain time interval (depending on the strength of the protein expression, time may vary from seconds to minutes). The film is then placed into the film developing machine (CP 1000 AGFA Healthcare N.V.). The developed film then can be stored and

further used to analyze the protein expression. For this purpose, blots were scanned using Epson Perfection 4990 scanner and analysed using ImageJ software.

The membrane can be either stored dry in a sealed plastic bag or used for the detection of different proteins, e.g. β-actin as loading control. To allow detection by different antibodies, the membrane has to be incubated in a „stripping buffer“ containing 0.2M glycine and 0.1% sodiumdodecyl sulfate (SDS), pH 2.2, to separate the primary and secondary antibodies from the proteins on the membrane.

3.13 Immunohistochemical stainings and microscopy

All the immunohistochemical stainings were conducted following standard procedures, described elsewhere.

3.13.1 Caspase 3, 8 and 9 staining

Sections were removed from the fridge and were allowed to dry for 30 minutes on a hot plate, followed by fixation in 4% paraformaldehyde in PBS for 30 min. Then the sections were washed in PBS, followed by a wash in milliQ water and in the case of caspase 3 staining additionally incubated with 10 mM $CuSO_4$ in 50 mM ammonium acetate buffer (pH 5.0) for 10 min to reduce lipofuscin-like autofluorescence. The sections were then subsequently washed in water, PBS and TBS for 5 minutes each wash, and permeabilized with 0,2% Triton-X100 in TBS. Antigene retrieval was performed using citrate buffer, pH 6, for 20 minutes in a microwave. Sections were then washed and blocked with 4% bovine serum albumine (BSA) for 1h, followed by an overnight incubation with primary antibodies against caspase 3 (1:250), caspase 8 (1:100) or caspase 9 (1:200). On the second day, sections were washed in TBS and incubated with a secondary Alexa fluor® 594 donkey anti-rabbit secondary antibody for caspase 3 and 9 (1:1000)

and Alexa fluor® 647 donkey anti-rabbit (1:250) for 2h at room temperature. The slices were then washed in TBS and water and covered in mounting medium (Vectashield, Vector Labs, containing 4',6-diamidino-2-phenylindole, DAPI, for counterstaining). At least 6 sections per mouse were used for the analysis.

3.13.2 8-hydroxyguanosine staining

Until the blocking step, sections were processed as described in the previous section. Sections were then washed and blocked with 10% donkey serum/TBS and then additionally blocked to prevent unspecific binding of primary antibody developed in mouse using Mouse On Mouse Blocking Kit (Vector Laboratories, Inc., Burlingame, CA), followed by incubation with the monoclonal mouse anti-8-hydroxyguanosine 1:1000 (Abnova GmbH Germany) overnight. Sections incubated with 10% donkey serum/TBS without primary antibody were used as negative controls and were provided on each slide. Additionally, we used RNase A treated samples, as controls for specificity of anti-8-hydroxyguanosine antibody for DNA as previously described (Strazielle *et al.* 2009). On the next day, sections were washed with TBS and then incubated with Alexa fluor® 647-coupled secondary antibody (Life Technologies, Carlsbad, CA). After the incubation, sections were washed and covered with Vectashield mounting medium for fluorescence (Vector Laboratories Inc., Burlingame, CA) containing 4',6-diamidino-2-phenylindole for counterstaining. Section images were acquired using an immunofluorescence microscope (Zeiss, Axioplan 2 imaging) connected to a digital camera (Zeiss) and a PC system with AxioVision imaging software. Images were analyzed using ImageJ software (National Institute of Mental Health, Bethesda, Maryland, USA). Data are presented as mean values of staining intensity per total area.

3.13.3 Quantification of lipofuscin autofluorescence

Lipofuscin accumulation in the pyramidal cells was measured as the presence of lipofuscin-like autofluorescence at 500-550 nm. Data are presented as mean values of fluorescence intensity measured in the whole CA3 region of the hippocampus.

3.13.4 BrdU labeling and cell counting

BrdU labeling and cell counted was carried out as described previously (Albayram et al. 2011). To label dividing cells, the mitotic marker 5-bromo-2'-deoxyuridine (BrdU; 50 mg/kg, Sigma) was dissolved in saline and administered intraperitoneally 4 times during 1 day with 2h intervals (proliferation protocol). The animals were sacrificed with CO_2 24h hours after the last injection and transcardially perfused with 4% paraformaldehyde in phosphate buffered saline to fix the brain tissue for further processing. The brains were then cryoprotected with 10% sucrose for 24h and frozen in isopentane. The brains were then embedded in Tissue Tek, and serial coronal free-floating sections (40 μm) were cut through the rostro-caudal axis of the hippocampus according to the mouse brain atlas (Paxinos and Franklin 2001); bregma -0,94mm - -3,340mm) using a cryostate and embedded in cryoprotection solution (Mineur et al., 2007) . Every 6th slide was used for one staining series, and 6 slices per hippocampus were used for quantification of BrdU labeled cells. Brain sections were stained with anti-BrdU rat IgG monoclonal antibody (1:500; Abcam) and Alexa fluor® 594-conjugated secondary antibody (goat anti-rabbit IgG; 1:500; Life Technologies). To better locate the labeled cells within the hippocampus and visualize the hippocampal regions, the sections were also stained with a mouse monoclonal antibody against NeuN (Alexa fluor® 488-conjugated; 1:250; Life Technologies). Since we used a proliferation protocol, no colocolization of BrdU with NeuN staining was expected; this was confirmed using a confocal microscope. The dentate gyrus area was determined with 10x objective (areas where the cells were quantified did not differ

significantly between the individuals, strains or or age groups), and BrdU-positive cells were counted in the subgranular zone of the dentate gyrus in 6 sections per hippocampus using 40x objective. The number of positive cells was then multiplied by the factor of 6, since every 6th section was used for the analysis.

3.14 Detection of mRNA expression

Real-time, quantitative polymerase chain reaction (qPCR) is usually used to determine gene expression in tissues. It has several advantages over some older techniques (like Northern blotting): small amounts of RNA are sufficient, and it is quite sensitive in comparison to Northern blots; it also provides quantitative information about the expression of certain genes of interest. In this work, the combination of real-time PCR with reverse trascription PCR was used to quantify mRNA expression. Differences in mRNA expression were determined using the following custom TaqMan® Gene Expression Assays (Applied Biosystems, Darmstadt, Germany): Mm00813830_m1 (DAGLα), Mm00523381_m1 (DAGLβ), Mm00449274_m1 (MAGL), Mm99999915_g1 (GAPDH), Mm00432621_s1 (CB1, Cnr1).

3.14.1 RNA isolation

Total RNA was extracted from brain tissue using the TRIzol® reagent (Life Technologies). TRIzol® reagent is a monophasic solution of phenol and isothiocyanate and is an improvement to the metod of Chomczynski (Chomczynski and Sacchi 1987). It maintains RNA integrity during lysis and homogenization and allows RNA isolation from small amounts of tissue. Tissue punches were kept on dry ice prior to RNA extraction and then transferred to 1.4 ml Precellys tubes with ceramic beads (peqLab, Erlangen, Germany), and 800 µl TRIzol® was pipetted into the tubes. The tubes were transferred to the Precellys centrifuge, where they were homogenized

3 times and kept 5 minutes on ice in between. The samples were then centrifuged at 11400 rpm for 10 min at 4°C, and the supernatant was transferred to a new 1.5 ml Eppendorf tube. Then 160 µl 1-bromo-3-chloropropane was added to it to separate the solution into an aqueous (containing RNA) and an organic phase (Note: 1-bromo-3-chloropropane is less toxic than chloroform which is usually used for the procedure and decreases the possibility of DNA contamination, as suggested by the manufacturer, Sigma-Aldrich). The tubes were vortexed for 30s, allowed to sit 3 minutes at room temperature and centrifuged at 11400 rpm for 10 minutes at 4°C. The resulting upper phase containing RNA was transferred to a fresh tube, and 400 µl isopropyl alcohol was added to it to precipitate RNA. The tubes were vortexed and allowed to sit for 10 minutes at room temperature, then centrifued at 11400 rpm for 10 min at 4°C. The resulting pellet contained the precipitated RNA. Supernatants were removed, and the pellet was washed with 1 ml 75% ethanol for 3 times, always followed by a centrifugation step (114000 rpm, 5 minutes, 4°C). The RNA pellet was then dried for 5-10 minutes at 50°C and then dissolved in 20 µl RNAse-free water (Qiagen, Germany) for 10 minutes at room temperature and subsequently for 5 minutes at 55°C. RNA concentration (ng/ml) was determined spectrophotometrically using NanoDrop 1000. In some experiments using older RNA, RNA quality was additionally analyzed with the Agilent 2100 bioanalyzer. The integrity of RNA was determined using the RNA 6000 Nano LabChip® Kit according to the instructions provided by the manufacturer. For the analysis, 1 µl RNA was loaded onto the chip. RNA samples were separated via electrophoresis on a microchip and subsequently detected with laser-induced fluorescence.

3.14.2 cDNA synthesis

RNA was transcribed to cDNA using the SuperScript First-Strand Synthesis System for RT-PCR Kit (Life Technologies, Carlsbad, CA, USA). Prior to cDNA synthesis, total RNA was diluted with RNAse-free or DEPC-treated water so that all samples had the same RNA concentration (total

volume: 10 µl). Then 1 µl of Oligo-dT was added to the samples, and they were incubated for 10 min at 70°C and then 3 min at 4°C in a PCR cycler machine (Biorad). 8 µl of master mix, containing 5x First Strand Buffer (5 µl per sample), 0,1M DTT (2 µl per sample) and 10 mM dNTP's (1 µl per sample) was subsequently pipetted into each tube, and the resulting probes were incubated at 42°C for 2 min and at 4°C in a PCR cycler, after which 1 µl of Reverse Transcriptase (RT) was given to each sample. The probes were then incubated at 42°C for 1h, followed by 15 min at 70°C (inactivation stage) and at least 10 min at 4°C. The resulting cDNA was again diluted with an appropriate amount of DEPC water. 40ng (9 µl) cDNA was used for each TaqMan reaction (per well). Samples to which RT had not been added were used as a control for genomic DNA contamination. Samples containing only DEPC water were used as a control for eventual contaminations.

3.14.3 Quantitative polimerase chain reaction (qPCR)

Differences in mRNA expression were determined by custom TaqMan® Gene Expression Assays (Applied Biosystems, Darmstadt, Germany) with 3-phosphate dehydrogenase (GAPDH) as a control to standardize the amount of target cDNA as described previously (Albayram et al. 2011). Samples were processed in a 7500 Real-Time PCR Detection System (Applied Biosystems, Darmstadt, Germany), and further analysis was performed using the 7500 Sequence Detection Software version 2.2.2 (Applied Biosystems, Darmstadt, Germany). Relative quantitative gene expression was calculated with the $2^{-\Delta\Delta C_t}$ method (Livak and Schmittgen 2001).

3.15 Ceramide measurements

3.15.1 Sample preparation

Before the lipid extraction and ceramide measurement which was performed at the Life & Medical Sciences Insitute (LIMES) institute, the samples were prepared using the following steps. First, the wet weight of each sample was determined. Then the sample was suspended in 1.6 ml of milliQ water with a glass homogenizer (Wheaton, Wheaton Millville, New Jersey, USA) on ice. 100 µl volume of the homogenized sample was used to determine the protein concentration by the BCA assay (as described above). The homogenized suspension was kept at -20°C until further analysis.

3.15.2 Lipid extraction, densitometric quantification and mass spectrometric profiling

Lipid extraction and further analysis of ceramide levels and ceramide species' profiling was carried out in the laboratory of Professor Konrad Sandhoff from the Life & Medical Sciences Insitute, University of Bonn, by Hany Farwanah, PhD.

To ensure maximal lipid yield, sequential extractions starting with chloroform/methanol/water (1:2:0.8; v/v/v) followed by chloroform/methanol (1:1; v/v), and ending with chloroform/methanol (2:1, v/v) were performed. The extraction steps were carried out over night at 40°C in a water bath. Afterwards, the extracts were pooled, and the solvents were evaporated under a stream of nitrogen. Further processing was performed as described previously elsewhere (Farwanah et al. 2009). However, no alkaline hydrolysis was conducted.

For quantification purposes, lipid extracts were initially applied onto silica HPTLC (Merck, Darmstadt, Germany) plates using Linomat® 4 (CAMAG, Berlin, Germany). The lipids were then separated by developing the plates twice in a horizontal chamber (CAMAG, Berlin, Germany) using a solvent mixture consisting of chloroform, methanol and acetic acid (190:10:1; v/v/v). The separated bands were visualized by dipping the plates into a solution of 10% $CuSO_4$ and 8% H_3PO_4 (w/v) and subsequently heating them on a TLC plate heater (CAMAG, Berlin, Germany) at 180°C for 15 min. The quantification was performed densitometrically using a TLC scanner 3

(CAMAG, Berlin, Germay) by relating the detected intensities to a previously comprised standard curve (Farwanah et al. 2009).

The profiling of the ceramide species was carried out using an LC/ESI-QTOF-MS method as described previously elsewhere (Farwanah et al. 2011).

3.16 Endocannabinoid measurements

All the endocannabinoid measurements were carried out at the lab of Professor B.Lutz at the Institute of Physiological Chemistry, University of Mainz, by R.Buchalla, PhD, with the technical support of C.Schwitter and R.Lerner.

3.16.1 Sample preparation

Hippocampus samples were stored at -80°C until analysis. Samples were weighed in the extraction tubes, spiked with 50 µl acetonitrile (ACN) containing internal standards, homogenized in 500 µl ice-cold 0.1 M formic acid using Precellys 24 (Bertin Technologies, Montigny-le-Bretonneux, France) and extracted with ethylacetate/hexane (9:1, v/v). The tubes were vortexed for 10 seconds, and centrifuged for 10 min at 8000 g and 4°C. The upper (organic) phase was removed, evaporated to dryness under a gentle stream of nitrogen at 37°C, re-dissolved in 500 µl ACN (all chemicals were from Fluka LC-MS grade) and analyzed by LC-MS/MS.

3.16.2 Chromatographic conditions

ECs were separated with a Phenomenex Luna 2.5 µm C18(2)-HST column, 100 mm x 2 mm, combined with a SecurityGuard pre-column (C18, 4 mm x 2 mm; Phenomenex, Aschaffenburg,

Germany) with solvents A: 0.1% FA in 20:80 ACN/water (v/v), and B: 0.1% FA in ACN, using the following gradient: 55-90% B (0-2 min), then held at 90% B (2-7.5 min), and re-equilibrated at 55% B (7.5-10 min). The column temperature was 25°C, the LC flow rate 0.3 ml/min, and the injection volume 10 µl.

3.16.3 Mass spectrometry detection

Positive and negative ions were analyzed simultaneously by combining two experiments in 'positive-negative-switching' mode. The Turbo V Ion Source was operated with the electrospray ('TurboIon') probe with nitrogen as curtain and nebulizer gas, and using the following settings: Temperature 550°C, curtain gas 40 psi, GS1 50 psi, GS2 50 psi, capillary voltage -4500 V (negative) and +4800 V (positive). The following precursor-to-product ion transitions were used for multiple-reaction monitoring (MRM): Experiment 1 (positive): AEA m/z 348.3 -> 62.1, AEA-d_4 m/z 352.3 -> 66.1, 2-AG m/z 379.1 -> 287.2, 2-AG-d_5 m/z 384.2 -> 287.2, OEA m/z 326.2 -> 62.1, OEA-d_2 m/z 328.2 -> 62.1, PEA m/z 300.2 -> 62.1, PEA-d_4 m/z 304.2 -> 62.1; Experiment 2 (negative): AA m/z 303.1 -> 259.1, AA-d_8 311.0 -> 267.0. Dwell times were 20 msec in Exp. 1, and 50 msec in Exp. 2, pause between MRM transitions was 5 msec, and settling time between Experiments 1 and 2 was 50 msec.

3.17 Image and statistical analysis

Statistical analysis was performed using GraphPad Prizm (Version 4.0) and *Statistica 6.0* software. Age- and genotype-related changes were analysed using two way ANOVA followed by Bonferroni's *post hoc* test. In cases where the influence of only one factor on the data was analyzed, one way ANOVA (in case of multiple groups) or Student's unpaired t-test (two groups)

were used (as indicated in the text). Correlation was assessed using Pearson's correlation coefficient (r).

4. Results

4.1 Mechanisms contributing to the aging phenotype of the CB1 knockout mice

In this section, the results of the studies investigating the influence of CB1 receptor presence on age-related changes in neurogenesis, apoptosis, oxidative stress, lysosomal function and autophagy are presented.

4.1.1 Age-related changes in the rate of neurogenesis in the dentate gyrus of the hippocampus of WT ($Cnr1^{+/+}$) and CB1 receptor knockout ($Cnr1^{-/-}$) mice

It has been previously shown that young $Cnr1^{-/-}$ animals exibit lower levels of neurogenesis compared to WT mice (Aguado et al. 2005; Aguado et al. 2007; Jin et al. 2004). In our group we observed that these mice have lower neuronal numbers in the CA3 region in the hippocampus already at 2 months of age (Bilkei-Gorzo et al. 2005), which could be a result of decreased neurogenesis. However, the neuronal loss was also present in the CA1 region in older mice and was further exacerbated in the CA3 region with increasing age (Bilkei-Gorzo et al. 2005). In the first part of the present work, the influence of neurogenesis on this decrease in neuronal numbers was investigated. It is known that neurogenesis is generally affected by aging (Villeda et al. 2011), and activating CB1 receptor signaling by using exogenous CB1 receptor agonists can partially restore it to normal levels in aged animals (Marchalant et al. 2009a; Marchalant et al. 2009b). To test the possibility that neurogenesis further decreased in aging in the knockout mice in comparison to their WT littermates, we compared the rate of neurogenesis between $Cnr1^{+/+}$ and $Cnr1^{-/-}$ mice at 2, 5 and 12-months of groups by quantifying BrdU-labeled neurons in the

dentate gyrus 24 hours after BrdU treatment (Albayram et al. 2011). The results presented in this section have been published as indicated and are partially reproduced from this publication (Albayram et al. 2011).

We used a staining against BrdU (see method section 3.13 for details) on free-floating sections to compare the rate of proliferation between the WT and the knockout mice and quantified the labeled cells in the whole dentate gyrus (DG) region. Fig. 4.1.1.1 shows a representative microphotograph of the DG region with BrdU-labeled proliferating cells (WT mouse, 2 months of age).

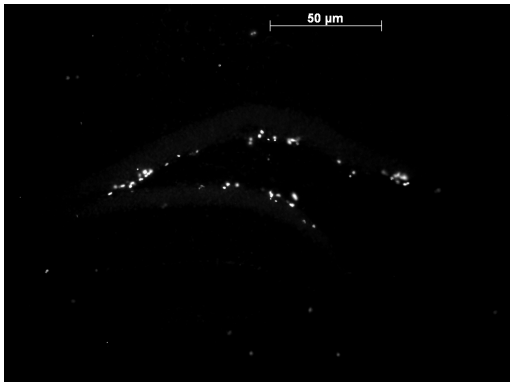

Fig.4.1.1.1. Respresentative photomicrograph of the proliferating cells labeled with BrdU in the whole dentate gyrus region of a young WT mouse. Scale bar: 50 µm.

We also used a NeuN-positive staining to better visualize the hippocampal region (see Fig. 4.1.1.2).

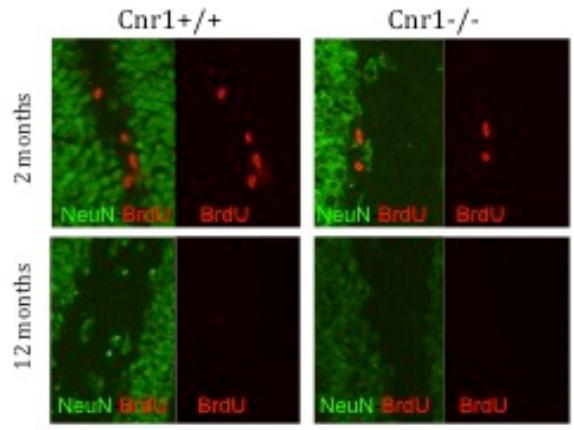

Fig.4.1.1.2. Representative confocal microphotographs showing proliferating cells labeled with BrdU (in red in the dentate gyrus of the hippocampus of a young (2 months old) and an old (12 months old) WT ($Cnr1^{+/+}$) and CB1 knockout ($Cnr1^{-/-}$) mouse. Mature neurons were labeled with an antibody against the neuron-specific protein NeuN (in green). From: Albayram et al, 2011.

A 48% reduction in the numbers of BrdU-labeled cells was found in the knockout strain at the age of 2 months in comparison to WT (Fig.4.1.1.3; $p<0.05$ in Bonferroni's post hoc test). There was a general effect of age on the amount of proliferating cells (age effect: $F_{2,22} = 26.44$, $p<0.001$), as well as a significant effect of interaction age x genotype ($F_{2,22} = 3.598$, $p<0.05$). However, the difference between the strains was present only in the young mice and seemed to disappear with increasing age: 5- and 12-month-old WT mice showed a low level of neurogenesis, similar to the knockout mice.

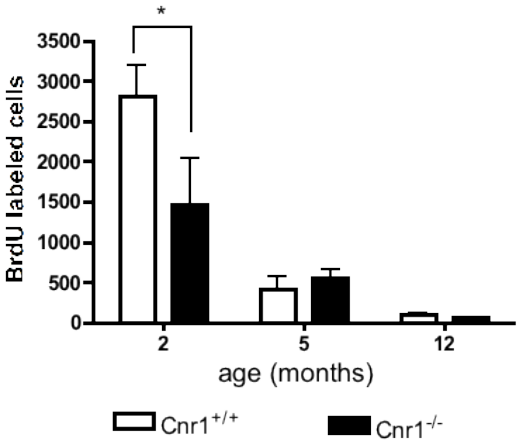

Fig.4.1.1.3. Quantification of BrdU-labeled, proliferating cells in the dentate gyrus of the hippocampus of WT and CB1 knockout mice of different ages (n=6). Data were analysed by two way ANOVA. The star (*) indicates $p<0.05$ in Bonferroni's post hoc test.

Thus, it can be excluded that the difference in neurogenesis plays a decisive role in the age-dependent decrease in neuronal numbers in the CB1 receptor knockout mice.

4.1.2 Age-related changes in pro-apoptotic markers in the CB1 receptor knockout mice

It has been shown previously that CB1 knockout mice are more sensitive to induced neuroinflammation and show elevated caspase 3 levels (e.g., in multiple sclerosis models) (Jackson et al. 2005; Pryce et al. 2003). Aging is generally is associated with increased neuroinflammation and it has been shown in our group that CB1 knockout mice have increased levels of pro-inflammatory cytokine IL6 in the hippocampus, along with higher numbers of activated, Iba1-positive microglia cells (Albayram et al. 2011). Therefore, there is a possibility that increased caspase 3 activation can contribute to the aging phenotype of CB1 knockout mice, particularly to the neuronal loss in the hippocampus. Caspase 3 expression in the hippocampus was evaluated by an immunohistochemical staining with an antibody specific to the activated form of caspase 3. Furthermore, the possibility of caspase 3 regulation through different mechanisms was evaluated: activation via caspase 9 (mitochondrial pathway) and via caspase 8 (extracellular pathway, e.g. via the activation of TNF receptors).

4.1.2.1 *Caspase 3-positive staining in the hippocampus of WT and CB1 receptor knockout mice*

Caspase 3 staining in the brains of 2-, 5- and 12-month-old $Cnr1^{+/+}$ and $Cnr1^{-/-}$ mice was evaluated using the area fraction function of ImageJ software (% of total area covered by the signal). Prior to analysis, a threshold was selected to exclude non-specific signals. The results of the analysis are presented in Fig.5.1.2.1. Data were analysed by two way ANOVA (age effect: $F_{2,113} = 37.38$, $p<0.001$; genotype effect: $F_{1,113} = 6.056$, $p<0.05$; interaction age x genotype: $F_{2,113} = 2.725$, $p = 0.07$).

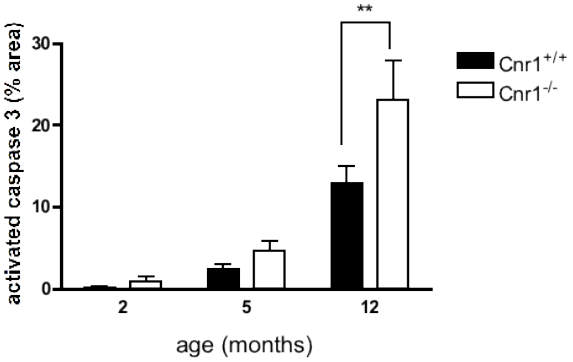

Fig.4.1.2.1. Levels of activated caspase 3 (presented as area fraction, %) in the CA3 region of the hippocampus of 2-,5- and 12-month-old $Cnr1^{+/+}$ and $Cnr1^{-/-}$ mice. ** indicate $p<0.01$ in Bonferroni's post hoc test).

As shown in Fig.4.1.2.1, it appears that old $Cnr1^{-/-}$ have significantly higher caspase 3 levels compared to their $Cnr1^{+/+}$ littermates ($p<0.01$ in Bonferroni's post hoc test).

4.1.2.2 *4.1.2.2. Age-related changes in caspase 8 and 9 expression in the hippocampus*

Caspase 3 activation can be achieved through two distinct pathways in the cell: via the mitochondrial pathway or the extracellular pathway. Therefore, activation markers for both pathways were studied. As an activation marker for the mitochondrial pathway, caspase 9

activation was assessed in the hippocampus of WT and CB1 knockout mice of different ages using a caspase 9-specific staining. The results are presented in Fig.4.1.2.2.1. Two way ANOVA revealed an age effect ($F_{2,90} = 41.81$, $p<0.001$) on caspase 9 levels in the hippocampus, and this effect was similar between the mice from both genotypes.

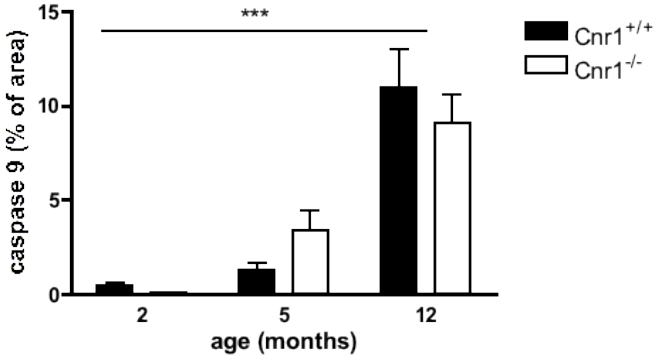

Fig.4.1.2.2.1. Caspase 9 levels in the hippocampus of WT and CB1 receptor knockout mice of different ages. (***p<0.001, age effect, two way ANOVA).

Since the antibody against caspase 9 is not specific to the activated form, a Western blot analysis was performed in order to confirm the results presented in Fig.4.1.2.2.1 for the 12-month-old mice, in which the elevation on caspase 3 levels (and the highest caspase 9 levels) was observed (n=5-6).

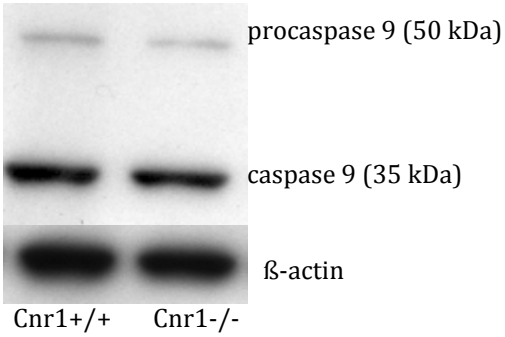

Fig.4.1.2.2.2. Representative Western blot from the hippocampus of 12-month-old WT and CB1 receptor knockout mice showing specific bands for procaspase 9 (50 kDa) and cleaved caspase 9 (approximately 35 kDa).

No difference in the amount of activated caspase 9 was observed between WT and CB1 knockout mice ($p>0.05$, unpaired t-test).

Furthermore, the levels of caspase 8 in the hippocampus were assessed using an immunohistochemical staining. The analysis results (represented as mean gray value) are shown in Fig.4.1.2.2.3. There was a genotype effect on the caspase 8 staining intensity ($F_{1,101} = 7.252$, $p<0.01$), which was most significant at 2 months of age ($p<0.01$ in Bonferroni's post hoc test). There was no significant effect of age on caspase 8 levels, although a tendency was observed (age effect: $F_{2,101} = 2.655$, $p=0.07$; interaction age x genotype: $F_{2,101} = 2.873$, $p=0.06$).

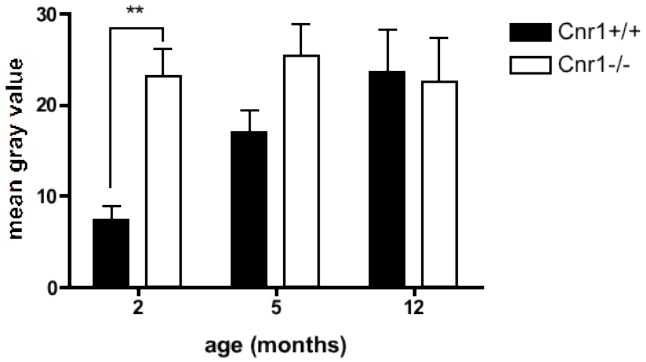

Fig.4.1.2.2.3. Caspase 8 levels in the hippocampus of WT and CB1 receptor knockout mice (n=3). **p<0.01 in Bonferroni's post hoc test.

4.1.3 Enhanced lipofuscin accumulation in the hippocampus of CB1 knockout mice

While performing the stainings described in section 4.1.2, an interesting effect could be observed: there was a strong fluorescence in the negative control samples in the absence of primary antibodies, and its intensity increased with age, being quite prominent in the knockout strain already at 5 months of age. Given the morphological, dot-like appearance (dots were more aggregate-like in the samples from older animals) and the spectral characteristics of this autofluorescence (maximum at 400-500 nm), as well as its age-related increase (it was practically absent in 2-month-old WT animals), we concluded that it indicates lipofuscin

accumulation in the hippocampus. Although in the old animals we could observe some lipofuscin-like dots in other brain regions, its accumulation was most prominent in the CA3 region of the hippocampus, where it has been quantified using unstained sections covered with Vectashield for fluorescence microscopy. Lipofuscin is a lipopigment consisting of aggregated products of lysosomal degradation, including oxidized and misfolded proteins, lipids, defective mitochondria etc. The studies presented in this section revealed an exacerbated age-related lipofuscin accumulation in the CA3 region of hippocampus in $Cnr1^{-/-}$ mice and were performed with the help of A.Bilkei-Gorzo, PhD, and K.Michel.

The intensity of lipofuscin autofluorescence in the CA3 area of the hippocampus, where it was most prominent, was compared between WT and $Cnr1^{-/-}$ mice at 2, 5 and 12-months of age. As a result of this analysis, a significant age-related increase in the intensity of lipofuscin autofluorescence (age effect: $F_{2,102}$ = 164.2 , $p<0.001$, two way ANOVA; Fig.4.1.3.1) could be shown. Accumulation of lipofuscin was significantly exacerbated in the $Cnr1^{-/-}$ mice compared to the age-matched wildtype mice (genotype effect: $F_{1,102}$ = 9.13, $p<0.01$). The difference between the strains was most prominent at 12 months of age (Bonferroni's post hoc test, $p<0.05$).

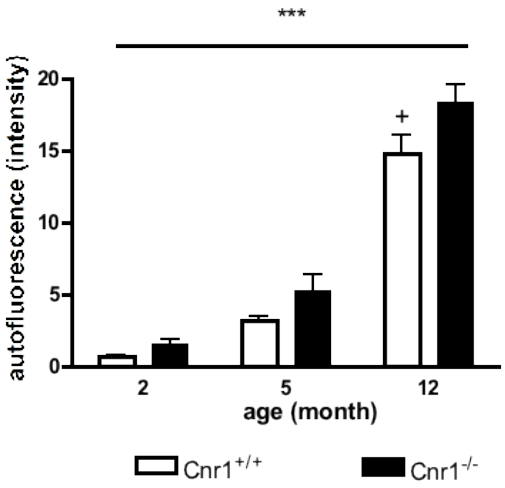

Fig.4.1.3.1. Quantitative analysis of lipofuscin-like autofluorescence in the hippocampus of WT ($Cnr1^{+/+}$) and CB1 receptor knockout ($Cnr1^{-/-}$) mice (n=3). Columns represent group mean values; error bars

represent standard error of mean (SEM). The cross (+) indicates significant difference between the groups according to Bonferroni *post hoc* test, p<0.05; ***p<0.001 (age effect, two way ANOVA).

A prominent example of lipofuscin-like fluoresence in the hippocampus in the absence of CB1 receptors is shown in Fig.4.1.3.1.

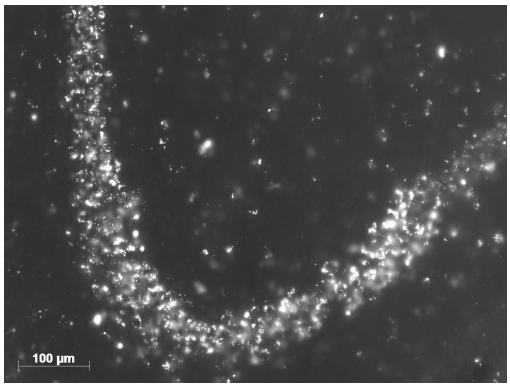

Fig.4.1.3.2. Representative image of lipofuscin-like autofluorescence in the hippocampus of a $Cnr1^{-/-}$ mouse at 12 months of age (CA3 region, unstained section).

The presence of lipofuscin in neurons was double-checked in the slices stained with an antibody against NeuN, which confirmed lipofuscin accumulation in neurons (data not shown).

4.1.4 Age-related changes in the oxidative stress markers in the brains of WT and CB1 receptor knockout mice

As shown in the previous section, an increased accumulation of lipofuscin was observed in the hippocampus of CB1 receptor knockout mice. Since oxidative stress is one of the main reasons that can cause lipofuscin accumulation (Brunk et al. 1992), the possibility that the oxidative damage is increased in the brain of the CB1 receptor knockout mice was investigated. Lipid peroxidation, protein carbonylation and oxidative damage to DNA were assessed as markers of age-related oxidative stress. Furthermore, as it was previously speculated that CB1 receptors are necessary for the protection against oxidative damage, we additionally assessed the

presence of oxidative stress markers (for lipid and protein oxidation) in different brain regions known to have a high CB1 receptor density (Herkenham et al. 1991a; Herkenham et al. 1991b; Herkenham et al. 1990; Mailleux and Vanderhaeghen 1992; Matsuda et al. 1993).

4.1.1.1 Lipid peroxidation

Lipid peroxidation was assessed by measuring the presence of thiobarbituric acid reactive substances (TBARS) in different brain parts (hippocampus, amygdala, cortex, striatum, cerebellum) of WT ($Cnr1^{+/+}$) and CB1 knockout ($Cnr1^{-/-}$) mice (see section 3.8.1) and expressed as malondialdehyde units per µg of protein. The results are shown in Fig.4.1.4.1. Surprisingly, no age-related increase in lipid peroxidation was observed in most of the regions studied, including striatum, cortex, hippocampus and cerebellum in both wildtype and knockout mice up to the age of 12-15 months (Fig.4.1.4.1 A, B, C, E). However, a significant age-related increase in lipid peroxidation was unexpectedly found in the amygdala (age effect: $F_{2,30} = 6.108$, $p<0.01$, two-way ANOVA; Fig.4.1.4.1 D). This effect was similar in both strains; a slight, albeit non-significant tendency towards higher peroxidation levels could be seen in the old $Cnr1^{-/-}$ mice.

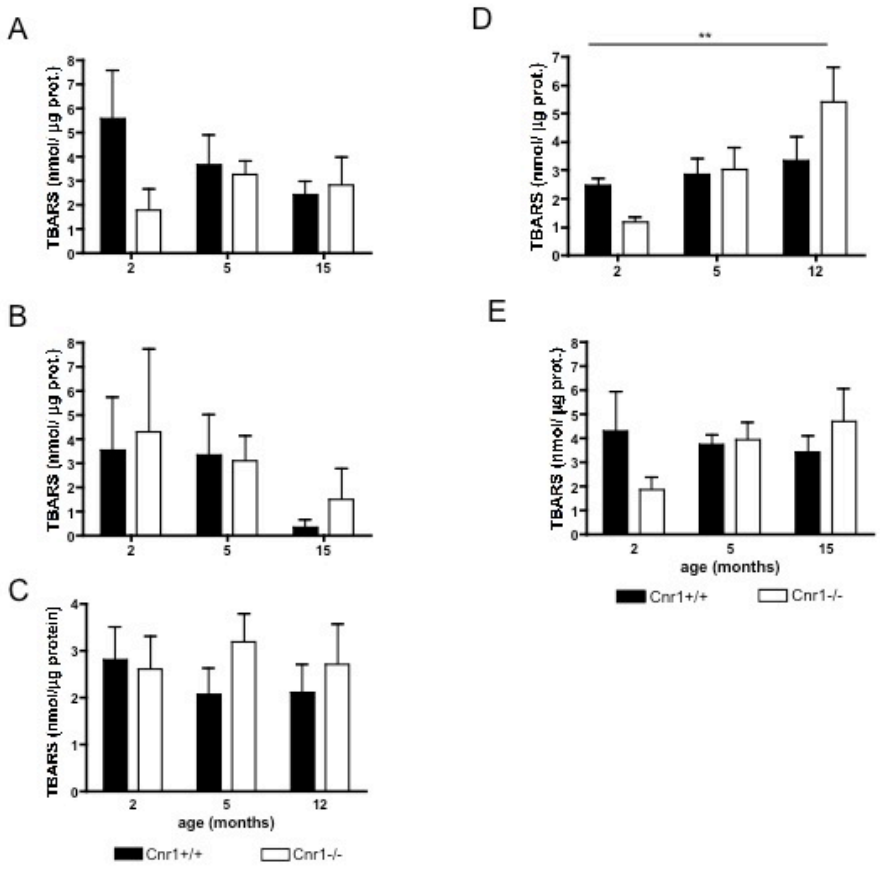

Fig.4.1.4.1. Peroxidized lipids (nmol per µg total protein) in different brain regions (A – striatum, B – cortex, C – hippocampus, D – amygdala, E – cerebellum) in young (2 months), mature (5 months) and old (12-15 months) $Cnr1^{+/+}$ and $Cnr1^{-/-}$ mice. Data were analyzed by two way ANOVA followed by Bonferroni's post hoc tests and respresented as mean value +/+ standard error of mean (SEM); $^{**}p<0.01$ (age effect, two way ANOVA).

Therefore, it is reasonable to conclude that there is no significant increase in lipid peroxidation in the $Cnr1^{-/-}$ mice. Also, no general increase in lipid peroxidation could be observed until the age of 12-15 months in most regions studied.

4.1.1.2 Protein carbonylation

Although no significant increase in the oxidative damage to lipids could be observed (4.1.4.1), one cannot exclude that other cellular macromolecules are affected by age-related oxidative

stress or oxidative stress presumably caused by CB1 receptor deletion. Therefore, protein oxidation was further assessed using an established oxidation marker, protein carbonylation (Hawkins et al. 2009). Proteins carbonyls were determined by the method of Levine using 2,4-DNPH as a marker (see section 3.8.2) by two independent assays: a colorimetric assay for determination of protein carbonyls and immunoblots using a specific antibody against 2,4-DNPH).

5.1.4.2.1. Detection of total protein carbonylation by a colorimetric assay

The amount of total protein carbonyls was determined in different brain regions in $Cnr1^{+/+}$ and $Cnr1^{-/-}$ from different age groups (2, 5 and 12 months of age). The results are presented in Fig.4.1.4.2.1. Like in the previous experiment, no increase in oxidative damage could be determined in cortex or cerebellum up to 12 months of age (Fig.4.1.4.2.1, C, D). However, a significant increase in the amount of protein carbonyls could be observed in the hippocampus (Fig.4.1.4.2.1, A; age effect: $F_{2,34} = 20.77$, ***$p<0.001$), as well as in the amygdala (Fig.4.1.4.2.1, B; age effect: $F_{2,32} = 15.78$, ***$p<0.001$). Interestingly, this increase was detected earlier in the amygdala, starting at 5 months, while in was evident in the hippocampus only at 12 months of age. No effect of genotype on protein carbonylation was observed ($p>0.05$).

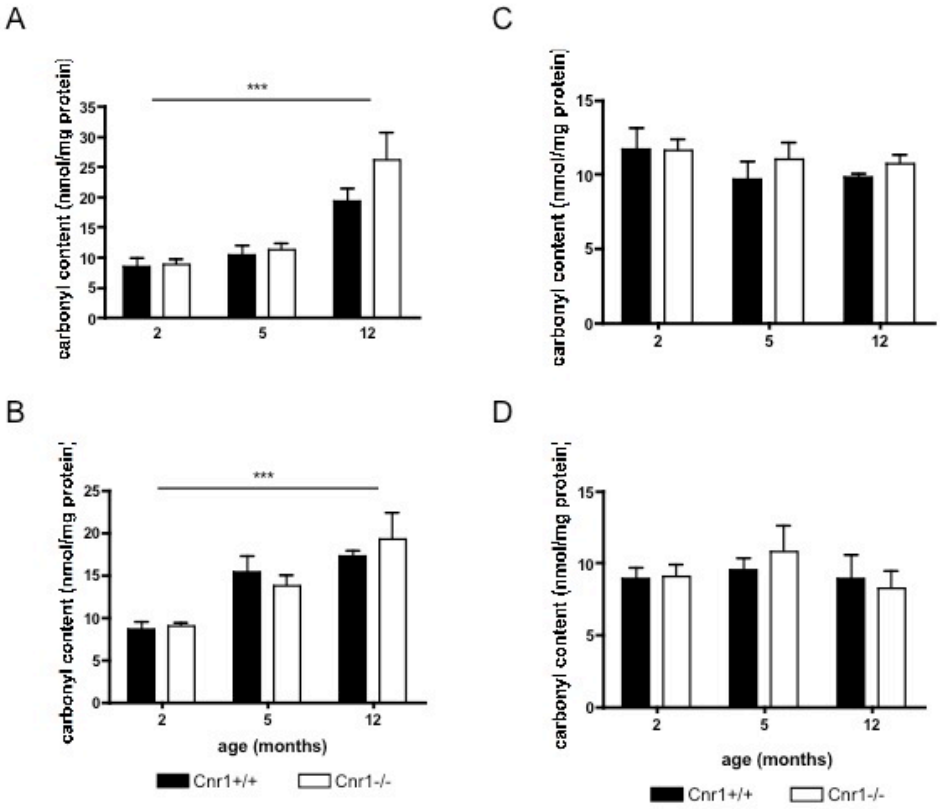

Fig.4.1.4.2.1 Carbonylated proteins (nmol per mg total protein) in different brain regions (A – hippocampus, B – amygdala, C – cortex, D – cerebellum) in young (2 months), mature (5 months) and old (12-15 months) $Cnr1^{+/+}$ and $Cnr1^{-/-}$ mice. Data were analyzed by two way ANOVA followed by Bonferroni's post hoc tests and represented as mean value +/+ standard error of mean (SEM); ***p<0.001 (age effect, two way ANOVA).

In conclusion, no significant increase in the total carbonyl content could be observed in the CB1 knockout mice compared to their WT littermates in any of the age groups studied.

4.1.4.2.2 Detection of carbonylation of individual proteins by 2D-PAGE followed by immunoblotting against 2,4-DNPH

Using two-dimensional Western blotting (separation of proteins with 2D-PAGE followed by immunoblotting) allows qualitative analysis of oxidized proteins (as opposed to colorimetric detection of *all* oxidized proteins in the tissue), which can be particularly important to identify proteins that are specifically modified in different conditions, for example, in aging or disease.

2D-Western blotting has been successfully applied to detect proteins differentially modified in the brain and cerebrospinal fluid of Alzheimer's disease patients (Aksenov et al. 2001; Castegna et al. 2002; Castegna et al. 2003; Korolainen et al. 2007), as well as in the brain of aging mice (Poon et al. 2004; Talent et al. 1998). Therefore, we sought to determine if there are differences in the patterns of oxidative damage (carbonylation) to individual proteins in the brains of WT ($Cnr1^{+/+}$) and CB1 receptor knockout ($Cnr1^{-/-}$) mice using a 2D-oxyblot method established in the course of the present work. We specifically concentrated on hippocampus and amygdala, since these were the only brain regions where we found an increase in the total amount of carbonylated proteins with increasing age (see previous section 4.1.4.2.1).

First, to prove that our method is sensitive enough to detect oxidatively modified (carbonylated) proteins, we used two samples from APP/PS1 transgenic mice (an established mouse model of AD; kindly provided by D.Terwel, PhD, from the laboratory of Professor M.Heneka, University Clinic, University of Bonn) as a positive control (Fig.4.1.4.2.2.1, right). It was possible to detect carbonylated proteins in the analyzed hippocampal sample (indicated by arrows). When compared to an oxyblot from an old WT mouse from our breeding colony (Fig.4.1.4.2.2.1, left), an altered spot pattern could be seen in the APP/PS1 transgenic mouse hippocampus without a massive increase in the number of carbonyl spots.

Fig.4.1.4.2.2.1. Presence of carbonylated proteins in the hippocampus of a WT (left) and an APP.PS1 mouse (right) at the age of 12 months. Arrows indicate oxidatively modified proteins.

The oxyblot technique was further used to compare the samples from the WT mice from different age groups (young, month-old and old, 12-month-old). The results from a representative experiment are shown in Fig.4.1.4.2.2.2.

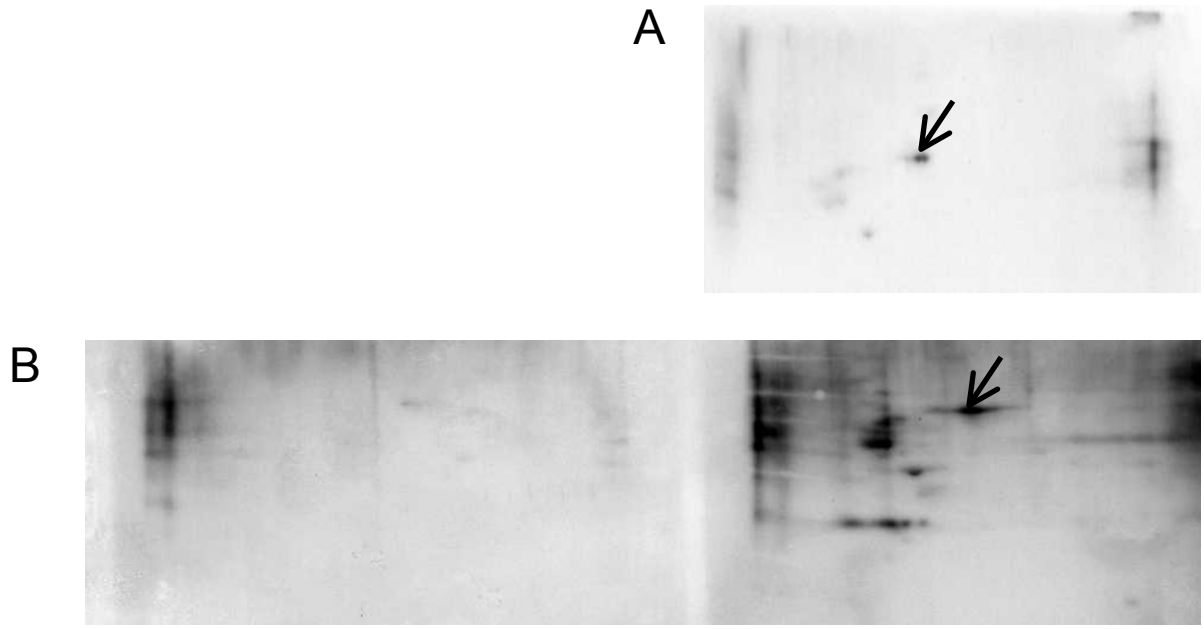

Fig.4.1.4.2.2.2. Oxidative damage to proteins increases with age. A – oxyblot from amygdala of a young WT mouse (2 months), B – oxyblot of amygdala of an old WT mouse (12 months; left – control without DNPH, right – DNPH-positive staining). Arrows indicate one of the carbonylated proteins present on both blots: the mean density of the spot increased from 0.06 (2-month-old) to 0.76 (12-month-old).

As presented in Fig.4.1.4.2.2.2 (A, B right), carbonylation of proteins in the amygdala was found to increase with age. Both the number of oxidized spots, as well as their density was increased in aged mice: an example indicated by arrow shows a protein spot, the oxidation of which was found to increase with age, as indicated by an increase in spot density from 0.06 (young) to 0.76 (old). 2,4-DNPH-positive staining was also proven to be specific (Fig.4.1.4.2.2.2, B left), as shown by the absence of specific staining on the blot not treated with the primary antibody against 2,4-DNPH (negative control).

Furthermore, the oxyblotting technique was used to determine the changes in protein carbonylation between the WT and CB1 knockout mice. It was shown in the previous section that there was no genotype effect on the amount of total protein carbonyls. However, one cannot exclude that some proteins are differentially modified in the knockout strain. To further address this question, oxyblots from amygdala and hippocampus samples from WT and CB1 knockout mice were performed. The representative results are shown in Fig.4.1.4.2.2.3.

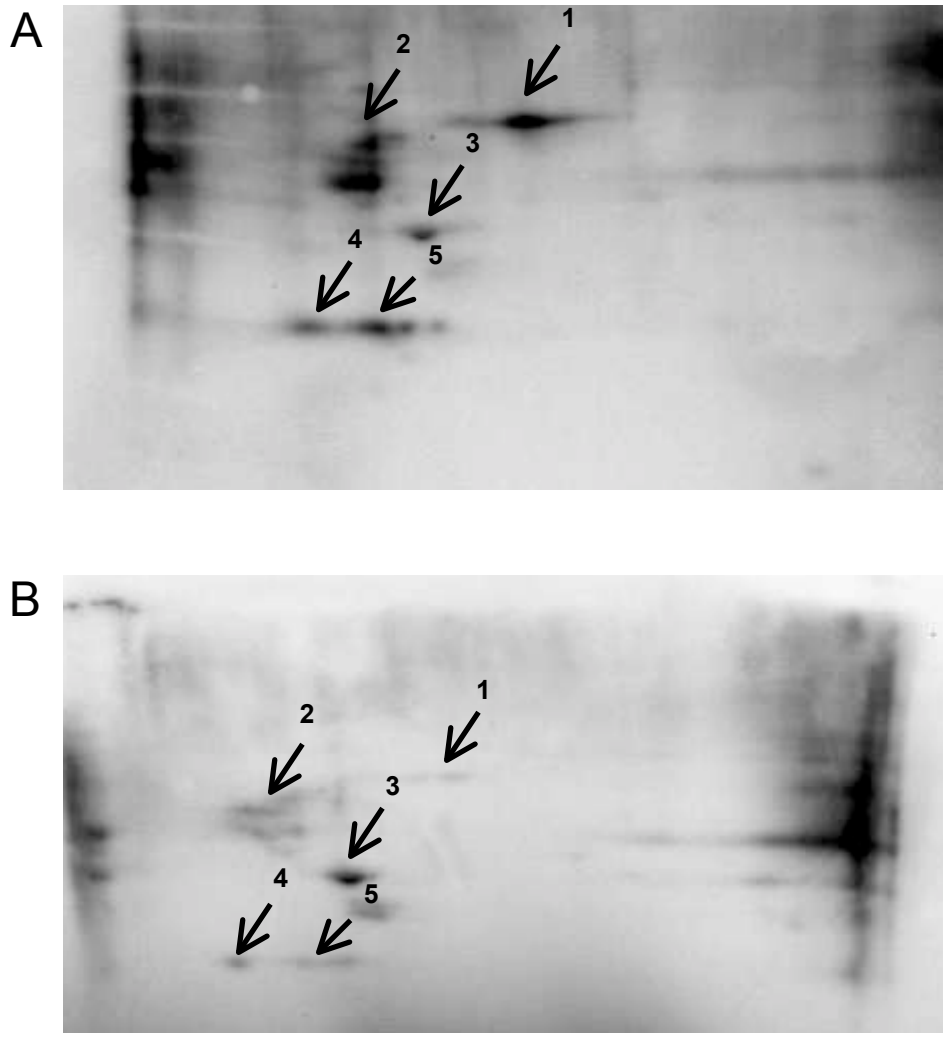

Fig.4.1.4.2.2.3. Presence of oxidatively modified proteins in the amygdala of old WT (A) and CB1 (B) knockout mice. Arrows and numbers (1-5) indicate analogous spots on both blots. No increase in the spot intensity was observed in the knockout strain, but rather more intense oxidation was observed in the blot from a WT mouse.

As presented in Fig. 4.1.4.2.2.3, there was no evident increase in the intensity of carbonyl-positive spots in the CB1 knockout mice. The pattern of protein oxidation was similar between the strains, as indicated by arrows showing analogous proteins. The spot intensity was rather higher in the WT strain in this example. Overall, no increase in protein oxidation in the knockout strain could be shown using the oxyblot technique, which supports the data from colorimetric assays.

Finally, the differences between the amount and the pattern of carbonylated proteins in different brain regions (amygdala and hippocampus) were assessed. As shown in Fig. 4.1.4.2.2.4, the pattern of carbonyl-positive spots was similar between these two regions, and a higher intensity of the spots could be observed in the amygdala.

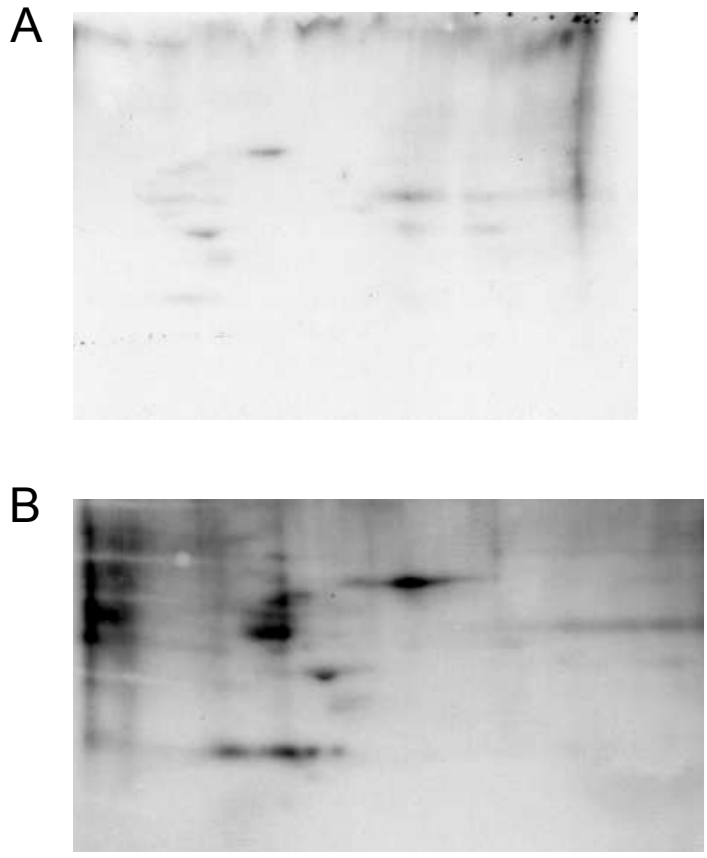

Fig.4.1.4.2.2.4. Difference in the carbonylation of proteins was assessed between the brain regions of interest. Images represent oxyblots from the hippocampus (A) and amygdala (B) from an old WT mouse (12 months). A similar oxidation pattern was observed, with higher intensity in the amygdala.

To sum it up, the oxyblot experiments supported the findings from the previous study: no increase in protein carbonylation could be observed in the knockout strain. Amygdala was again found to be more sensitive to oxidative damage.

4.1.1.3 Oxidative damage to DNA

Finally, the oxidative damage to DNA was identified using an immunostaining against 8-hydroxyguanosine, one of the markers for oxidized DNA (Bowers et al. 2004). RNAse-treated samples were used as a control to prove the specificity of the staining for DNA (Strazielle et al. 2009). The data from 3 independent experiments were combined and analyzed using Image J software. Data represent mean gray values per CA3 region (total number of slices analyzed, n=12-21). A significant effect of age on the presence of 8-hydroxyguanosine, marker for DNA oxidation, was observed in both strains ($F_{2,92}$ = 37.28, p<0.001), but the intensity of staining showing DNA damage was found to increase with age (Fig.4.1.4.3.1) similarly in the WT and CB1 knockout mice.

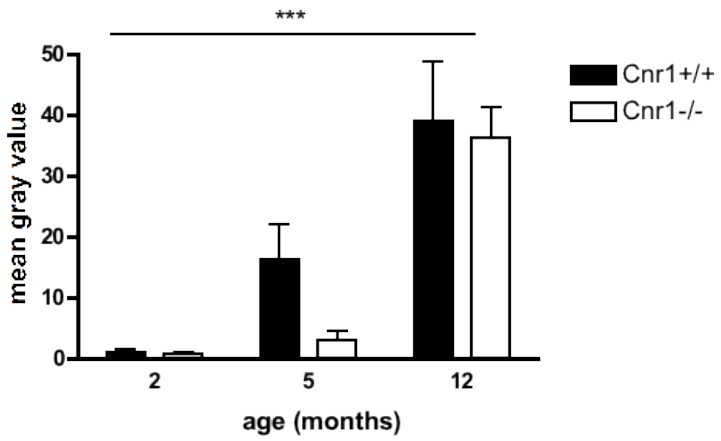

Fig.4.1.4.3.1. Analysis of 8-hydroxyguanosine-positive staining (mean gray value) in the CA3 region of the hippocampus of young (2 months), mature (5 months) and old (12-15 months) $Cnr1^{+/+}$ and $Cnr1^{-/-}$ mice (n=12-21 slices total). Data were analyzed by two way ANOVA followed by Bonferroni's post hoc tests and represented as mean value +/- standard error of mean (SEM). ***p<0.001(age effect, two way ANOVA).

Data presented in Fig. 4.1.4.3.1 indicate that, although a significant age-related increase in DNA oxidation was observed with increasing age, no genotype effect on the presence of 8-hydroxyguanosine-positive staining in the hippocampus was found, indicating that there was no difference in DNA oxidation between the two strains. An example of 8-hydroxyguanosine-positive staining in the CA3 region is shown in Fig.4.1.4.3.2.

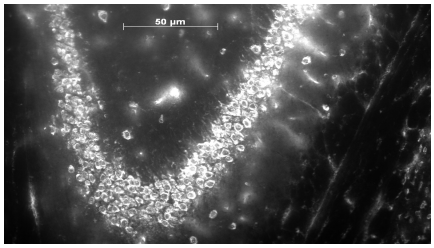

Fig.4.1.4.3.2. Representative microphotograph showing 8-hydroxyguanosine-positive staining in the CA3 region (CB1 knockout mouse, 12 months old). Scale bar: 50µm.

Overall, the results presented in section 4.1.4 suggest that oxidative damage to cellular macromolecules increases with age in mice (the increase being evident mostly at 12 months of age) but this age-related change is not further exacerbated in the absence of CB1 receptors. Moreover, it was found that hippocampus and amygdala seem to be more sensitive to age-related oxidative damage than other brain regions, such as cortex and cerebellum.

4.1.5 Expression of lysosomal protease cathepsin D is decreased in the hippocampus of Cnr1-/- mice

The results presented in the previous section indicate that oxidative stress cannot account for the accelerated lipofuscin accumulation in the CB1 receptor knockout mice, because none of the oxidative stress markers investigated were elevated in the brain in the absence of the CB1 receptors. Therefore, other possible reasons for lipofuscin accumulation were investigated. It is known, for instance, that lysosomal deficits often lead to accumulation of toxic waste products,

such as lipofuscin (Brunk and Terman 2002; Koike et al. 2000; Nakanishi and Wu 2009; Terman and Brunk 2004). These deficits are often traced to deficiencies in different lysosomal enzymes, one of them being cathepsin D, which can also be used as a lysosomal marker. Cathepsin D deficiency in mice has been shown to induce a condition similar to neuronal ceroid lipofuscinosis in humans (Koike et al. 2000), which results in a massive accumulation of autofluorescent pigment (ceroid or lipofuscin) in the brain and various behavioural deficits. Therefore, the expression of cathepsin D was assessed in the hippocampus of young and old WT and $Cnr1^{-/-}$ mice by Western blot analysis. Cathepsin D exists in several isoforms: it is synthesized as a precursor (43 kDa) and is later on processed to form the mature, active isoforms – heavy chain (approximately 30 kDa), and light chain (14kDa) (Erickson et al. 1981).

The results of cathepsin D expression analysis are presented in Fig.4.1.5.1. A generally reduced expression of cathepsin D in both age groups of $Cnr1^{-/-}$ mice could be observed (genotype effect: $F_{1,14} = 40.38$, $p<0.001$ for the precursor form, $F_{1,14} = 18.33$, $p<0.001$ for the heavy chain, $F_{1,14} = 24.39$, $p<0.001$ for the light chain). Interestingly, there was an age-related change in the expression of the precursor and mature (heavy chain) forms of cathepsin D: while the expression of the precursor form decreased (age effect: $F_{1,14} = 9.903$, $p<0.01$; Fig.4.1.5.1, A), the expression of mature, heavy chain cathepsin D increased with age (age effect: $F_{1,14} = 21.96$, $p<0.001$; Fig.4.1.5.1, B). This, indicates an alteration in cathepsin D processing in aging – a shift towards an enhanced production of the mature, active isoform (Heinrich et al. 1999). There was no age-related change in the expression of the light chain isoform (age effect: $F_{1,14} = 1.608$, $p>0.05$; Fig.4.1.5.1, C). The lack of interaction between age and genotype effects indicates that the age-related changes in the expression of cathepsin D isoforms are similar in WT and CB1 knockout mice.

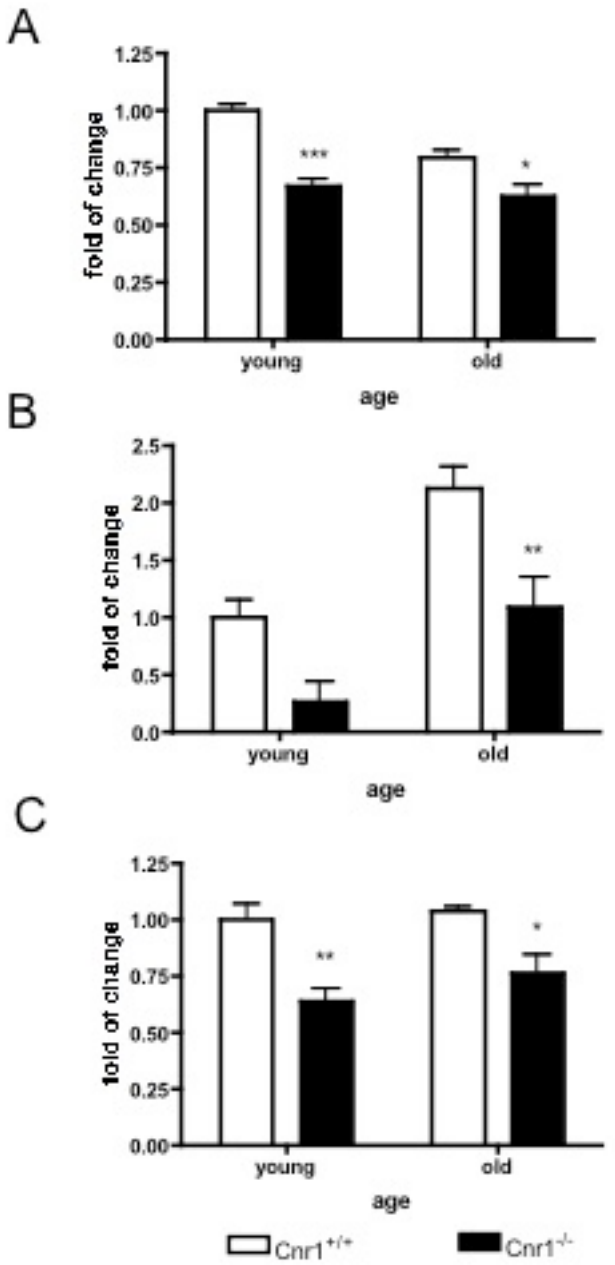

Fig.4.1.5.1. Results of Western blot analysis of the expression of different cathepsin D isoforms (A - precursor form, 43 kDa; B – mature, heavy chain, ≈30 kDa; C – mature, light chain, 14 kDa) in the hippocampus of $Cnr1^{+/+}$ and $Cnr1^{-/-}$ mice (n=4-5). Data are expressed as as fold of change in relation to mean value of respective cathepsin D isoform expression in the hippocampus of young WT mice. Stars (*, **, ***) indicate $p<0.05$, $p<0.01$, $p<0.001$ in the Bonferroni's post hoc test, respectively. From: Piyanova et al, under revision.

A typical cathepsin D Western blot is shown in Fig.4.1.5.2.

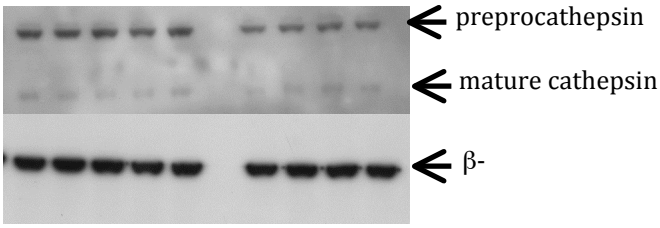

Fig.4.1.5.2. A representative Western blot example showing samples from young WT (n = 5, left) and CB1 knockout mice (n = 4, right). Arrows indicate the specific bands for the precursor and mature (heavy chain) forms of cathepsin D and β-actin. The blot was first probed with an antibody against cathepsin D (top), stripped and re-probbed with an antibody against β-actin (bottom) to ensure equal loading. Additionally, background substraction was performed for all samples before the normalization.

4.1.6 Similar total ceramide content and ceramide species' profile in WT and Cnr1-/- mice

In the previous section, the evidence that CB1 receptor affects cathepsin D expression levels was presented. This effect could be both direct and indirect. One of the factors that can affect cathepsin D production in the lysosome is ceramide (Heinrich *et al.* 1999), which belongs to a family of lipid molecules that are produced via acid sphingomyelinase in the lysosomes (Kitatani *et al.* 2008), among other pathways. It is also known that CB1 receptor activation can induce ceramide synthesis via different pathways – by inducing sphyngomyelin hydrolysis, as well as via serine palmitoyltransferase (SPT) pathway (Carracedo *et al.* 2004; Velasco *et al.* 2005). Therefore, it is possible that ceramide levels are decreased in CB1 knockout mice leading to disturbances in ceramide signaling, which in turn could influence cathepsin D production. To address this question, total and individual ceramide levels in the hippocampal samples of young (2-month-old) and old (12-month-old) WT and $Cnr1^{-/-}$ mice were measured by high performance thin layer chromatography (HPTLC) after total lipid extraction, as described in section 3.15. All ceramide measurements were performed in the laboratory of Professor K.Sandhoff (Life and Medical Sciences Institute, University of Bonn) by H.Farwanah, PhD. These

results together with previously presented data on oxidative stress and cathepsin D expression have been submitted for publication and are currently under review.

Data from total ceramide content measurements by HTPLC are presented in Fig.5.1.6.1. There was no effect of age ($F_{1,18}$ = 0.136, p>0.05) or genotype ($F_{1,18}$ = 0.037, p>0.05) on the total ceramide content, as determined by two way ANOVA (Fig.5.1.6.1).

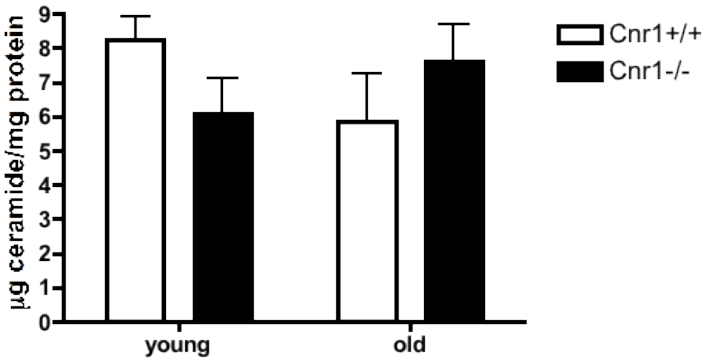

Fig.4.1.6.1. Total ceramide levels in young (2-month-old) and old (12-month-old) WT and CB1 knockout mice. Data are expressed in μg per mg total protein, n=4-8.

Since individual ceramides have different roles in the cell, possible changes in the ceramide profile in WT and $Cnr1^{-/-}$ mice with increasing age could also affect cathepsin D production. Therefore, an initial qualitative profiling of different ceramide species was performed. Profiling of ceramide species was done using high performance liquid chromatography (LC) coupled with electrospray ionization (ESI)-quadrapole/time of flight hybrid mass spectrometry (QTOF-MS) method (Farwanah et al. 2011). Although there were no significant differences in the ceramide profile of WT and CB1 knockout mice (Fig.4.1.6.2), C16 ceramides were only present at detectable levels in aged mice, indicating a tendency to increased C16 ceramide levels in aging.

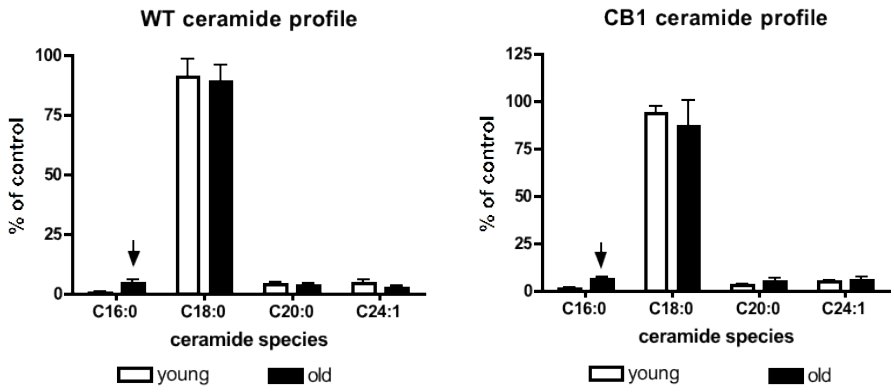

Fig.4.1.6.2. Ceramide profiles of WT and CB1 receptor knockout mice of different ages. Arrow indicates a tendency for age-related increase in C16 ceramides.

In conclusion, no changes in total or individual ceramide levels were observed in the knockout strain, indicating that life-long absence of CB1 receptors does not affect ceramide production. No age effect to total ceramide levels could be observed as well, however, C16 ceramides were present at detectable levels only in the old mice.

4.1.7 LC3 and p62 levels are altered in Cnr1-/- mice

Lipofuscin accumulation can affect autophagy and prevent fusion between the lysosomes and autophagosomes, in this way further contributing to the impairment of clearance of damaged, oxidized macromolecules. Also, a deficiency in cathepsin D synthesis can result in autophagy deficits, since normal lysosomal function is a crucial counterpart of autophagy. Therefore, the levels of basic markers of autophagy, LC3 and p62, were assessed in the hippocampus of CB1 receptor knockout mice and their WT littermates of different ages. Because the Western blots for autophagy markers could not be properly established in our lab, these experiments were performed in collaboration with C.-A.Rossi, PhD, in the laboratory of D.Bano, PhD, and Professor P.Nicotera at the DZNE (Deutsches Zentrum für Neurodegenerative Erkrankungen), and the resulting data are presented here (also submitted for publication as part of the manuscript number 4 in the publication list).

The levels of autophagy markers LC3 and p62 in the hippocampus of young (2-month-old) and old (12-month-old) $Cnr1^{+/+}$ and $Cnr1^{-/-}$ mice were assessed by Western blot analysis. The accumulation of LC3-II isoform is considered to be a marker for the upregulation of autophagosomal formation (Klionsky et al 2008). The amount of LC3-II was almost two times higher in 12-month-old $Cnr1^{-/-}$ compared to age-matched WT mice, indicating autophagy upregulation (Fig.5.1.7.1; genotype effect: $F_{1,12} = 5.73$, $p<0.05$, interaction age x genotype: $F_{1,12} = 5.852$, $p<0.05$).

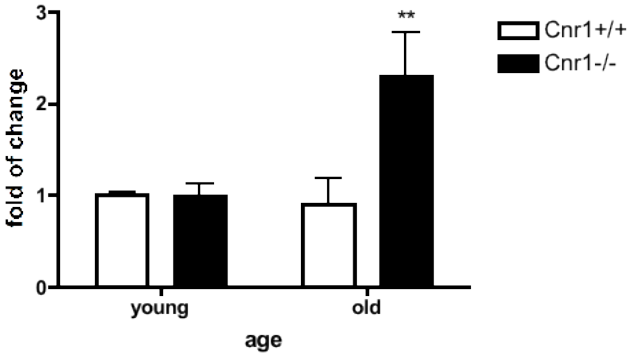

Fig.4.1.7.1 LC3-II levels in the hippocampus of young and old $Cnr1^{+/+}$ and $Cnr1^{-/-}$ mice (n=3-5), $^{**}p<0.01$ in Bonferroni's post hoc test.

This was consistent with the finding that old $Cnr1^{-/-}$ animals also had lower p62 levels as compared to WT mice (Fig.4.1.7.2; genotype effect: $F_{1,12} = 28.13$, $p<0.001$).

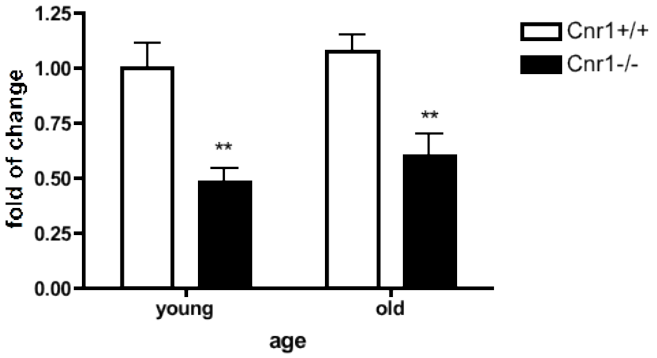

Fig.4.1.7.2. p62 levels in the hippocampus of young and old $Cnr1^{+/+}$ and $Cnr1^{-/-}$ mice (n=4-5); **p<0.01 in Bonferroni's post hoc test.

Lower p62 levels together with higher LC3-II presence indicate enhanced autophagy in the hippocampus of old CB1 receptor deficient mice. Interestingly, there was no upregulation of LC3-II in the young $Cnr1^{-/-}$ mice (Fig.4.1.7.1) but these mice also had a lower p62 level (Fig.4.1.7.2; p<0.01 in Bonferroni's post hoc test). This could indicate a general decrease in p62 expression in the absence of CB1 receptors.

Representative Western blots for LC3 and p62 are shown in Fig.4.1.7.3 and 4.1.7.4, respectively.

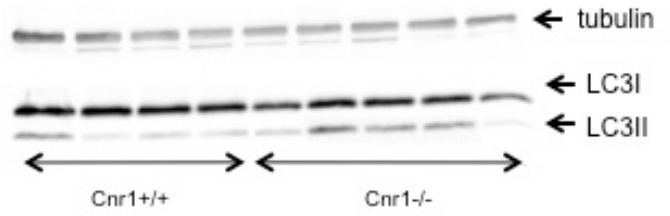

Fig.4.1.7.3. A representative Western blot used to quantify the LC3-II expression in the hippocampus of the old mice. The first sample from the right side was excluded from the analysis because of its poor quality.

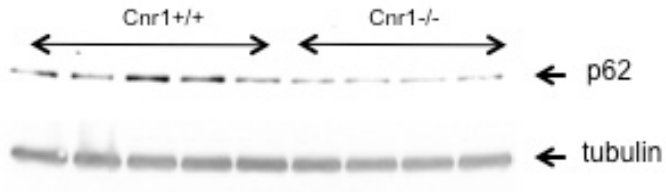

Fig.4.1.7.4. A representative Western blot used to quantify the p62 level in the hippocampus of the old mice.

4.1.8 Akt/mTOR phosphorylation levels are unchainged in the absence of CB1 receptors

Mammalian target of rapamycin (mTOR) is one of the major regulators of cellular aging and autophagy (Santos et al. 2011). Since signs of autophagy upregulation had been observed in old CB1 knockout animals, we decided to check the levels of mTOR phosphorylation, as well as phosphorylation of Akt (also known as protein kinase B), the activity of which regulates the phosphorylation of mTOR. However, no significant changes in mTOR phosphorylation level in aging could be observed between WT and CB1 knockout animals (see Fig.4.1.8) using two way ANOVA analysis.

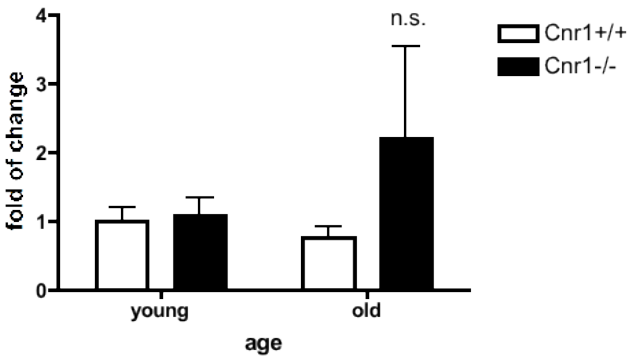

Fig.4.1.8.1. Analysis of age-related changes in the mTOR phosphorylation state in WT and CB1 receptor knockout mice (n=4-5). Data represent p-mTOR/mTOR ratio (fold of change to control – yount WT mean value); n.s. = not significant.

Although a tendency towards an increase in mTOR phosphorylation in the absence of CB1 receptors was observed, it was not significant due to high variation between different samples.

Akt signaling pathway has been related to CB1 receptor activation (Ozaita et al. 2007), and the activation of Akt is known to influence the mTOR pathway related to the autophagy function. Consistent with the results presented in Fig.4.1.8.1 (showing no change in the basal level of mTOR phosphorylation as a consequence of CB1 receptor deletion), no change in the levels of phosphorylated Akt could be observed in either young (2-month-old) or old (12-month-old) CB1 receptor knockout mice.

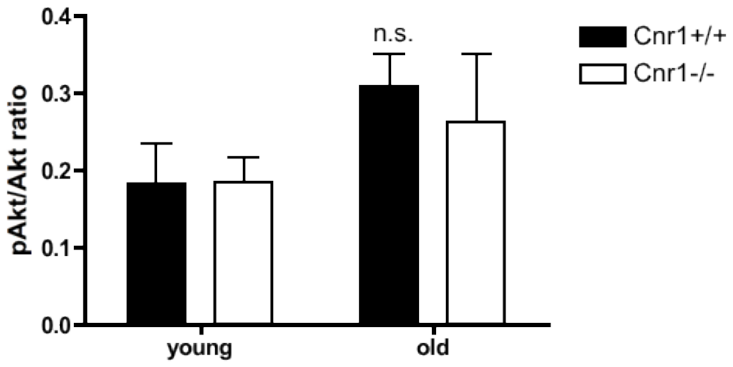

Fig.4.1.8.2. Phosphorylated Akt/total Akt ratio in young (2-month-old) and old (12-month-old) WT ($Cnr1^{+/+}$) and CB1 receptor knockout ($Cnr1^{-/-}$) mice. No effect of age or genotype on Akt phosphorylation was observed ($p>0.05$, two way ANOVA).

4.2 Age-related changes of the endocannabinoid system

Several studies suggest that some components of the endocannabinoid system undergo age-related changes, for instance, an age-related decrease in CB1 receptor expression (Berrendero et al. 1998; Canas et al. 2009; Romero et al. 1998) and coupling was reported in the forebrain. In some studies, diminished anandamide levels were found in aging in the CB1 knockout mice (Maccarrone et al. 2001; Maccarrone et al. 2002), while others found no significant differences in the endocannabinoid (EC) levels in aging in different brain regions in WT or CB1 knockout mice (Wang et al. 2003). Therefore, there is still a lack of knowledge about age-related changes of 2-AG and other endocannabinoids in the hippocampus. Thus, the goal of this study was to determine age-related changes in the endocannabinoid system, concentrating on 2-AG levels and the enzymes responsible for the metabolism of 2-AG, since it is the major ligand of the CB1 receptor and the age-related changes of the enzymatic machinery related to it have never been described before. Additionally, the age-related changes in the levels of several other endocannabinoids (anandamide, AEA, oleoylethanolamine, OEA, and palmithoylethanolamine, PEA, as well as their both precursor and dedradation product arachidonic acid, AA) were determined. The results presented in this section have been submitted for a publication (see publication list, number 5) and are partially reproduced from this paper.

4.2.1 Expression of DAGLα progressively decreases in aging in C57BL6/J mice

As shown in Fig.4.2.1.1, the expression of DAGLα mRNA was significantly downregulated with increasing age (n=3-5; one-way ANOVA, 4 groups, $F = 8.953$, $p<0.01$). The expression of DAGLα in young, 2-month-old mice was significantly higher than at 17 ($p<0.05$, Bonferroni's post hoc test) and 26 months of age ($p<0.01$, Bonferroni's post hoc test). There were no significant changes in DAGLβ, MAGL or CB1 receptor expression (n=4-6; one-way ANOVA, $p>0.05$),

although there was a tendency (p=0.07) towards a decrease in MAGL expression with increasing age.

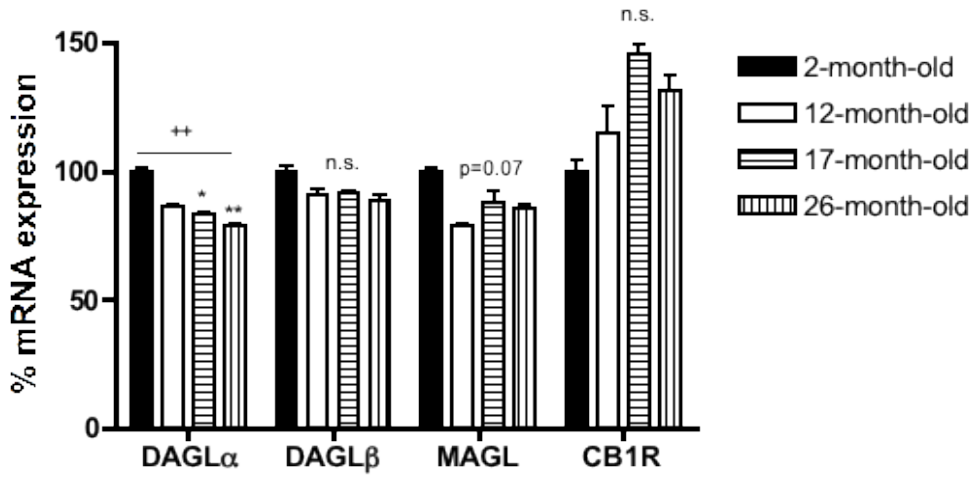

Fig.4.2.1.1. Expression of enzymes involved in 2-AG metabolism and CB1 receptor in the hippocampus of C57B6/J mice from different age groups (2 months, 12 months, 17 months, 26 months). The data were analyzed by one-way ANOVA followed by Bonferroni's post hoc tests (if p-value in ANOVA was <0.05): ++ indicates age effect on DAGLα expression, p<0.01; *p<0.05, Bonferroni's post hoc test; **p<0.01, Bonferroni's post hoc test; n.s. = not significant.

To test if the observed effects are general and not restricted to our mouse colony, the gene expression experiments were then repeated with a separate group of C57BL6/J mice from a different breeding colony (Charles River, France; n=7-8). The mRNA expression of DAGLα, DAGLβ, MAGL and CB1 receptor in young (2-month-old) and old (15-month-old) mice (Fig. 5.2.1.2) was compared. As depicted in Fig. 5.2.1.2, an age-related decrease in DAGLα expression was observed again (p<0.05, unpaired t-test). A significant decrease in MAGL expression was also found (Fig. 5.2.1.2; p<0.05, unpaired t-test), presumably due to higher animal numbers, since a similar tendency was observed in the previous experiment (Fig. 5.2.1.1). There were no age-dependent changes in DAGLβ or CB1 expression (p>0.05, unpaired t-test). So, the results of the first study were successfully replicated using animals from an independent breeding colony.

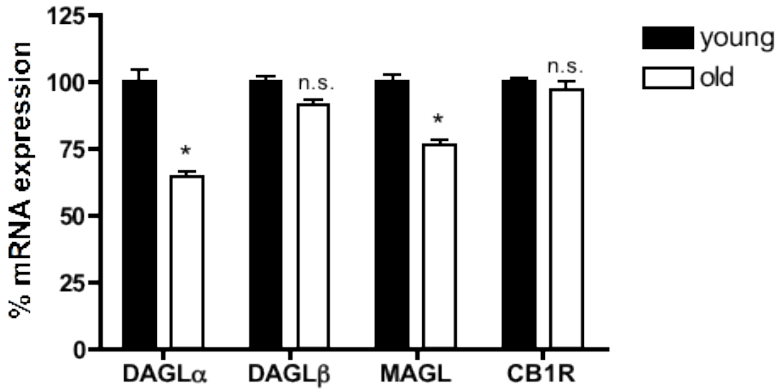

Fig.4.2.1.2. Expression of DAGLα, DAGLβ, MAGL and Cnr1 (CB1R) mRNA in the hippocampus of young (2-month-old) and old (15-month-old) C57B6/J mice from a different animal facility. *p<0.05, unpaired t-test with Welch's correction; n.s. = not significant.

Interestingly, when the expression data from both experiments were combined, one could observe a significant correlation between the expression of DAGLα and MAGL, as well as DAGLβ and MAGL (r = 0,41; n=29 in both cases). This effect was further investigated separately in young and old animals. In the young animals, a significant correlation between the expression of MAGL and DAGLβ was present (r = 0.56; n = 14), whereas in the old mice the correlation between MAGL and DAGLα was significant (r = 0.78; n = 15).

4.2.2 2-arachidonoylglycerol (2-AG) levels do not significantly change with age in the C57BL6/J mice

Next, the effect of the age-related changes in the expression of enzymes on the tissue levels of 2-AG was investigated. As depicted in Fig.4.2.2.1, hippocampal 2-AG levels do not undergo a significant age-dependent change: the amount of 2-AG is not significantly reduced in the 15-month-old mice in comparison to 2-month-old mice. Neither the expression of the synthesizing enzymes DAGLα and DAGLβ or the degrading enzymes MAGL correlates with the 2-AG level (data not shown), which means that other factors contribute to the regulation of the concentration of 2-AG which is usually produced on demand and rapidly degraded.

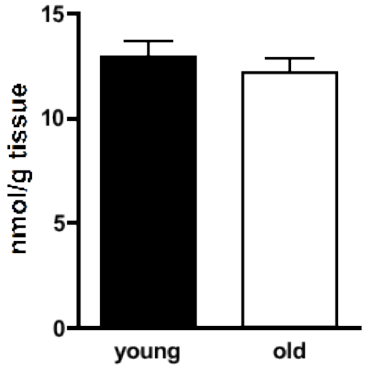

Fig.4.2.2.1. 2-AG levels in the hippocampus of young (2-month-old) and old (15-month-old) C57BL6/J mice (data expressed as mean values +/- SEM, nmol/g tissue). No significant difference in 2-AG levels was observed between young and old mice.

However, an interesting effect was observed when closely investigating individual differences in 2-AG levels: 2-AG levels were highly variable in the young mice, so that three separate groups with similar 2-AG levels within the group (indicated by circles) could be distinguished (see Fig.4.2.2.2).

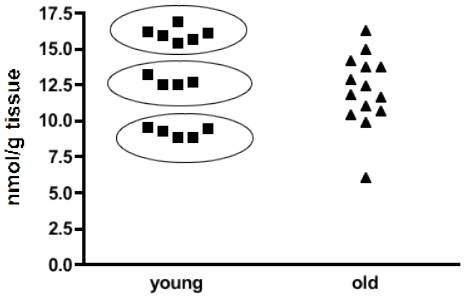

Fig.4.2.2.2. Individual differences in 2-AG levels in the young and old C57BL6/J mice (n=15 for young mice, n=14 for old mice).

Whether this variability has functional consequences for physiology or behavior of mice, remains unknown. Interestingly, this clear distribution of individual differences in 2-AG levels seems to disappear with age, becoming more homogenous.

4.2.3 Age effect on the levels of AEA, AA, OEA and PEA in the hippocampus of C57BL6/J mice

Finally, the effect of age on the concentrations of other endocannabinoids in the hippocampus was assessed. Previously, such changes have been reported for anandamide in the CB1 receptor knockout mice but not their WT littermates (Maccarrone et al. 2001; Maccarrone et al. 2002). However, the oldest mice used for EC measurements in those studies were 6 months old. In this study using 15-month-old mice, no age-related changes in the concentration of anandamide could be found ($p>0.05$; Fig.4.2.3.1). The age-related changes in the levels of two other endocannabinoids normally found in the brain – oleoylethanolamide (OEA) and palmithoylethanolamide (PEA) – were also measured. The levels of OEA were unchanged in aged animals ($p>0.05$; Fig.4.2.3.1). However, a significant age-related increase in the level of PEA was observed ($p<0.01$; Fig.4.2.3.1).

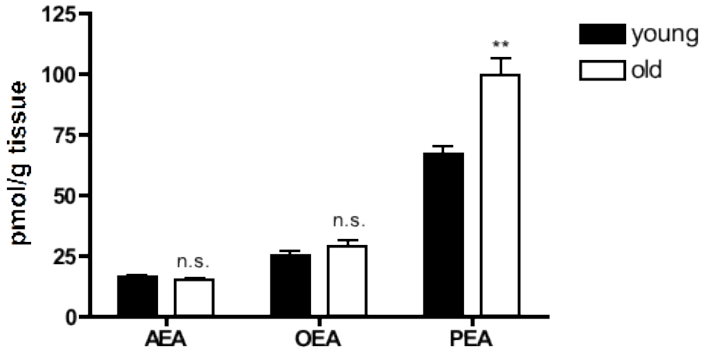

Fig.4.2.3.1. Endocannabinoid levels in the hippocampus of young (2-month-old) and old (15-month-old) C57BL6/J mice (data expressed as mean values +/- SEM, pmol/g tissue). **p<0.01, unpaired t-test, n.s. = not significant.

Arachidonic acid (AA) levels were also measured in the hippocampus of young and old C57BL6/J mice. AA is the common metabolite of the studied endocannabinoids and can be their precursor, as well as degradation product. However, it can also participate in many other metabolic pathways in the cell, for example, it can be a precursor to prostaglandins (Nomura et al. 2011), and thus contribute to age-related neuroinflammation, therefore, maintaining stable AA levels in aging might be particularly important. In this study, no change in AA levels could be detected in aged mice in comparison to young mice (see Fig.4.2.3.2).

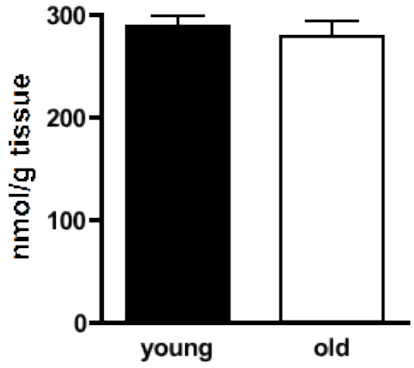

Fig.4.2.3.2. Arachidonic acid levels in the hippocampus of young (2-month-old) and old (15-month-old) C57BL6/J mice (data expressed as mean values +/- SEM, nmol/g tissue). No significant age-related change was observed ($p>0.05$, unpaired t-test).

When investigating correlation between the levels of different endocannabinoids (see Table 5.2.3; n = 29), a significant correlation between 2-AG and AEA levels (r = 0.40), as well as a correlation between 2-AG and AA (r = 0.42) and AEA and AA (r = 0.71) could be shown. OEA also correlated positively with AA (r = 0.4) and with PEA (r = 0.69).

Table 4.2.3. Pearson's correlation coefficients (r values) for the different endocannabinoids (AEA, 2-AG, OEA, PEA) and arachidonic acid (AA) measured in the hippocampus of young (2-month-old) and old (15-

month-old) C57BL6 mice. Significant correlations between the levels of different endocannabinoids are shown in bold (2-AG and AEA, OEA and PEA, AEA and AA, OEA and AA, 2-AG and AA).

Endocannabinoids	AEA	2-AG	AA	PEA	OEA
AEA	-	**0.40**	**0.71**	0.08	0.26
2-AG	**0.40**	-	**0.42**	-0.20	-0.20
AA	**0.71**	**0.42**	-	0.25	**0.40**
PEA	0.08	-0.20	0.25	-	**0.69**
OEA	0.26	-0.20	**0.4**	**0.69**	-

4.2.4 Age-related changes in DAGLα, DAGLβ and MAGL, as well as endocannabinoid levels in the absence of CB1 receptor

Finally, the possibility that the expression of DAGLs and MAGL in aging, as well as endocannabinoid levels could be influenced by CB1 receptor activity was investigated. Therefore, mRNA expression experiments were again performed in the hippocampus of young (-2-month-old) and old (12-month-old) WT and CB1 receptor knockout mice. RNA isolation for this experiment was performed with the kind help of D.Mauer.

As depicted in Fig. 4.2.4.1, age has a general effect on DAGLα expression in WT and CB1 knockout mice. The expression of DAGLα significantly differs between the age groups (two way ANOVA, $F_{1,25} = 5.303$, $p < 0.05$). There was a 20% decrease in DAGLα expression in 12-month-old WT mice and a 31% decrease in 12-month-old CB1 knockout mice. There was an age effect on DAGLβ expression as well (age effect, $F_{1,27} = 6.921$, $p < 0.05$, although it was only significant in the CB1 knockout mice ($p < 0.05$ in Bonferroni´s post hoc test). Interestingly, DAGLβ expression

generally lower in the absence of CB1 receptors (genotype effect, $F_{1,27} = 8.931$, $p < 0.01$). MAGL expression in the hippocampus of CB1 knockout mice is higher by 24% at 2 months of age and is lower by 13% at 12 months of age in comparison to WT (age effect, $F_{1,26} = 13.37$,$p < 0.01$; interaction age x genotype, $F_{1,26} = 6.333$, $p < 0.05$). In the WT mice, only a minor change of 3% in aging is observed.

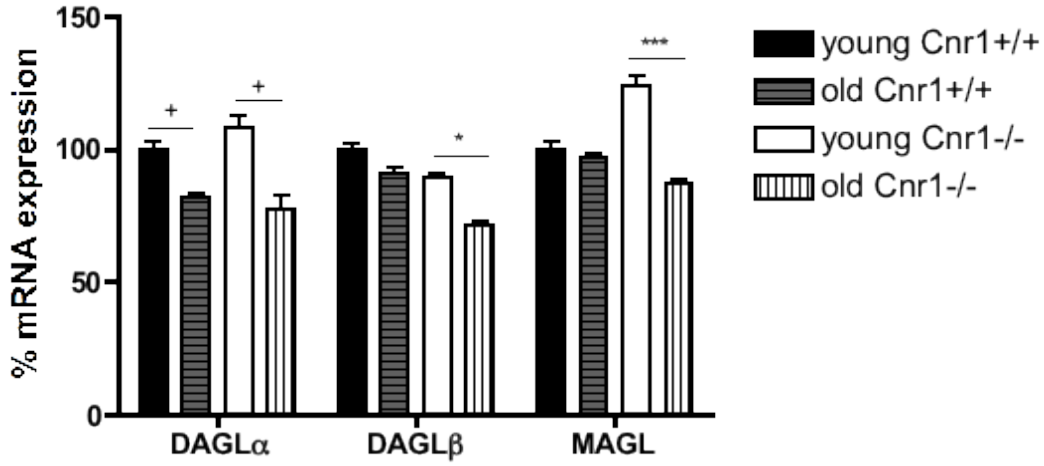

Fig.4.2.4.1. DAGLα, DAGLβ and MAGL expression in the hippocampus of WT and CB1 knockout mice differentially changes with aging. Data are expressed as mean value +/- standard error of mean (% of control – mean expression in the young WT mice). $^{+}p<0.05$ (age effect); $*p<0.05$, $***p<0.001$, Bonferroni's post hoc test.

Furthermore, it was tested if the indicated differences in the enzyme expression between the two strains can affect endocannabinoid levels. Therefore, the levels of 2-AG and AA, as well as AEA were measured in the hippocampus of young and old WT and CB1 receptor knockout mice. The results are presented in Fig.4.2.4.2. 2-AG content in the hippocampus of WT mice significantly decreases with age but increases in the CB1 knockout mice, as shown by two way ANOVA (interaction age x genotype, $F_{1,16} = 13.36$, $p < 0.01$). Arachidonic acid levels significantly decrease with age in both genotypes, although CB1 animals have generally lower AA levels (age effect: $F_{1,16} = 8.299$, $p < 0.05$; genotype effect, $F_{1,16}=15.86$, $p < 0.01$; $p < 0.05$ in Bonferroni's post hoc test). Anandamide levels do not show any significant changes in aging in both genotypes.

Surprisingly, in this experiment a significant age-related decrease in the levels of 2-AG was found in the WT mice. This was consistent with reduced levels of AA in old WT mice, since the alterations in the levels of AA were found to correspond to changes in 2-AG levels in previous studies (Gao et al. 2010). A significant correlation between AA and 2-AG levels was also found in this work (see section 4.2.3).

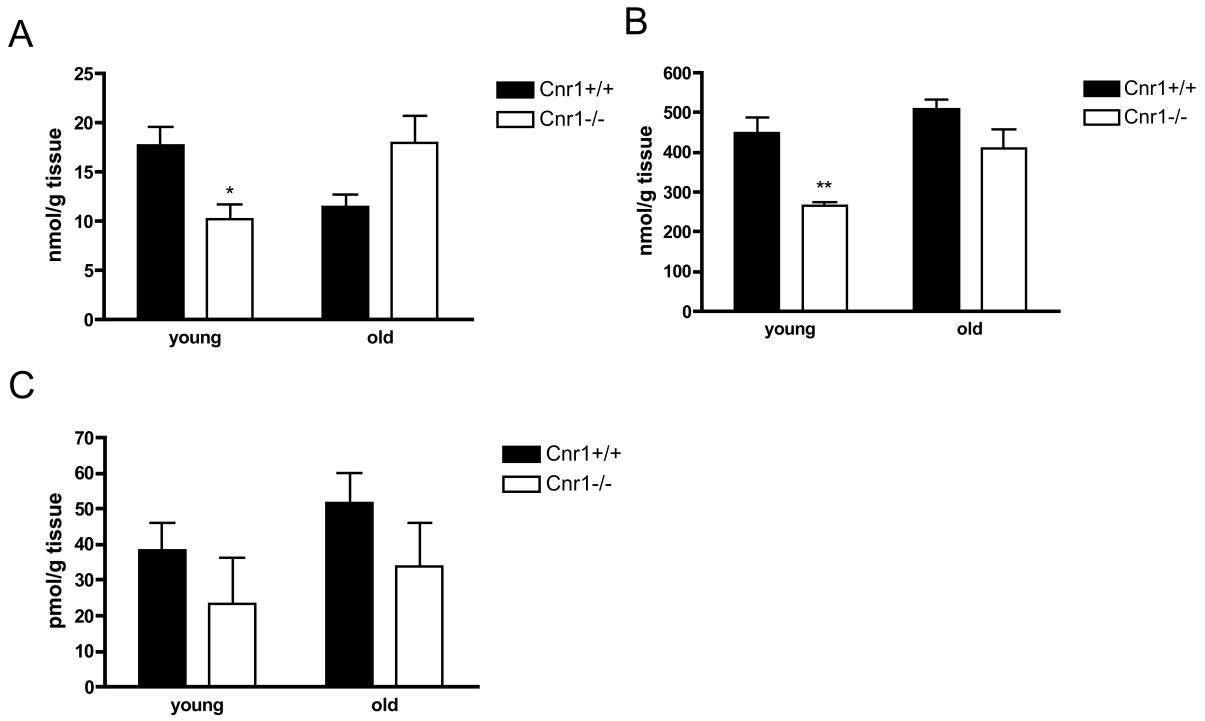

Fig.4.2.4.2. Age-related changes in the 2-AG (A), arachidonic acid (AA; B) and anandamide (AEA; C) levels in the hippocampus of WT and CB1 knockout mice (n=5). Data are expressed as mean value +/- standard error of mean. * and ** indicate $p < 0.05$ and $p<0.01$ in Bonferroni's post hoc test.

Overall, the results presented in this section indicate that the presence of CB1 receptors regulates the expression of other components of the endocannabinoid system, as well as 2-AG levels.

5. Discussion

5.1 Mechanisms contributing to accelerated aging of the CB1 receptor knockout mice

Several possible mechanisms contributing to the aging phenotype of the mice lacking CB1 receptors have been investigated. In this section, the results of these studies are discussed in the same order, in which the findings were presented in the „Results“ section.

5.1.1 Changes in neurogenesis and apoptosis are probably not responsible for the lower neuronal number in old $Cnr1^{-/-}$ mice

In this study, age-related changes in the rate of neurogenesis were assessed in the CB1 receptor knockout ($Cnr1^{-/-}$) mice and their WT ($Cnr1^{+/+}$) littermates in different age groups. The results showed that, although young $Cnr1^{-/-}$ mice had impaired neurogenesis (almost 50% lower proliferation than in the WT), similar to previously published data (Jin et al. 2004), this prominent difference between the strains disappeared with age. This finding was rather surprising, because a similar difference between the genotypes in different age groups was expected. However, since a dramatic reduction in the rate of neurogenesis was also observed in the aged wildtype animals, the difference to CB1 knockout animals was no longer present. These findings suggest that age-related reduction in neurogenesis not related to the CB1 receptor activity.

Furthermore, the contribution of pro-apoptotic mechanisms to the age-related decrease in neuronal numbers was assessed. Since CB1 knockout mice show elevated caspase 3 levels in inflammation-related disease models (Jackson et al. 2005; Pryce et al. 2003), the theory that caspase 3 activation is exacerbated in old mice lacking CB1 receptors was tested. As shown in Fig.5.1.2.1, old $Cnr1^{-/-}$ indeed seem to have significantly higher caspase 3 levels compared to

their $Cnr1^{+/+}$ littermates. However, later we found that this staining was contaminated by lipofuscin which had been found to accumulate with aging, especially in the $Cnr1^{-/-}$ mice. Several techniques have been establish to diminish the impact of lipofuscin autofluorescence on caspase 3 staining, such as treatment of the brain slices with 10 mM $CuSO_4$ in 50 mM ammonium acetate buffer and substracting the background staining from negative control samples with the primary antibody. However, in spite of this, the lipofuscin was still present in the pictures analysed, so we cannot totally exclude that it interfered with the staining results. Therefore, additional studies have to be performed to support the fact that caspase 3 activation is higher in the old CB1 knockout mice, for example, using cleavage of poly(ADP-ribose) polymerase (PARP), catalyzed by caspase 3, as a read-out. Also, it is not quite clear, which cellular pathway can lead to the activation of caspase 3. There is no significant increase in the caspase 9 activation in the old CB1 knockout mice, which is also true for the caspase 8. Caspase 8 presence was significantly elevated in the young, but not old knockout animals, which would suggest an activation of the extrinsic apoptotic pathway. Interestingly, it has been shown that CB1 receptor knockout mice show an increased phosphorylation of Fas-associated protein with death domain (FADD) in several brain regions (Alvaro-Bartolome et al. 2010). FADD is known to mediate apoptosis by interacting with caspase 8, and an increase in its phosphorylation is considered to be non-apoptotic. Therefore, the authors of the study suggest that CB1 receptor activity has a tonic control on the level of FADD phosphorylation. This theory could not be confirmed by studies with CB1 receptor antagonist rimonabant, so this effect must be rather moderate (Alvaro-Bartolome et al. 2010). The modulation of FADD/caspase 8 complexes by CB1 receptor activity deserves further studies.

5.1.2 A possible mechanism responsible for increased lipofuscin accumulation in the CB1 knockout animals

In this work, it has been demonstrated for the first time that CB1 receptor activity might play an important role in the maintenance of protein homeostasis, which is very important in aging (Bishop et al. 2010). CB1 receptor knockout mice show signs of accelerated lipofuscin

accumulation in the hippocampus with increasing age, accompanied by changes in autophagy and lysosomal degradation capacity (diminished expression of cathepsin D). Although these results have to be further extended to functional studies of the autophagy and lysosomal function *in vitro* and the mechanism of these changes is not quite clear yet, this evidence suggestes that CB1 receptors influence the clearance of damaged macromolecules. In Fig.5.1.2.1 a simplified mechanism for autophagic clearance is depicted. Normally, the damaged macromolecules (e.g., proteins) can be either directly taken up by the lysosomes or transported to assembling autophagosomes, which then fuse with the lysosomes to get access to the lysosomal hydrolases and cathepsins that are able to degrade cellular trash.

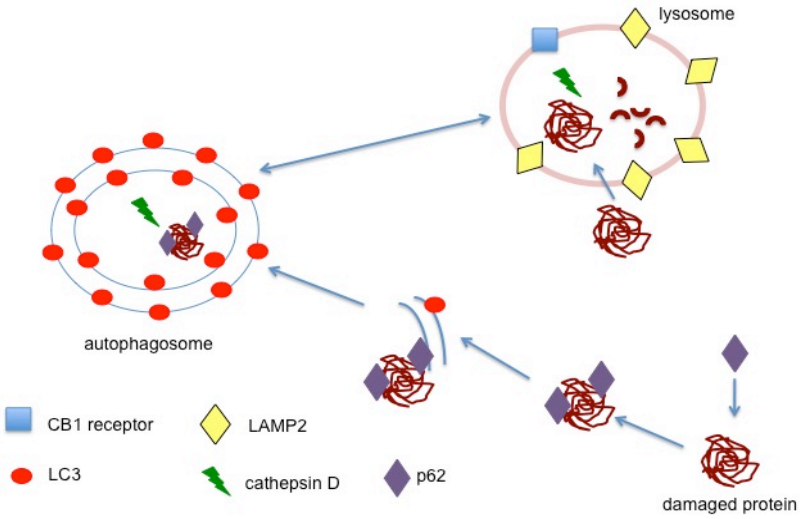

Fig.5.1.2.1. Normal clearance of damaged proteins (or other macromolecules and organelles) by the autophagolysosomal pathway. LAMP2 = lysosomal-associated membrane protein 2.

However, when this mechanism is not working properly, damaged macromolecules can accumulate in the cell, interfering with its normal functions. A hypothetical mechanism of the changes in the autophagy-lysosomal degradation pathway in the CB1 knockout mice is presented in Fig.5.1.2.2.

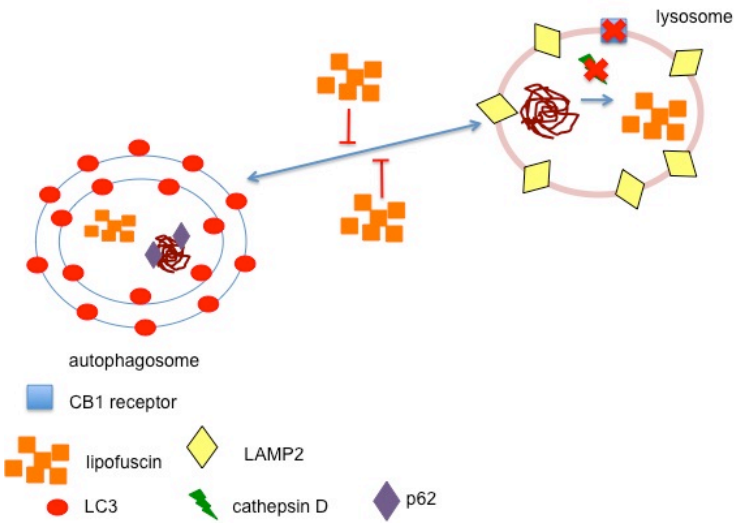

Fig.5.1.2.2. Hypothesized changes in the autophagolysosomal pathway in the absence of CB1 receptor leading to lipofuscin accumulation. LAMP2 = lysosomal-associated membrane protein 2.

In the absence of CB1 receptor, the expression of cathepsin D is decreased, which might lead to a decrease in lysosomal degradation capacity and accumulation of lipofuscin. Lipofuscin then further impairs the fusion of autophagosomes with the lysosomes, which exacerbates its own accumulation. Although the production of new autophagosomal membranes seems to be exacerbated in the CB1 knockout mice (as indicated by higher LC3-II and lower p62 levels in the old Cnr1$^{-/-}$ mice), autophagy cannot exert its protective ability on the accumulation of damaged macromolecules because the cathepsin D amount is insufficient and lipofuscin is basically undegradable. In addition, lipofuscin accumulation is also elevated in the old WT mice. This can be explained by the fact that the CB1 receptor expression and activity is known to decrease with age (Berrendero et al. 1998; Romero et al. 1998), which can contribute to lipofuscin accumulation in the WT mice. We have also shown (Piyanova et al, under revision) that there is an accumulation of lipofuscin in the microglia cells of CB1 knockout mice. Microglia cells are known to phagocytose neurons that accumulate lipofuscin but are also unable to degrade it. It this case, this accumulation might be exacerbated because of the decrease in cathepsin D expression which can also compromise normal lysosomal function in the microglia cells. Moreover, preliminary studies with conditional CB1 knockout mice indicate that neither GABA- nor glutamatergic neuron-specific CB1 knockouts are prone to the accumulation of lipofuscin,

which leaves the possibility that the absence of CB1 receptors on another cell type (possibly microglia) is responsible for this phenotype. This hypothesis can be tested in the future, when the conditional knockout mice for other cell types are available. In addition, the mechanism by which CB1 receptor absence influences cathepsin D expression has to be further investigated. The possibility that it can happen via ceramide synthesis has been excluded in the present work. There could be a direct effect of CB1 knockout on the expression of cathepsin D, which can be tested by mRNA expression analysis. It seems that the absence of CB1 receptors also influences the basal expression of p62, since the levels of p62 were lower in CB1 knockout mice in both age groups, although younger mice did not exhibit signs of eleveated autophagy. It has been published that p62 deficiency can result in neurodegeneration and accumulation of damaged proteins (Ramesh Babu et al. 2008), therefore, it could also contribute to the CB1 phenotype. It also remains to be shown, by which pathway CB1 receptors can possible modulate autophagy. It has been shown previously that cannabinoids can activate autophagy in glioma cells by inhibiting the Akt/mTOR pathway (Salazar et al. 2009). In this work, no change in the basal mTOR phosphorylation has been observed in the absence of CB1 receptors, which is consistent with a published report (Puighermanal et al. 2009). It could be interesting to investigate mTOR phosphorylation using neuronal cell cultures from WT and CB1 knockout mice under autophagy-stimulating conditions. It is also worth to consider other autophagy-modulating pathways, for example beclin 1-mediated pathway (Rubinsztein et al. 2011).

5.2 **Aging of the endocannabinoid system**

In the second part of the present work, the age-related changes of the endocannabinoid system itself have been investigated, focusing on the enzymes responsible for the metabolism of 2-AG. It could be shown that the expression of DAGLα, the primary enzyme responsible for the 2-AG synthesis in the brain, goes down with increasing age, and this effect was demonstrated in two independent animal colonies. Moreover, it has been found that the expression of DAGLα and

DAGLβ (which was not significantly altered with age in the WT mice) correlates with the expression fo MAGL, the main degradation enzyme for 2-AG, indicating that degradation and synthesis of 2-AG are tighly regulated. Interestingly, there is an age-related shift in this regulation: while in the young mice coordination of DAGLβ and MAGL levels seems to be of major importance, the correlation between DAGLα and MAGL becomes significant with increasing age. Indeed, a decrease in MAGL expression in aging could also be demonstrated, although it was not as prominent as in the case of DAGLα. Surprisingly, these changes in enzyme availability did not affect the levels of 2-AG: they remained unchainged with age and also did not correlate with the expression of the enzymes. This means that the amount of enzymes produced in the aged animlas is enough to maintain normal basal 2-AG levels; however, this may change in the case of urgent need for EC production, e.g. in the case of increased extracellular glutamate levels. In a situation like that, the available pool of enzymes might not be enough to produce a required amount of 2-AG, which may then contribute to age-related pathologies (like an increase in neurotoxicity and oxidative stress). CB1 receptor mRNA expression did not change with age, however, a decrease in CB1 receptor protein levels have been demonstrated in our lab (by O.Albayram; data not shown). Additionally, the levels of other endocannabinoids (AEA, OEA, PEA), as well as arachidonic acid were assessed in the hippocampus. Only PEA levels were significantly elevated with increasing age – this might be a compensatory effect, since PEA has been shown to have anti-inflammatory and neuroprotective properties (Koch et al. 2011; Lo Verme et al. 2005), thus its increase in aging is rather beneficiary. In a previous study, a decrease in PEA levels was reported with age (Maccarrone et al, 2001), however, this study used much younger (6-month-old) mice, so this is probably an age-dependent effect. A significant correlation between the levels of different EC and AA has also been observed, which is logical, because it can be a precursor, as well as a metabolic product for most of the EC.

Finally, it has been demonstrated that the presence of CB1 receptors affects other components of the EC system. There were profound changes in the expression of 2-AG metabolic enzymes in the CB1 knockout mice: young $Cnr1^{-/-}$ mice had higher MAGL levels in comparison with their WT

littermates, as well as generally lower DAGLβ levels, which further decreased with age. This coincided with lower 2-AG levels in the young CB1 knockout mice, which were then elevated in the old mice. This effect in the old mice might be compensatory, since 2-AG is known to have neuroprotective properties (Panikashvili et al. 2001), which are only partially CB1R-dependent. In the same experiment, WT littermates of the CB1 knockout mice showed decreased 2-AG levels, which was not observed in the experiment with mice from a different animal colony. This might be explained by the fact that steady-state EC levels are very unstable and can be influenced by many factors and can often vary between different animal facilities and laboratories (Buczynski and Parsons 2010). Also, the animal numbers were different in these two experiments: there were only 5 specimens available in the group from our animal facility versus 14 specimens from old animals from Charles River. Given a rather high variation typical for the EC levels, this significant effect could be achieved by chance. Further experiments are needed to confirm that there is a basal change in the 2-AG levels in aging. Probably, these future experiments should involve other techniques for EC measurement, such as microdialisis, which is gaining acceptance as opposed to the usual postmortem measurement techniques (Buczynski and Parsons 2010).

6. Conclusions and outlook

In the present work, we investigated the contribution of several mechanisms to the aging phenotype of the CB1 receptor knockout mice. We can conclude that age-related changes in neurogenesis are similar in the CB1 knockout mice and their WT littermates. We also demonstrate that CB1 receptors play an important role in maintaining normal lysosomal and autophagy function and preventing lipofuscin accumulation. In addition, we show that the endocannabinoid system undergoes age-related changes that might contribute to age-related pathological changes in the brain. However, several open questions deserving further studies still remained. Future studies will have to elucidate the pathways, by which CB1 receptors can influence autophagy and lysosomal function. Also, it has to be shown, which cell type is responsible for the accelerated lipofuscin accumulation in the CB1 knockout mice. Further studies using conditional knockout mice and ulstrastructural analysis techniques will address this question. Finally, the studies of age-related changes in the endocannabinoid system have to be extended to other mouse strains or even other species to test if this effect is common among vertebrates, and additional parameters (like changes in the enzyme activity) will be investigated.

7. Publications

1. A.Ju.Zhigalov, **A.A. Pyanova**, A.Ya.Kaplan. Statistical structure of EEG alpha waves in adolescence with schizophrenic spectrum disorders and age-matched normals. Int J of Psychophysiol 2008, Vol 69, 3, P. 256
2. Albayram O, Alferink J, Pitsch J, **Piyanova A**, Neitzert K, Poppensieker K, Mauer D, Michel K, Legler A, Becker A, Monory K, Lutz B, Zimmer A, Bilkei-Gorzo A. Role of CB1 cannabinoid receptors on GABAergic neurons in brain aging. *Proc Natl Acad Sci U S A* 2011 Jul 5; 108(27):11256-61. Epub 2011 Jun 20
3. Bilkei-Gorzo A, Drews E, Albayram Ö, **Piyanova A**, Gaffal E, Tueting T, Michel K, Mauer D, Maier W, Zimmer A. Early onset of aging-like changes is restricted to cognitive abilities and skin structure in $Cnr1^{-/-}$ mice. *Neurobiol Aging* 2012 Jan; 33(1):200.e11-22. Epub 2010 Aug 17
4. **Piyanova A**, Albayram O, Rossi CA, Farwanah H, Michel K, Nicotera P, Sandhoff K, Bilkei-Gorzo A. CB1 receptor activity influences cathepsin D expression and lipofuscin accumulation (under revision at *Mechanisms of Ageing and Development*)
5. **Piyanova A**, Buchalla R, Michel K, Schwitter C, Albayram O, Lutz B, Zimmer A, Bilkei-Gorzo A. Age-related changes in the endocannabinoid system: focusing on 2-arachidonoylglycerol and the enzymes responsible for its metabolism (submitted to *Journal of Neurochemistry*)
6. Albayram O, **Piyanova A**, Imbeault S, Miro X, Michel K, Racz I, Bilkei-Gorzo A*, Zimmer A*. Low dose of Δ^9-THC restores cognitive functions and synaptogenesis in old mice through an epigenetic mechanism (submitted)

* - equal contribution

8. Conference abstracts

1. A.Bilkei-Gorzo, B.Schürmann, D.Mauer, **A.Piyanova,** K.Michel, A.Zimmer. Age-dependent changes in animals lacking CB1 receptor. 12th Meeting of the Hungarian Neuroscience Society. Budapest, Hungary, January 22-24, 2009
2. **A.Piyanova**, A.Zimmer, A.Bilkei-Gorzo. Accumulation of oxidative damage to cellular macromolecules does not precede the onset of age-related memory deficits in Cnr1-/- mice. COST B30 Training School "Cellular neuropathology: *in vitro* models", Kiev, Ukraine, June 3-7 2010 ***(travel grant award)***
3. **A.Piyanova**, O.Albayram, K.Michel, A.Bilkei-Gorzo, A.Zimmer. Accumulation of oxidative damage to cellular macromolecules does not precede the onset of age-related memory deficits in *Cnr1-/-* mice. Workshop of the DFG Research Unit 926 "The Endocannabinoid System: From Physiology to Pathophysiology", Bonn, Germany, June 16-19, 2010
4. **A.Piyanova**, O.Albayram, K.Michel, A.Bilkei-Gorzo, A.Zimmer. Accumulation of oxidative damage to cellular macromolecules does not precede the onset of age-related memory deficits in *Cnr1-/-* mice. 7th FENS Forum of European Neuroscience, Amsterdam, The Netherlands, July 3-7 2010
5. **A.Piyanova**, O.Albayram, K.Michel, R.Buchalla, A.Zimmer, A.Bilkei-Gorzo. Uncovering molecular mechanisms of early-onset age-related memory deficits in *Cnr1-/-* mice. Semester Meeting of the Bonner Forum Biomedizin, Bonn, Germany, February 11-12, 2011
6. **A.Piyanova**, O.Albayram, K.Michel, R.Buchalla, A.Zimmer, A.Bilkei-Gorzo. Uncovering molecular mechanisms of early-onset age-related memory deficits in *Cnr1-/-* mice. 9th Göttingen Meeting of the German Neuroscience Society, Göttingen, Germany, March 23-27, 2011
7. **A.Piyanova**, O.Albayram, K.Michel, R.Buchalla, B.Lutz, A.Zimmer, A.Bilkei-Gorzo. Uncovering molecular mechanisms of early-onset age-related memory deficits in CB1

receptor knockout mice. 8th IBRO World Congress of Neuroscience, Florence, Italy, July 14-18, 2011

8. **A.Piyanova**, O.Albayram, K.Michel R.Buchalla, C.Schwitter, B.Lutz, A.Zimmer, A.Bilkei-Gorzo. Age-related changes in the endocannabinoid levels, oxidative stress and lysosomal activity in mice lacking CB1 receptor. IACM 6th Conference on Cannabinoids in Medicine and 5th European Workshop on Cannabinoid Research, Bonn, Germany, September 8-10, 2011
9. **A.Piyanova**, O.Albayram, K.Michel R.Buchalla, C.Schwitter, B.Lutz, A.Zimmer, A.Bilkei-Gorzo. Age-related changes in the endocannabinoid levels, oxidative stress and lysosomal activity in mice lacking CB1 receptor. Semester Meeting of the Bonner Forum Biomedizin, Bonn, Germany, February 3-4, 2012

9. Acknowledgements

Last but not least section of this work is dedicated to thanking everyone who helped and supported me during the last 3.5 years! So here we go. First of all, I would like to thank my supervisor, Andras Bilkei-Gorzo, who was so much more than just a supervisor to me: a teacher, a friend and one of the most inspiring scientists I have ever known. You brought the real meaning to the word „Doktorvater" during these last years! I hope some day you will revolutionize aging research, like we have always dreamed of ☺ Here I would also like to say thanks to the third indispensable part of our little „aging group" – my lab mate Önder (a.k.a. „Dr.Love") for helping me to become really patient (with all the noise you were making in our office☺). But, seriously, I also learned a lot from you – you are one of the few natural talents I have known in this field, and you have become one of my best friends over the years. So here is to the PNAS paper and to all our future papers! And to finish it off with the „aging people" I would like to thank Kerstin for all her excellent support during these years – technical and friendly. You are the best assistant one could wish for, Andras is very lucky. Next, I would like to thank Andreas (Professor Andreas Zimmer) for, of course, accepting me to his lab and challenging me with an interesting research project, for letting me practice my organizational skills (organizing the lab retreat!) and for all the interesting scientific discussions that we have had, but also for creating a very nice, friendly atmosphere at the institute. Who knew it can be fun to do science? ☺ Speaking of fun, I would also like to thank all my great colleagues at the Institute of Molecular Psychiarty, especially those ones who I had a chance to get to know a little bit better from their non-scientific side: Bruno, Irene, Kim, and of course Ildi („the best half" of Andras). I would also like to thank everyone who contributed to this work in any technical or intellectual way, especially Anne for all the help with the genotyping of the CB1 knockout mice, as well as all our collaboration partners mentioned in the text for the great work they have done.

Finally, I would like to thank my second reviewer, Professor Gerhard von der Emde, for agreeing to do this hard job and I wish you all the luck with the new zebrafish aging project.

And not to forget the most important part: this work was supported by a grant from the DFG (Deutsche Forschungsgemeinschaft) to Forschergruppe 926 (FOR 926) „Physiology and Pathophysiology of the Endocannabinoid System“.

10.References

Aguado T, Monory K, Palazuelos J, Stella N, Cravatt B, Lutz B, Marsicano G, Kokaia Z, Guzman M, Galve-Roperh I (2005) The endocannabinoid system drives neural progenitor proliferation. FASEB J 19: 1704-6

Aguado T, Romero E, Monory K, Palazuelos J, Sendtner M, Marsicano G, Lutz B, Guzman M, Galve-Roperh I (2007) The CB1 cannabinoid receptor mediates excitotoxicity-induced neural progenitor proliferation and neurogenesis. J Biol Chem 282: 23892-8

Aksenov MY, Aksenova MV, Butterfield DA, Geddes JW, Markesbery WR (2001) Protein oxidation in the brain in Alzheimer's disease. Neuroscience 103: 373-83

Albayram O, Alferink J, Pitsch J, Piyanova A, Neitzert K, Poppensieker K, Mauer D, Michel K, Legler A, Becker A, Monory K, Lutz B, Zimmer A, Bilkei-Gorzo A (2011) Role of CB1 cannabinoid receptors on GABAergic neurons in brain aging. Proc Natl Acad Sci U S A 108: 11256-61

Alvaro-Bartolome M, Esteban S, Garcia-Gutierrez MS, Manzanares J, Valverde O, Garcia-Sevilla JA (2010) Regulation of Fas receptor/Fas-associated protein with death domain apoptotic complex and associated signalling systems by cannabinoid receptors in the mouse brain. Br J Pharmacol 160: 643-56

Bano D, Agostini M, Melino G, Nicotera P (2011) Ageing, neuronal connectivity and brain disorders: an unsolved ripple effect. Mol Neurobiol 43: 124-30

Benard G, Massa F, Puente N, Lourenco J, Bellocchio L, Soria-Gomez E, Matias I, Delamarre A, Metna-Laurent M, Cannich A, Hebert-Chatelain E, Mulle C, Ortega-Gutierrez S, Martin-Fontecha M, Klugmann M, Guggenhuber S, Lutz B, Gertsch J, Chaouloff F, Lopez-Rodriguez ML, Grandes P, Rossignol R, Marsicano G (2012) Mitochondrial CB(1) receptors regulate neuronal energy metabolism. Nat Neurosci

Berrendero F, Romero J, Garcia-Gil L, Suarez I, De la Cruz P, Ramos JA, Fernandez-Ruiz JJ (1998) Changes in cannabinoid receptor binding and mRNA levels in several brain regions of aged rats. Biochim Biophys Acta 1407: 205-14

Bilkei-Gorzo A, Drews E, Albayram O, Piyanova A, Gaffal E, Tueting T, Michel K, Mauer D, Maier W, Zimmer A (2010) Early onset of aging-like changes is restricted to cognitive abilities and skin structure in Cnr1(-/-) mice. Neurobiol Aging

Bilkei-Gorzo A, Drews E, Albayram O, Piyanova A, Gaffal E, Tueting T, Michel K, Mauer D, Maier W, Zimmer A (2012) Early onset of aging-like changes is restricted to cognitive abilities and skin structure in Cnr1(-/-) mice. Neurobiol Aging

Bilkei-Gorzo A, Racz I, Valverde O, Otto M, Michel K, Sastre M, Zimmer A (2005) Early age-related cognitive impairment in mice lacking cannabinoid CB1 receptors. Proc Natl Acad Sci U S A 102: 15670-5

Bishop NA, Lu T, Yankner BA (2010) Neural mechanisms of ageing and cognitive decline. Nature 464: 529-35

Bisogno T, Di Marzo V (2010) Cannabinoid receptors and endocannabinoids: role in neuroinflammatory and neurodegenerative disorders. CNS Neurol Disord Drug Targets 9: 564-73

Bisogno T, Howell F, Williams G, Minassi A, Cascio MG, Ligresti A, Matias I, Schiano-Moriello A, Paul P, Williams EJ, Gangadharan U, Hobbs C, Di Marzo V, Doherty P (2003) Cloning of the first sn1-DAG lipases points to the spatial and temporal regulation of endocannabinoid signaling in the brain. J Cell Biol 163: 463-8

Blagosklonny MV (2007) Program-like aging and mitochondria: instead of random damage by free radicals. J Cell Biochem 102: 1389-99

Blagosklonny MV (2008) Aging: ROS or TOR. Cell Cycle 7: 3344-54

Blagosklonny MV (2010) Linking calorie restriction to longevity through sirtuins and autophagy: any role for TOR. Cell Death Dis 1: e12

Bowers R, Cool C, Murphy RC, Tuder RM, Hopken MW, Flores SC, Voelkel NF (2004) Oxidative stress in severe pulmonary hypertension. Am J Respir Crit Care Med 169: 764-9
Brown AJ (2007) Novel cannabinoid receptors. Br J Pharmacol 152: 567-75
Bruce AJ, Baudry M (1995) Oxygen free radicals in rat limbic structures after kainate-induced seizures. Free Radic Biol Med 18: 993-1002
Brunk UT, Jones CB, Sohal RS (1992) A novel hypothesis of lipofuscinogenesis and cellular aging based on interactions between oxidative stress and autophagocytosis. Mutat Res 275: 395-403
Brunk UT, Terman A (2002) The mitochondrial-lysosomal axis theory of aging: accumulation of damaged mitochondria as a result of imperfect autophagocytosis. Eur J Biochem 269: 1996-2002
Buczynski MW, Parsons LH (2010) Quantification of brain endocannabinoid levels: methods, interpretations and pitfalls. Br J Pharmacol 160: 423-42
Calabrese EJ, Bachmann KA, Bailer AJ, Bolger PM, Borak J, Cai L, Cedergreen N, Cherian MG, Chiueh CC, Clarkson TW, Cook RR, Diamond DM, Doolittle DJ, Dorato MA, Duke SO, Feinendegen L, Gardner DE, Hart RW, Hastings KL, Hayes AW, Hoffmann GR, Ives JA, Jaworowski Z, Johnson TE, Jonas WB, Kaminski NE, Keller JG, Klaunig JE, Knudsen TB, Kozumbo WJ, Lettieri T, Liu SZ, Maisseu A, Maynard KI, Masoro EJ, McClellan RO, Mehendale HM, Mothersill C, Newlin DB, Nigg HN, Oehme FW, Phalen RF, Philbert MA, Rattan SI, Riviere JE, Rodricks J, Sapolsky RM, Scott BR, Seymour C, Sinclair DA, Smith-Sonneborn J, Snow ET, Spear L, Stevenson DE, Thomas Y, Tubiana M, Williams GM, Mattson MP (2007) Biological stress response terminology: Integrating the concepts of adaptive response and preconditioning stress within a hormetic dose-response framework. Toxicol Appl Pharmacol 222: 122-8
Canas PM, Duarte JM, Rodrigues RJ, Kofalvi A, Cunha RA (2009) Modification upon aging of the density of presynaptic modulation systems in the hippocampus. Neurobiol Aging 30: 1877-84
Carracedo A, Geelen MJ, Diez M, Hanada K, Guzman M, Velasco G (2004) Ceramide sensitizes astrocytes to oxidative stress: protective role of cannabinoids. Biochem J 380: 435-40
Castegna A, Aksenov M, Thongboonkerd V, Klein JB, Pierce WM, Booze R, Markesbery WR, Butterfield DA (2002) Proteomic identification of oxidatively modified proteins in Alzheimer's disease brain. Part II: dihydropyrimidinase-related protein 2, alpha-enolase and heat shock cognate 71. J Neurochem 82: 1524-32
Castegna A, Thongboonkerd V, Klein JB, Lynn B, Markesbery WR, Butterfield DA (2003) Proteomic identification of nitrated proteins in Alzheimer's disease brain. J Neurochem 85: 1394-401
Chomczynski P, Sacchi N (1987) Single-step method of RNA isolation by acid guanidinium thiocyanate-phenol-chloroform extraction. Anal Biochem 162: 156-9
Conrad CC, Choi J, Malakowsky CA, Talent JM, Dai R, Marshall P, Gracy RW (2001) Identification of protein carbonyls after two-dimensional electrophoresis. Proteomics 1: 829-34
Cota D, Steiner MA, Marsicano G, Cervino C, Herman JP, Grubler Y, Stalla J, Pasquali R, Lutz B, Stalla GK, Pagotto U (2007) Requirement of cannabinoid receptor type 1 for the basal modulation of hypothalamic-pituitary-adrenal axis function. Endocrinology 148: 1574-81
Cuervo AM (2008) Autophagy and aging: keeping that old broom working. Trends Genet 24: 604-12
Di Marzo V (2011) Endocannabinoid signaling in the brain: biosynthetic mechanisms in the limelight. Nat Neurosci 14: 9-15
Di Marzo V, Bifulco M, De Petrocellis L (2004) The endocannabinoid system and its therapeutic exploitation. Nat Rev Drug Discov 3: 771-84
Donadelli M, Dando I, Zaniboni T, Costanzo C, Dalla Pozza E, Scupoli MT, Scarpa A, Zappavigna S, Marra M, Abbruzzese A, Bifulco M, Caraglia M, Palmieri M (2011) Gemcitabine/cannabinoid combination triggers autophagy in pancreatic cancer cells through a ROS-mediated mechanism. Cell Death Dis 2: e152

Dubey A, Forster MJ, Lal H, Sohal RS (1996) Effect of age and caloric intake on protein oxidation in different brain regions and on behavioral functions of the mouse. Arch Biochem Biophys 333: 189-97
Dunlop RA, Brunk UT, Rodgers KJ (2009) Oxidized proteins: mechanisms of removal and consequences of accumulation. IUBMB Life 61: 522-7
Erickson AH, Conner GE, Blobel G (1981) Biosynthesis of a lysosomal enzyme. Partial structure of two transient and functionally distinct NH2-terminal sequences in cathepsin D. J Biol Chem 256: 11224-31
Farwanah H, Kolter T, Sandhoff K (2011) Mass spectrometric analysis of neutral sphingolipids: Methods, applications, and limitations. Biochim Biophys Acta
Farwanah H, Wirtz J, Kolter T, Raith K, Neubert RH, Sandhoff K (2009) Normal phase liquid chromatography coupled to quadrupole time of flight atmospheric pressure chemical ionization mass spectrometry for separation, detection and mass spectrometric profiling of neutral sphingolipids and cholesterol. J Chromatogr B Analyt Technol Biomed Life Sci 877: 2976-82
Follo C, Ozzano M, Mugoni V, Castino R, Santoro M, Isidoro C (2011) Knock-down of cathepsin D affects the retinal pigment epithelium, impairs swim-bladder ontogenesis and causes premature death in zebrafish. PLoS One 6: e21908
Gallily R, Breuer A, Mechoulam R (2000) 2-Arachidonylglycerol, an endogenous cannabinoid, inhibits tumor necrosis factor-alpha production in murine macrophages, and in mice. Eur J Pharmacol 406: R5-7
Gao Y, Vasilyev DV, Goncalves MB, Howell FV, Hobbs C, Reisenberg M, Shen R, Zhang MY, Strassle BW, Lu P, Mark L, Piesla MJ, Deng K, Kouranova EV, Ring RH, Whiteside GT, Bates B, Walsh FS, Williams G, Pangalos MN, Samad TA, Doherty P (2010) Loss of retrograde endocannabinoid signaling and reduced adult neurogenesis in diacylglycerol lipase knock-out mice. J Neurosci 30: 2017-24
Godlewski G, Offertaler L, Wagner JA, Kunos G (2009) Receptors for acylethanolamides-GPR55 and GPR119. Prostaglandins Other Lipid Mediat 89: 105-11
Golden TR, Hinerfeld DA, Melov S (2002) Oxidative stress and aging: beyond correlation. Aging Cell 1: 117-23
Gowran A, Campbell VA (2008) A role for p53 in the regulation of lysosomal permeability by delta 9-tetrahydrocannabinol in rat cortical neurones: implications for neurodegeneration. J Neurochem 105: 1513-24
Gray DA, Woulfe J (2005) Lipofuscin and aging: a matter of toxic waste. Sci Aging Knowledge Environ 2005: re1
Harman D (1956) Aging: a theory based on free radical and radiation chemistry. J Gerontol 11: 298-300
Hawkins CL, Morgan PE, Davies MJ (2009) Quantification of protein modification by oxidants. Free Radic Biol Med 46: 965-88
Heinrich M, Wickel M, Schneider-Brachert W, Sandberg C, Gahr J, Schwandner R, Weber T, Saftig P, Peters C, Brunner J, Kronke M, Schutze S (1999) Cathepsin D targeted by acid sphingomyelinase-derived ceramide. EMBO J 18: 5252-63
Herkenham M, Groen BG, Lynn AB, De Costa BR, Richfield EK (1991a) Neuronal localization of cannabinoid receptors and second messengers in mutant mouse cerebellum. Brain Res 552: 301-10
Herkenham M, Lynn AB, de Costa BR, Richfield EK (1991b) Neuronal localization of cannabinoid receptors in the basal ganglia of the rat. Brain Res 547: 267-74
Herkenham M, Lynn AB, Little MD, Johnson MR, Melvin LS, de Costa BR, Rice KC (1990) Cannabinoid receptor localization in brain. Proc Natl Acad Sci U S A 87: 1932-6
Hill MN, McLaughlin RJ, Bingham B, Shrestha L, Lee TT, Gray JM, Hillard CJ, Gorzalka BB, Viau V (2010) Endogenous cannabinoid signaling is essential for stress adaptation. Proc Natl Acad Sci U S A 107: 9406-11
Jackson SJ, Pryce G, Diemel LT, Cuzner ML, Baker D (2005) Cannabinoid-receptor 1 null mice are susceptible to neurofilament damage and caspase 3 activation. Neuroscience 134: 261-8

Jin K, Xie L, Kim SH, Parmentier-Batteur S, Sun Y, Mao XO, Childs J, Greenberg DA (2004) Defective adult neurogenesis in CB1 cannabinoid receptor knockout mice. Mol Pharmacol 66: 204-8
Kim SH, Won SJ, Mao XO, Jin K, Greenberg DA (2005) Involvement of protein kinase A in cannabinoid receptor-mediated protection from oxidative neuronal injury. J Pharmacol Exp Ther 313: 88-94
Kitatani K, Idkowiak-Baldys J, Hannun YA (2008) The sphingolipid salvage pathway in ceramide metabolism and signaling. Cell Signal 20: 1010-8
Klionsky DJ, Cuervo AM, Dunn WA, Jr., Levine B, van der Klei I, Seglen PO (2007) How shall I eat thee? Autophagy 3: 413-6
Koch M, Kreutz S, Bottger C, Benz A, Maronde E, Ghadban C, Korf HW, Dehghani F (2011) Palmitoylethanolamide protects dentate gyrus granule cells via peroxisome proliferator-activated receptor-alpha. Neurotox Res 19: 330-40
Koike M, Nakanishi H, Saftig P, Ezaki J, Isahara K, Ohsawa Y, Schulz-Schaeffer W, Watanabe T, Waguri S, Kametaka S, Shibata M, Yamamoto K, Kominami E, Peters C, von Figura K, Uchiyama Y (2000) Cathepsin D deficiency induces lysosomal storage with ceroid lipofuscin in mouse CNS neurons. J Neurosci 20: 6898-906
Komatsu M, Waguri S, Koike M, Sou YS, Ueno T, Hara T, Mizushima N, Iwata J, Ezaki J, Murata S, Hamazaki J, Nishito Y, Iemura S, Natsume T, Yanagawa T, Uwayama J, Warabi E, Yoshida H, Ishii T, Kobayashi A, Yamamoto M, Yue Z, Uchiyama Y, Kominami E, Tanaka K (2007) Homeostatic levels of p62 control cytoplasmic inclusion body formation in autophagy-deficient mice. Cell 131: 1149-63
Koppel J, Davies P (2008) Targeting the endocannabinoid system in Alzheimer's disease. J Alzheimers Dis 15: 495-504
Korolainen MA, Nyman TA, Nyyssonen P, Hartikainen ES, Pirttila T (2007) Multiplexed proteomic analysis of oxidation and concentrations of cerebrospinal fluid proteins in Alzheimer disease. Clin Chem 53: 657-65
Lapointe J, Hekimi S (2010) When a theory of aging ages badly. Cell Mol Life Sci 67: 1-8
Levine RL (2002) Carbonyl modified proteins in cellular regulation, aging, and disease. Free Radic Biol Med 32: 790-6
Levine RL, Williams JA, Stadtman ER, Shacter E (1994) Carbonyl assays for determination of oxidatively modified proteins. Methods Enzymol 233: 346-57
Lichtman AH, Blankman JL, Cravatt BF (2010) Endocannabinoid overload. Mol Pharmacol 78: 993-5
Livak KJ, Schmittgen TD (2001) Analysis of relative gene expression data using real-time quantitative PCR and the 2(-Delta Delta C(T)) Method. Methods 25: 402-8
Lo Verme J, Fu J, Astarita G, La Rana G, Russo R, Calignano A, Piomelli D (2005) The nuclear receptor peroxisome proliferator-activated receptor-alpha mediates the anti-inflammatory actions of palmitoylethanolamide. Mol Pharmacol 67: 15-9
Low P (2011) The role of ubiquitin-proteasome system in ageing. Gen Comp Endocrinol 172: 39-43
Lu T, Pan Y, Kao SY, Li C, Kohane I, Chan J, Yankner BA (2004) Gene regulation and DNA damage in the ageing human brain. Nature 429: 883-91
Maccarrone M, Attina M, Bari M, Cartoni A, Ledent C, Finazzi-Agro A (2001) Anandamide degradation and N-acylethanolamines level in wild-type and CB1 cannabinoid receptor knockout mice of different ages. J Neurochem 78: 339-48
Maccarrone M, Valverde O, Barbaccia ML, Castane A, Maldonado R, Ledent C, Parmentier M, Finazzi-Agro A (2002) Age-related changes of anandamide metabolism in CB1 cannabinoid receptor knockout mice: correlation with behaviour. Eur J Neurosci 15: 1178-86
Mailleux P, Vanderhaeghen JJ (1992) Distribution of neuronal cannabinoid receptor in the adult rat brain: a comparative receptor binding radioautography and in situ hybridization histochemistry. Neuroscience 48: 655-68

Marchalant Y, Brothers HM, Norman GJ, Karelina K, DeVries AC, Wenk GL (2009a) Cannabinoids attenuate the effects of aging upon neuroinflammation and neurogenesis. Neurobiol Dis 34: 300-7
Marchalant Y, Brothers HM, Wenk GL (2009b) Cannabinoid agonist WIN-55,212-2 partially restores neurogenesis in the aged rat brain. Mol Psychiatry 14: 1068-9
Marsicano G, Moosmann B, Hermann H, Lutz B, Behl C (2002) Neuroprotective properties of cannabinoids against oxidative stress: role of the cannabinoid receptor CB1. J Neurochem 80: 448-56
Martinez-Vicente M, Talloczy Z, Wong E, Tang G, Koga H, Kaushik S, de Vries R, Arias E, Harris S, Sulzer D, Cuervo AM (2010) Cargo recognition failure is responsible for inefficient autophagy in Huntington's disease. Nat Neurosci 13: 567-76
Massi P, Valenti M, Bolognini D, Parolaro D (2008) Expression and function of the endocannabinoid system in glial cells. Curr Pharm Des 14: 2289-98
Matsuda LA, Bonner TI, Lolait SJ (1993) Localization of cannabinoid receptor mRNA in rat brain. J Comp Neurol 327: 535-50
McCarron RM, Shohami E, Panikashvili D, Chen Y, Golech S, Strasser A, Mechoulam R, Spatz M (2003) Antioxidant properties of the vasoactive endocannabinoid, 2-arachidonoyl glycerol (2-AG). Acta Neurochir Suppl 86: 271-5
Mechoulam R, Fride E, Di Marzo V (1998) Endocannabinoids. Eur J Pharmacol 359: 1-18
Miller TW, Forbes JT, Shah C, Wyatt SK, Manning HC, Olivares MG, Sanchez V, Dugger TC, de Matos Granja N, Narasanna A, Cook RS, Kennedy JP, Lindsley CW, Arteaga CL (2009) Inhibition of mammalian target of rapamycin is required for optimal antitumor effect of HER2 inhibitors against HER2-overexpressing cancer cells. Clin Cancer Res 15: 7266-76
Miquel J, Economos AC, Fleming J, Johnson JE, Jr. (1980) Mitochondrial role in cell aging. Exp Gerontol 15: 575-91
Mulder J, Aguado T, Keimpema E, Barabas K, Ballester Rosado CJ, Nguyen L, Monory K, Marsicano G, Di Marzo V, Hurd YL, Guillemot F, Mackie K, Lutz B, Guzman M, Lu HC, Galve-Roperh I, Harkany T (2008) Endocannabinoid signaling controls pyramidal cell specification and long-range axon patterning. Proc Natl Acad Sci U S A 105: 8760-5
Muller FL, Lustgarten MS, Jang Y, Richardson A, Van Remmen H (2007) Trends in oxidative aging theories. Free Radic Biol Med 43: 477-503
Nakanishi H (2003) Neuronal and microglial cathepsins in aging and age-related diseases. Ageing Res Rev 2: 367-81
Nakanishi H, Amano T, Sastradipura DF, Yoshimine Y, Tsukuba T, Tanabe K, Hirotsu I, Ohono T, Yamamoto K (1997) Increased expression of cathepsins E and D in neurons of the aged rat brain and their colocalization with lipofuscin and carboxy-terminal fragments of Alzheimer amyloid precursor protein. J Neurochem 68: 739-49
Nakanishi H, Wu Z (2009) Microglia-aging: roles of microglial lysosome- and mitochondria-derived reactive oxygen species in brain aging. Behav Brain Res 201: 1-7
Nakanishi H, Zhang J, Koike M, Nishioku T, Okamoto Y, Kominami E, von Figura K, Peters C, Yamamoto K, Saftig P, Uchiyama Y (2001) Involvement of nitric oxide released from microglia-macrophages in pathological changes of cathepsin D-deficient mice. J Neurosci 21: 7526-33
Navarro A, Sanchez Del Pino MJ, Gomez C, Peralta JL, Boveris A (2002) Behavioral dysfunction, brain oxidative stress, and impaired mitochondrial electron transfer in aging mice. Am J Physiol Regul Integr Comp Physiol 282: R985-92
Nomura DK, Morrison BE, Blankman JL, Long JZ, Kinsey SG, Marcondes MC, Ward AM, Hahn YK, Lichtman AH, Conti B, Cravatt BF (2011) Endocannabinoid hydrolysis generates brain prostaglandins that promote neuroinflammation. Science 334: 809-13
O'Sullivan SE, Kendall DA (2010) Cannabinoid activation of peroxisome proliferator-activated receptors: potential for modulation of inflammatory disease. Immunobiology 215: 611-6
Oeppen J, Vaupel JW (2002) Demography. Broken limits to life expectancy. Science 296: 1029-31
Ozaita A, Puighermanal E, Maldonado R (2007) Regulation of PI3K/Akt/GSK-3 pathway by cannabinoids in the brain. J Neurochem 102: 1105-14
Palkovits M (1983) Punch sampling biopsy technique. Methods Enzymol 103: 368-76

Panikashvili D, Simeonidou C, Ben-Shabat S, Hanus L, Breuer A, Mechoulam R, Shohami E (2001) An endogenous cannabinoid (2-AG) is neuroprotective after brain injury. Nature 413: 527-31
Paradisi A, Oddi S, Maccarrone M (2006) The endocannabinoid system in ageing: a new target for drug development. Curr Drug Targets 7: 1539-52
Pertwee RG (1997) Pharmacology of cannabinoid CB1 and CB2 receptors. Pharmacol Ther 74: 129-80
Poon HF, Castegna A, Farr SA, Thongboonkerd V, Lynn BC, Banks WA, Morley JE, Klein JB, Butterfield DA (2004) Quantitative proteomics analysis of specific protein expression and oxidative modification in aged senescence-accelerated-prone 8 mice brain. Neuroscience 126: 915-26
Pryce G, Ahmed Z, Hankey DJ, Jackson SJ, Croxford JL, Pocock JM, Ledent C, Petzold A, Thompson AJ, Giovannoni G, Cuzner ML, Baker D (2003) Cannabinoids inhibit neurodegeneration in models of multiple sclerosis. Brain 126: 2191-202
Puighermanal E, Marsicano G, Busquets-Garcia A, Lutz B, Maldonado R, Ozaita A (2009) Cannabinoid modulation of hippocampal long-term memory is mediated by mTOR signaling. Nat Neurosci 12: 1152-8
Ramesh Babu J, Lamar Seibenhener M, Peng J, Strom AL, Kemppainen R, Cox N, Zhu H, Wooten MC, Diaz-Meco MT, Moscat J, Wooten MW (2008) Genetic inactivation of p62 leads to accumulation of hyperphosphorylated tau and neurodegeneration. J Neurochem 106: 107-20
Reinheckel T, Korn S, Mohring S, Augustin W, Halangk W, Schild L (2000) Adaptation of protein carbonyl detection to the requirements of proteome analysis demonstrated for hypoxia/reoxygenation in isolated rat liver mitochondria. Arch Biochem Biophys 376: 59-65
Reznick AZ, Packer L (1994) Oxidative damage to proteins: spectrophotometric method for carbonyl assay. Methods Enzymol 233: 357-63
Romero J, Berrendero F, Garcia-Gil L, de la Cruz P, Ramos JA, Fernandez-Ruiz JJ (1998) Loss of cannabinoid receptor binding and messenger RNA levels and cannabinoid agonist-stimulated [35S]guanylyl-5'O-(thio)-triphosphate binding in the basal ganglia of aged rats. Neuroscience 84: 1075-83
Rozenfeld R, Devi LA (2008) Regulation of CB1 cannabinoid receptor trafficking by the adaptor protein AP-3. FASEB J 22: 2311-22
Rubinsztein DC, Marino G, Kroemer G (2011) Autophagy and aging. Cell 146: 682-95
Salazar M, Carracedo A, Salanueva IJ, Hernandez-Tiedra S, Lorente M, Egia A, Vazquez P, Blazquez C, Torres S, Garcia S, Nowak J, Fimia GM, Piacentini M, Cecconi F, Pandolfi PP, Gonzalez-Feria L, Iovanna JL, Guzman M, Boya P, Velasco G (2009) Cannabinoid action induces autophagy-mediated cell death through stimulation of ER stress in human glioma cells. J Clin Invest 119: 1359-72
Santos RX, Correia SC, Cardoso S, Carvalho C, Santos MS, Moreira PI (2011) Effects of rapamycin and TOR on aging and memory: implications for Alzheimer's disease. J Neurochem 117: 927-36
Sastre J, Pallardo FV, Vina J (2003) The role of mitochondrial oxidative stress in aging. Free Radic Biol Med 35: 1-8
Settembre C, Fraldi A, Jahreiss L, Spampanato C, Venturi C, Medina D, de Pablo R, Tacchetti C, Rubinsztein DC, Ballabio A (2008a) A block of autophagy in lysosomal storage disorders. Hum Mol Genet 17: 119-29
Settembre C, Fraldi A, Rubinsztein DC, Ballabio A (2008b) Lysosomal storage diseases as disorders of autophagy. Autophagy 4: 113-4
Stranahan AM, Mattson MP (2012) Recruiting adaptive cellular stress responses for successful brain ageing. Nat Rev Neurosci
Strazielle C, Jazi R, Verdier Y, Qian S, Lalonde R (2009) Regional brain metabolism with cytochrome c oxidase histochemistry in a PS1/A246E mouse model of autosomal dominant Alzheimer's disease: correlations with behavior and oxidative stress. Neurochem Int 55: 806-14

Talent JM, Kong Y, Gracy RW (1998) A double stain for total and oxidized proteins from two-dimensional fingerprints. Anal Biochem 263: 31-8
Terman A, Brunk UT (2004) Lipofuscin. Int J Biochem Cell Biol 36: 1400-4
Valenti M, Vigano D, Casico MG, Rubino T, Steardo L, Parolaro D, Di Marzo V (2004) Differential diurnal variations of anandamide and 2-arachidonoyl-glycerol levels in rat brain. Cell Mol Life Sci 61: 945-50
Vara D, Salazar M, Olea-Herrero N, Guzman M, Velasco G, Diaz-Laviada I (2011) Anti-tumoral action of cannabinoids on hepatocellular carcinoma: role of AMPK-dependent activation of autophagy. Cell Death Differ 18: 1099-111
Vaughn LK, Denning G, Stuhr KL, de Wit H, Hill MN, Hillard CJ (2010) Endocannabinoid signalling: has it got rhythm? Br J Pharmacol 160: 530-43
Velasco G, Galve-Roperh I, Sanchez C, Blazquez C, Haro A, Guzman M (2005) Cannabinoids and ceramide: two lipids acting hand-by-hand. Life Sci 77: 1723-31
Villeda SA, Luo J, Mosher KI, Zou B, Britschgi M, Bieri G, Stan TM, Fainberg N, Ding Z, Eggel A, Lucin KM, Czirr E, Park JS, Couillard-Despres S, Aigner L, Li G, Peskind ER, Kaye JA, Quinn JF, Galasko DR, Xie XS, Rando TA, Wyss-Coray T (2011) The ageing systemic milieu negatively regulates neurogenesis and cognitive function. Nature 477: 90-4
Walls KC, Klocke BJ, Saftig P, Shibata M, Uchiyama Y, Roth KA, Shacka JJ (2007) Altered regulation of phosphatidylinositol 3-kinase signaling in cathepsin D-deficient brain. Autophagy 3: 222-9
Wang L, Liu J, Harvey-White J, Zimmer A, Kunos G (2003) Endocannabinoid signaling via cannabinoid receptor 1 is involved in ethanol preference and its age-dependent decline in mice. Proc Natl Acad Sci U S A 100: 1393-8
Wong E, Cuervo AM (2010) Autophagy gone awry in neurodegenerative diseases. Nat Neurosci 13: 805-11
Yamasaki R, Zhang J, Koshiishi I, Sastradipura Suniarti DF, Wu Z, Peters C, Schwake M, Uchiyama Y, Kira J, Saftig P, Utsumi H, Nakanishi H (2007) Involvement of lysosomal storage-induced p38 MAP kinase activation in the overproduction of nitric oxide by microglia in cathepsin D-deficient mice. Mol Cell Neurosci 35: 573-84